Contribution to the development of spinal functional magnetic resonance imaging as a tool in the investigation of spinal cord physiology

A Thesis

Submitted to the Faculty of Graduate Studies

In Partial Fulfillment of the Requirements

For the Degree of

Doctor of Philosophy

In Physiology

By

Jennifer Kornelsen

6761906

Department of Physiology

University of Manitoba

Winnipeg, Manitoba

©

THE UNIVERSITY OF MANITOBA

FACULTY OF GRADUATE STUDIES

*****

COPYRIGHT PERMISSION

Contribution to the Development of Spinal Functional Magnetic Resonance Imaging as a Tool in the Investigation of Spinal Cord Physiology

BY

Jennifer Kornelsen

A Thesis/Practicum submitted to the Faculty of Graduate Studies of The University of Manitoba in partial fulfillment of the requirement of the degree

Of

DOCTOR OF PHILOSOPHY

Jennifer Kornelsen © 2006

Permission has been granted to the Library of the University of Manitoba to lend or sell copies of this thesis/practicum, to the National Library of Canada to microfilm this thesis and to lend or sell copies of the film, and to University Microfilms Inc. to publish an abstract of this thesis/practicum.

This reproduction or copy of this thesis has been made available by authority of the copyright owner solely for the purpose of private study and research, and may only be reproduced and copied as permitted by copyright laws or with express written authorization from the copyright owner.

Abstract:

It is important, in order to further establish spinal fMRI as a valuable clinical and research tool, to expand the repertoire of stimuli and responses that can be assessed by this method. The specific contributions to the development of spinal functional magnetic resonance imaging were carried out in four studies. The first study aimed to develop a lower limb movement task suitable for functional imaging. A pedal was designed, built and tested, and healthy human volunteers participated in alternating flexion and extension ankle movements during a single-shot fast spin-echo imaging sequence. Active and passive pedaling was performed by all volunteers. Images were found to be sufficiently unaffected by motion. Neuronal activity was detected in the dorsal and ventral horns bilaterally in both conditions, however there was less activity overall in response to passive pedaling. Active and passive pedaling each incurred signal changes of approximately 12%. The second study aimed to improve the volume coverage of the spinal cord with increased resolution. This was achieved with a sagittal orientation imaging method of the cervical spinal cord during thermal stimulation. The third study employed the new imaging technique for the lumbar spinal cord and the previously tested movement task was carried out with a spinal cord injured population. Neuronal activity was detected in the lumbar cord caudal to the injury site in all injured volunteers. Active pedaling incurred more neuronal activity than passive pedaling, similar to the healthy volunteers studied in part one of the thesis. Signal intensity changes of 13.6% and 15.0% were recorded for active and passive participation, respectively. The fourth study of the thesis aimed to discriminate true neuronal activity from false positive activity in a spinal functional imaging study by means of a cluster analysis. It was shown that true neuronal activity-related signal changes that occur in the gray matter tend to occur in the 5%-15% signal intensity range, and that apparent activation surrounding the cord tended to occur in the above 15% signal intensity range. The overall goal of contributing to the development and advancement of spinal fMRI towards reliable research and practical clinical use was achieved.

Acknowledgments

I would like to thank, first and foremost, Dr. Patrick Stroman for being the most fantastic supervisor. His support, advice, and encouragement was much appreciated throughout the duration of my studies. I found him to be an excellent teacher and an inspiring mentor. Most importantly, he is terribly funny. And patient, for example. Thank you, Patrick!

I would like to thank my committee members, Dr. Brian Schmidt, Dr. Karen Ethans, Dr. Kris Malisza, and Dr. Brent Fedirchuk, as well as department head Dr. Janice Dodd, for all the help and support they have provided during my studies. Their input was invaluable and appreciated.

I would like to thank my fellow ThesisWatchers members, Jane Lawrence, Myriam Lafreniere-Roula, and Katinka Stecina for their friendship. These brilliant women are a constant source of inspiration for me.

I would like to thank my husband, Derek, for his unwavering confidence in my abilities. Last, but not least, I would like to thank my son, Sam, for being a constant reminder that there are more important things in life than a thesis.

General Introduction

Although MRI has been used to anatomically image the spinal cord for a number of years, it has only recently been successful in investigating functional processes. The purpose of this dissertation is to contribute to the development of spinal fMRI as a tool for investigating spinal cord physiology. In order to reach this goal, a number of studies were conducted. First, a spinal fMRI study was carried out that involved healthy volunteers imaged while participating in lower limb movement tasks. Second, we have adjusted the method to obtain images in the sagittal orientation. The numerous difficulties with developing this technique are outlined in the introduction. Third, once imaging in the sagittal orientation was established in the cervical cord, we used the technique to image the lumbar cord of spinal cord injured volunteers employing the same tasks used with the healthy volunteers, both to further validate the sagittal imaging method and also to see if spinal fMRI could detect neuronal function caudal to an injury site. Fourth, a paper considering the implications of a cluster analysis of this data ends the manuscript component of this work. In order to appreciate the unique contribution this project brings to the literature, a review of the MR basics and fMRI studies that lead up to this body of work are outlined, and the relevant spinal cord physiology is provided to assist in the comprehension of the imaging results. The four manuscripts are then included in the dissertation to describe the rationale, methods, results and discussion of the above mentioned studies. Finally, an overall discussion concludes the dissertation.

Introduction to MRI

MRI basics

There are a number of excellent texts describing the principles of magnetic resonance imaging (MRI) (Chakeres and Schmalbrock, 1992; Moonen and Bandettini, 1999; Jezzard, Matthews and Smith, 2001). The basic principles underlying MRI as presented in this Introduction to MRI: MRI Basics section can be found in these texts. However, the text by Jezzard, Matthews and Smith provides a clear, thorough and pleasant overview of the topic. For a more detailed explanation of the information presented here, I recommend this resource. Additionally, for a straight forward review of the relevant basic MR physics, see Bitar et al. (2006).

Magnetic resonance imaging is based on the magnetic properties of certain elements. The largest nuclear magnetic moment that naturally occurs in abundance is that of hydrogen as its nucleus is a single proton. The magnetic moment is a measure of the strength of the magnet. Only nuclei with an odd number of protons and/or neutrons have a magnetic moment, as even numbered protons align in a way that cancel each other out. The same is true for neutrons. The water in blood, interstitial fluid, and intracellular fluid is the biggest source of hydrogen in the body. The nucleus of hydrogen has a large magnetic moment. The magnitude of a magnetic moment of a nucleus is related to its spin, which is a constant physical property. When no external field is present, the orientation of a magnetic moment is random due to its thermal motion. A magnetic moment in a static magnetic field can be in only one of two possible states, either aligned parallel to the field or against it (anti-parallel). Each state has a specific energy. When placed in the magnet, after a few seconds the magnetic moments achieve

equilibrium where they either align parallel with the static magnetic field or anti-parallel to it. Since the energy of the parallel state is the lower of the two, more magnetic moments are in this state, according to MR convention. It is the net magnetization of the sample, the difference between the number of parallel and anti-parallel magnetic moments, that is observed. The "magnetization" is the net magnetic moment per unit volume. The magnetic field is the static field of the MR system and is called B_0 (with the z axis being defined as parallel to B_0). The magnetization depends on the magnetic field strength and the temperature. Increasing B_0 increases the number of protons that align parallel to B_0, as opposed to anti-parallel. Increasing temperature increases the random forces that tend to push the magnetic moments out of alignment into a more random orientation. The equilibrium magnetization, M_0, is the net total magnetic field of the magnetic moments. This magnetization is aligned parallel to the B_0 field, is parallel to the z axis, and is zero in the transverse (xy) plane.

When the magnetization is in the equilibrium state, it does not produce a detectable MR signal. In order for a signal to be detected, the magnetization must first be disturbed from equilibrium. The energy needed to cause an energy transition or a change of the magnetic moments from being parallel to the field to anti-parallel is at the same frequency as the precession of the magnetic moments in that field. This is called the resonance condition. Protons precess at a resonance frequency that is proportional to B_0, and this is defined by the Larmor Equation:

$$\omega_0 = \gamma B_0$$

where omega (ω_0) is the resonance frequency and gamma (γ) is a gyromagnetic constant. Each type of nucleus has a specific spin and gyromagnetic ratio. By applying an

oscillating magnetic field that stays in phase with the rotation of the magnetic moments and keeps pushing them in the same direction, this field is then also at the right energy to give energy to the magnetic moments. As a result, we can use a low intensity magnetic field, given that it is at the right frequency, to have a strong influence on the magnetization.

At the equilibrium state, the magnetization is parallel to B_0 and does not move. To get it to move away from B_0, a weak magnetic moment which is oscillating at the Larmor frequency is used. The Larmor frequency is in the radio frequency range, which is approximately 64 MHz at 1.5 Tesla. This magnetic field that is used to tip it away, B_1, needs to be at a 90 degree angle to B_0. If it were parallel, it would only add to the field, but at a right angle it is able to cause the magnetization to precess out of alignment with B_0. The magnetization is precessing around the net field, and so by changing the direction of the field that we add at the same speed as the magnetization, this effect accumulates. The magnetization rotates away from the alignment with B_0. With a brief pulse of the B_1 field it is possible to rotate the magnetization completely into the transverse (xy) plane. This brief pulse is called the radio-frequency (RF) pulse. The absorption of RF waves, which causes the spins to change their orientation from parallel to anti-parallel, is referred to as perturbation. With the application of an RF wave, M_0 spirals down towards the transverse plane. When the RF is turned off, three simultaneous effects occur. One, the absorbed RF energy dissipates away into thermal energy as the magnetic moments relax back to equilibrium. The signal we detect is from the magnetic moments rotating in phase, to produce a time-varying magnetization that induces an electric current in an MR coil. Two, the excited spins begin to return to original

orientation (T1 relaxation). And three, the initially in-phase excited protons begin to dephase (T2 and T2* relaxation). Relaxation times are physical properties of the water environment (in terms of biological tissues). Relaxation refers to the return of the spins to a stable low energy or random state after they have been excited or altered. Relaxation implies, therefore, that the spin system is returning to a state of equilibrium. Further explanation of these concepts can be found in Bitar et al. (2006).

There are a number of sources of field variation over which the experimenter has no control. There is, however, a field variation intentionally produced by applying gradients. Gradients are produced by coils of wire situated in the magnet that can be turned on and off. They are meant to produce a magnetic field that is parallel to B_0 but vary linearly in magnitude along one of the axes. At the center of the magnet and at the center of the coil the magnetic field produced is zero. Moving along the axis, the field magnitude changes. Gradients can be produced in any direction by applying gradients in two or three directions at a time.

With the gradients applied and an RF pulse applied on a particular frequency, it is possible to produce an effect on a selected region of space. This means that in one position in the field, the magnetic moments are precessing at whatever particular frequency the RF pulse is applied. On either side of this position the precessing frequency is different enough to no longer have an effect. If a gradient is applied in the y direction, moving away from the zero center of the magnet toward the spot where the moments are precessing at the appropriate frequency (that of the RF pulse) creates an effect in a particular location. The bandwidth of the RF pulse will determine what range of frequencies will be affected. This is what enables slice selection.

After the RF pulse has been applied, the moments have rotated away from the z axis to the transverse plane. However, because of the gradient along the axis these moments are all precessing at different rates, slower on one side of the slice and gradually faster on the other side of the slice. No signal can be obtained because all the different orientations cause the magnetization to sum to a net field of zero. For that reason, a slice refocusing gradient is applied in the opposite direction which puts all the moments back into phase but in the transverse plane.

Once the RF pulse is removed, if the moments are all in phase, they produce a strong signal. If they are not precessing at the same frequency, they will in time become out of phase and the signal will decrease. The location of the moments is determined by applying a linear magnetic field gradient. This gradient identifies the location of the signal in space based on its frequency. The signal detected is the sum of all the signals; therefore if it is known how much signal is at each frequency then it can be known how much signal is coming from each position in space.

The signal that is obtained is a spatially encoded signal. This is detected with a gradient on and is the inverse Fourier Transform of the signal distribution along the gradient direction. This signal is recorded along a one dimensional space, along the transverse magnetization distributed along the x axis. It is called frequency encoding because it makes use of changing the frequency of the MR signal depending on its position in space. To get a two dimensional image, encoding needs to occur in a second direction. This is accomplished by phase encoding, which is done by applying a gradient in a different direction, such as along the y axis, for a brief amount of time and then turning it off before the signal is acquired (See Figure 1). This is similar to taking a

signal from a point on the x axis with the gradient on; this alters the phase of the signal depending on its position. By continuously changing the gradient along the y axis repeated measures of the signal are obtained in two dimensions. These signals recorded in the two dimensions make up k-space. By measuring the entire k-space it is then possible to use the inverse Fourier Transform to get a two dimensional image. To get a three dimensional image another phase encoding is used.

Figure 1: Illustration of a typical spin-echo pulse sequence.

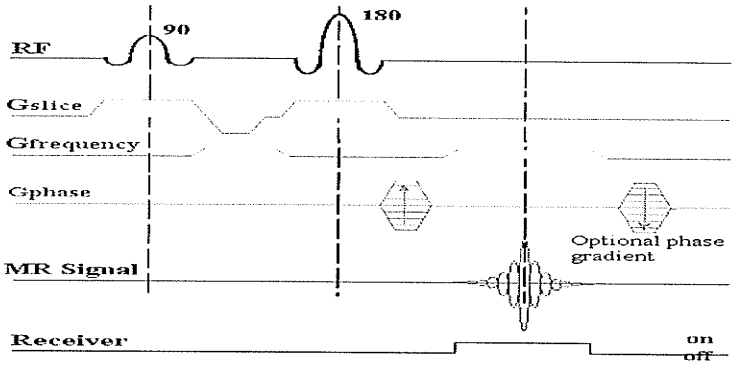

The signal obtained immediately following the tipping of the moments away from B_0, as they are precessing together in one direction in the x axis, begins to decay quickly. When the spins are first tilted down to the (xy) plane they are all in phase. Some spins are faster or slower than others, and so they begin to dephase quickly. The result is that the signal fades or decays. The speed of precession depends on the magnetic field experienced by the proton. Isolated protons feel only B_0. Protons near other protons have interacting magnetic fields. If one proton's field increases the field of the second proton, the second proton will precess faster. If the first field opposes the main field,

then the second proton will precess slower. As soon as the spins move apart, both return to their original frequency, but at different phases. This interaction is called the spin-spin interaction and these cause cumulative loss of phase across excited spins resulting in an overall loss of signal. This decay caused by the different moments becoming out of phase due to the interaction of other nearby moments is called free induction decay. Once the moments point in all directions in the transverse plane the net signal is zero. This spin-spin relaxation is the random interaction between two spins that cause a cumulative loss of signal and is known as transverse or T2 relaxation. The T2 decay curve is

$$M_{xy} = M_0 \exp(-t/T_2)$$

Each tissue type has a particular T2 value and this value is determined primarily by its environment with little relation to field strength. T2 decay is the exponential loss of signal resulting from purely random spin-spin interactions in the transverse plane.

In practice, the T2 signal decays faster than the T2 decay curve would predict. T2 decay is a function of purely random interactions between spins and assumes an homogeneous field. An approximated decay time which takes into account these purely random effects plus the fixed effects such as hardware flaws or different magnetic susceptibilities of tissues is called T2*. T2*, then, is a measure of all the factors leading to dephasing. T2* is dependent on the homogeneity of the magnetic field. If the magnetic field is very inhomogeneous, then the T2* relaxation is short, since the differences in the precessional rates are broad from one region in the magnet to the next. In general, the better the quality of the uniform field, the higher the signal, and the higher the signal, the better the image quality.

Gradient echo imaging uses a gradient to knock the spins out of phase in the transverse magnetization and then reverses the gradient to make the magnetization come back into phase and go beyond it out of phase again (See Figure 2). Because the signal is at its largest when all spins are in phase, gradient echo can detect a strong signal while the gradient is on. Due to free induction decay, the signal decays exponentially after the RF pulse is turned off. By applying a gradient the decay would occur faster until no signal was left. By reversing the gradient, that effect would be cancelled out and the signal would be large again. This does not effect the interactions between spins or the magnetization susceptibilities. If the signal is at the center of this echo, it would be smaller than that recorded following the RF pulse and would still be decaying at the time T2*. The time that passes between the RF pulse and the echo signal is called the echo time (TE), and this is dependent on T2*, and so images obtained in this way are called T2*-weighted. A longer echo time has more T2* weighting.

A spin-echo sequence uses an RF pulse to rotate the magnetization 180° to reverse the phase distribution, which refocuses the magnetization (See Figure 2). Following the 90° pulse all the magnetization is tipped into the transverse plane, and the signal would be strong. This would begin to decay due to free induction decay. If a 180° pulse was given at time t, the moments would rotate 180° and then continue to be subject to the field variations that were originally causing their decay after the 90° pulse. However, the magnetization is now moving back into phase, and at the time t following the 180° pulse it will reach maximum signal again, however, reduced due to transverse relaxation. In other words, at the time TE (equal to 2*t), all the spins are back in phase, and they produce a large signal called a spin echo. Immediately after a 90° RF pulse, the

magnetization is along the y axis. At half the TE, after the spins have been dephasing, a 180° RF pulse is applied which flips the dephased spins on the X axis. During the second half of TE the spins rephase. At TE, the spins have rephased and an echo of the opposite sign is formed. The 180° pulse can be repeated when the spins all come back into phase at TE and begin to go out of phase again. This process can be repeated over and over as long as the pure T2 decay has some signal left. The TE in spin-echo sequences is the time between the center of the 90° pulse and the echo center. The signal obtained in this sequence is dependent on the TE and the transverse relaxation time (T2) so this signal and the image obtained by this method are T2-weighted.

Figure 2: Comparison of the Spin-echo and Gradient-echo events.

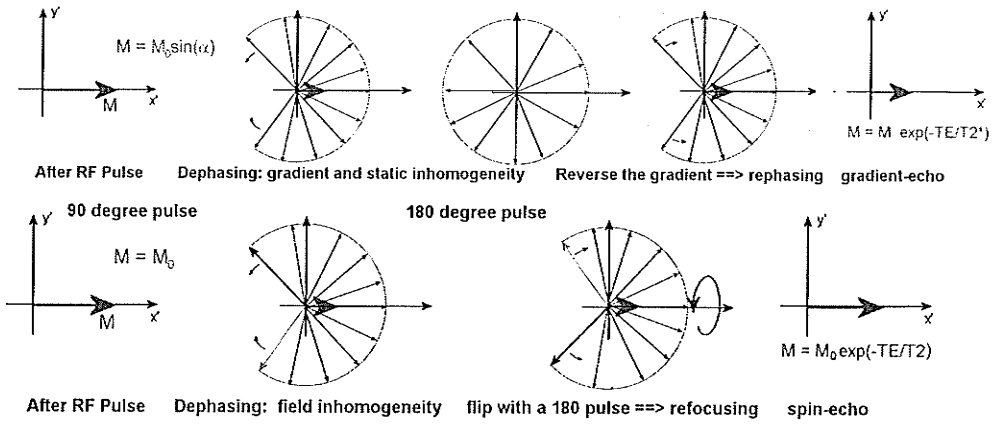

After an RF pulse, the moments are relaxing back toward equilibrium, and the rate of this relaxing and coming back to B_0 is called the longitudinal relaxation time, T1. T1-weighting is dependent on how far the magnetization was tipped away from B_0 by the RF pulse and also by how long is given for it to relax before another pulse is applied.

This time between pulses is called the repetition time, TR. As TR increases the amount of T1 contribution to a signal decreases. The recovery rate is unique for every tissue, and this is what enables MRI to differentiate different types of tissue. The T1 recovery curve is defined as

$$M_z = M_0 [1-\exp(-t/T_1)]$$

The T1 relaxation time is a measure of how rapidly the spins realign with the static magnetic field. T1 is also referred to as spin-lattice relaxation, which refers to the fact that the T1 relaxation process involves excited anti-parallel spins releasing energy back into the lattice as they return to parallel. The transition from anti-parallel to parallel is not instantaneous for the whole collection of magnetic moments, but occurs over a short interval. The rate at which the spins realign with the main magnetic field is an exponential function with time. The spins begin to realign rapidly but this slows as it approaches equilibrium. The time constant at which this transition occurs is the T1 relaxation rate. The different rates of T1 relaxation are related to how rapidly the higher energy spins can realign and dissipate the excess energy. Individual spins flip instantaneously, but the probability of them flipping decreases as the system approaches equilibrium.

Proton spin density is the number per volume of hydrogen nuclei that produce the signal in an MR experiment. This signal is composed of the sum of all the individual spins with magnetic properties that can be affected in an MR experiment. The more spins per volume, the higher the net magnetization, M_0, and the higher the maximum possible signal in a voxel. A voxel is a "volume element", that is, the volume spanned by a "pixel" or "picture element" in an image.

Spatial encoding is applied to the signal by applying a linear gradient. By doing this, a known change in the resonance frequency can be caused. The change in frequency is directly proportional to the distance from the center of the magnet. If the change in frequency is applied for a period of time, a change in phase is caused that is directly proportional to the distance from the center of the magnet. The MR coil records the signal. The received signal is the sum of the signal from all the protons within the sensitive volume of the MR coil. The strength of the signal at each frequency, however, is directly related to the number of excited protons at each position along the gradient.

The Fourier Transform (FT) decomposes a signal into the sum of sine waves with varying frequencies, phases, and amplitudes. Frequency is a measure of how rapidly the process makes a complete cycle per unit of time. The more cycles per time, the higher the frequency. Amplitude is the measure of the maximum change over the cycle; in MR this is a measure of the maximum signal intensity. Phase describes an arbitrary starting point of the cycle. The FT of a data set is useful if you wish to see how much contribution you have from different frequencies of oscillation, which is particularly important in MRI. The FT process decodes the individual components and creates a complex repeating curve or signal. An inverse FT is used to calculate the signal that is generated from the sum of multiple different simple phases, amplitude and frequency signals. In MR, the inverse FT is used to create signals composed of specific frequencies and also to predict the expected signal pattern of multiple sources. The FT is used to determine the strength of the signal at each frequency and thus produce an image.

This technique is similar in theory, but much faster than the original technique used to produce an image. Mansfield (1973) published work involving the application of

gradients to a magnetic field with a sequence that involved imaging half of k-space using a zigzag pattern, resulting in faster imaging. Lauterbur (1973) employed the technique of applying gradients in several directions to obtain an MR spectra from different angles and from the spectra developed a two dimensional back projection image, the first image produced from an MR spectra. This was followed a few years later by the first NMR image of human tissue (Damadian et al., 1977). Lauterbur and Mansfield were awarded the Nobel Prize in Medicine in 2004 for this contribution to the development of MRI.

MRI of the spinal cord

The composition of the gray matter of the spinal cord is similar to that of the brain, with approximately 80% water, 10% protein, and 10% phospholipids (Chakeres and Schmalbrock, 1992). Neuronal cell bodies contain a large amount of aqueous cytoplasm, which contributes to higher water content in gray matter than white matter. The higher water content increases proton density and lengthens T1 and T2 relaxation times (See Figure 3). The spinal cord and roots are surrounded by cerebrospinal fluid (CSF). This CSF flow is pulsatile due to cardiac and respiratory movements and the motion is periodic. Pulsatile flow creates several image artefacts and signal loss (Chakeres and Schmalbrock, 1992). The CSF currents are formed as CSF circulates around the dentate ligaments, resulting in regional flow-related signal changes. The areas of greatest CSF turbulence are adjacent to the anterolateral and posterolateral aspects of the spinal cord, where focal signal void is seen on axial spin-echo images (Chakeres and Schmalbrock, 1992). Several techniques can be used to minimize CSF pulsation artefacts. These include cardiac gating and flow compensation gradients.

Figure 3: Sagittal anatomical MR images showing T1 and T2 weighting contrast differences.

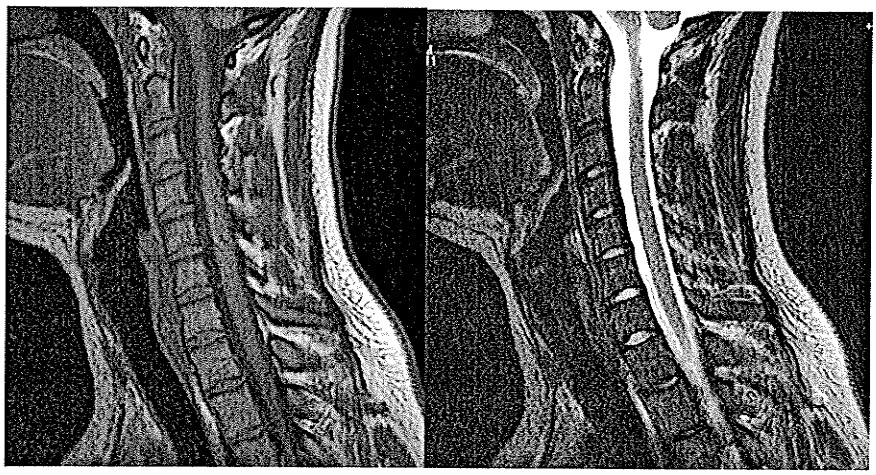

Functional MRI

Magnetic resonance imaging of neuronal function in the brain (fMRI) is a recent addition to the world of diagnostic imaging (Ogawa et al., 1990, 1992, 1993). This application has quickly become a commonly used tool in medical and research fields for imaging brain activity since it was first shown to be successful by Ogawa (1990). For a review of the different methodologies and applications of functional versus anatomical MRI, see Talos et al., 2006. Functional MRI is based on acquiring repeated MR images of an area of interest, usually in the brain, in order to describe a time series. Subtle changes in the MR images can thus be detected between periods of time when different tasks are being performed, and these image changes are inferred to reflect the changes in neuronal activity between the different tasks (Ogawa, 1998, or for a review see Lauritzen and Gold, 2003). As a result, fast imaging methods are preferred (see Figure 4), motion and other sources of signal variance cause confounding effects, and the results can

demonstrate only differential changes between tasks being compared. All fMRI methods are influenced by these requirements. FMRI of the spinal cord (spinal fMRI) is a recent application of this technology (Yoshizawa et al., 1996; Stroman et al., 1999). The application of fMRI to the spinal cord requires specific modification to the conventional brain fMRI methodology, but the theory of conventional brain fMRI applies. In order to further the advancement of spinal fMRI, particular attention to the artefact and error sources is required (for a review, see Tabor et al., 1998). Although advances have been made in this area, further work is required before the method is optimal for clinical purposes.

Figure 4: Illustration of a typical fast spin-echo sequence.

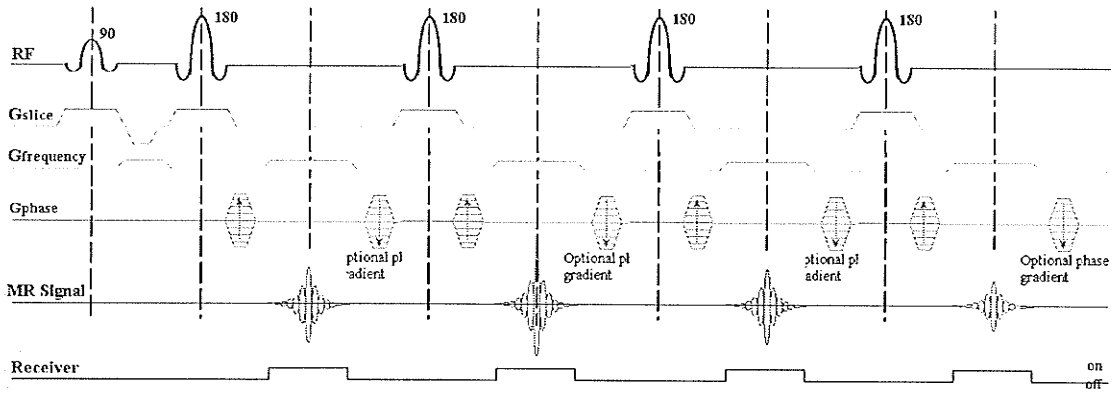

Blood Oxygenation-Level Dependent Theory

FMRI reveals neuronal function indirectly by way of changes in blood flow and blood oxygen levels that occur near metabolically active gray matter. Blood oxygen-level dependant (BOLD) contrast is linked to the metabolic activity that occurs in active

neuronal tissues (Ogawa et al., 1990; Menon et al., 1992). When neuronal firing rates increase, nerve cell bodies take up more oxygen. To compensate, an over-abundant increase in blood supply to neurons occurs resulting in a decrease in the concentration of deoxygenated hemoglobin and an increase of oxygenated hemoglobin. When the iron in the hemoglobin is bound to oxygen it is diamagnetic, whereas iron not bound to oxygen is paramagnetic (Pauling and Coryell, 1936). Deoxygenated hemoglobin in blood acts as an MR contrast agent which alters local magnetization relaxation times and this causes the MR signal to decay more quickly, whereas oxygenated hemoglobin is diamagnetic and does not contribute to relaxation. At the time of recording, the MRI signal is stronger from metabolically active areas because the signal has not decayed as quickly as in the adjacent less active tissues. The BOLD changes can be detected with T2* weighted MRI methods affording indices of local hemodynamic changes that are induced by changes in neural activity (Ogawa et al., 1992). A brightening of the image reflects an increase in the blood oxygenation and indicates an increase in neuronal activity. A darkening of the image reflects a decrease in blood oxygenation and indicates a decrease in neuronal activity (Logothetis et al., 2001, 2004). However, the image intensity changes are subtle, typically a few percent, in the brain. The MR image intensity, seen as image brightness, increases as the neuronal spiking rate increases (Logothetis et al., 2001, 2004). The BOLD contrast changes are larger with T2*-weighted data in gradient-echo imaging than with T2-weighted data in spin-echo imaging, because T2* is sensitive to magnetic susceptibility effects in the blood in addition to the transverse relaxation time (T2). This also makes T2* more sensitive to magnetic field inhomogeneities at different tissue interfaces because of the different magnetic susceptibilities of the tissues.

Signal Enhancement by Extra vascular water Protons Theory

Another dominant contrast mechanism in spinal fMRI is due to signal enhancement from extravascular water protons (SEEP) which is more closely related to the blood flow increase to the active neural tissues (Stroman et al., 2002, 2003a,b). Other studies have also confirmed the existence of a second contrast mechanism (Wong et al., 2004; Li et al., 2005; Ng et al., 2006). When blood flow increases, the intravascular pressure also increases, particularly on the arterial side of the capillary system. This pressure change alters the normal fluid balance and increases fluid movement across blood vessel walls into extracellular space, resulting in a slight increase of water protons near active neural tissues. This movement of water across vessel walls into extracellular space has been shown in PET studies (Ohta et al., 1996; Fujita et al., 1997). Water also accompanies solutes that are transported across cell membranes, which means that fluid balance across the membrane can be controlled by active transport and passive diffusion. The movement of ions, such as Na^+ and K^+, across the cell membrane during an action potential is so small in number that it cannot be expected to contribute to the MR signal. The water that accompanies these ions as they cross the cell membrane, however, could be expected to contribute to the MR signal. Glial cells are also important in MR imaging because they are 5-10 times more numerous than neurons and occupy about half of the volume of the central nervous system. Astrocytes, a type of glial cell, serve to maintain the extracellular concentrations of glutamate (Bouzier-Sore et al., 2002; Pellerin and Magistretti, 2003). They are involved in taking up glutamate from the synapse, converting it to glutamine, and releasing it back into the synapse for reuptake and repackaging by the neuron. In the process of taking up glutamate, the astrocytes use

sodium dependant transporters which move three Na^+ and one H^+ into the cell and one K^+ out of the cell, with water moving into the cell during this exchange (Nedergaard et al, 2002). Astrocytes are connected by gap junctions and therefore function as a continuous large fluid volume, as well. Astrocytes are therefore important in the effective functioning of a neuron as well as inhibiting propagation of neuronal signalling and should be considered to play an important role in fMRI. The impact that astrocyte function has on fMRI is only recently come into appreciation (for a review, see Raichle & Minton, 2006). Finally, it is well accepted that glial cells swelling occurs near areas of neuronal discharge (Andrew and MacVicar, 1994), and this likely contributes as a source of SEEP contrast.

Hemodynamic response function

The signal change observed in fMRI lags behind the onset of stimulation or motor activity. The time difference between stimulation or activity and the associated neuronal response is on the order of tens or hundreds of milliseconds. The hemodynamic change measured by fMRI does not reach its peak for 4 to 8 seconds. The relationship between the change in neuronal activity and the corresponding hemodynamic change is called the hemodynamic response function (Haxby, et al., 1998).

Functional MRI of the spinal cord

The application of fMRI to the spinal cord is a logical extension of its use in the brain but has been slow to develop due to the many challenges with the method. There are now a number of groups that are working on spinal fMRI and the work published has shown promising results and shows that the difficulties with obtaining functional MR imaging of the spinal cord can be overcome (Stroman et al., 2001; Mackey et al., 2003;

Wong et al., 2004; Brookes et al., 2004). The use of fMRI for investigating spinal cord activity is ideal because the spinal cord is contained within the vertebral column and is otherwise assessable by physical examination techniques or by invasive measures. The physical examination technique employed by the ASIA assessment scale gives information regarding cord function but does not give information about the condition of the spinal cord caudal to an injury.

A number of issues stand in the way of obtaining high quality functional spinal cord images with fMRI. The spinal cord is housed in the vertebral column where magnetic susceptibilities between bone, cartilage and tissue result in different fields within this material and field gradients at the boundaries. These gradients cause distortion and loss of signal in MR images. The lungs, which run anterior to the spinal cord along most of its length, also produce these magnetic susceptibility issues, as well as the field distortion caused by the fluctuation of breathing. Cerebrospinal fluid flows around the spinal cord and within the spinal canal, which presents another challenge because of the motion artefacts induced and because of the motion this causes of the spinal cord itself. Also, the short (approximately 45 cm) length of the spinal cord and its small cross section is another problem because a trade off is required between image resolution and the volume of tissue that can be imaged in an amount of time appropriate for MR imaging.

The challenges of the small dimensions of the spinal cord are overcome with appropriate choices of slice orientation, image resolution and slice thickness. The problem is the need for a high signal to noise ratio (SNR). The small dimensions of the spinal cord and the distribution of the white and gray matter within being even smaller, as

well as the surrounding CSF, make it necessary to obtain high resolution data in order to avoid mixing of gray and white matter and CSF into a voxel. The signal from a voxel depends on the volume of tissue/fluid it contains and a larger voxel provides a higher SNR. A balance must be found to produce adequate resolution and an adequate SNR.

Motion is problematic in spinal fMRI. In order for a comparison to be meaningful when detecting a signal from a voxel repeatedly in time, the voxel needs to contain the same volume of tissue consistently throughout the time series. Given the small dimensions of the spinal cord, even slight movement can change the distribution of gray and white matter and CSF in the voxel. This problem is further complicated by the pulsatile flow of CSF that moves the spinal cord with each heart beat. Nearby tissues also move and create image artefacts that contribute to confounding the signal, such as those arising from the lungs, heart, and other organs. To compensate, it is possible to reduce artefacts arising from moving tissues and fluids by use of flow compensation gradients applied in the rostral-caudal direction. Also, spatial saturation pulses are used to eliminate signal from regions anterior to the spine. Respiratory gated acquisition was not used in our studies, as it was not shown to improve the data obtained in previous proton-density weighted spin-echo imaging studies (Stroman et al., 1999). A recent article addressed the effects of cardiac gating and showed that the majority of noise in spinal fMRI is cardiac in origin (Brooks et al., 2004). However, no steps were taken in the papers presented herein to correct for this as the investigation into the modelling of this noise source is currently in progress.

Despite all of these issues, it has been determined that images of acceptable quality can be obtained of spinal cord function by using a proton-density weighted spin-

echo imaging sequence with short echo times. This technique provides the highest image quality in the spinal cord because it has the least sensitivity to spatial variations in the static magnetic field arising from magnetic susceptibility differences, which is a major difficulty with spinal cord imaging. This method does not provide high sensitivity to the BOLD effect, but does reveal areas of signal change which correspond to areas of neuronal activity in the spinal cord, as shown by many groups (Stroman et al., 2003a,b,c; Wong et al., 2004; Li et al., 2005; Ng et al., 2006). A spin-echo study by Stroman et al. (2003b) revealed that fMRI signal changes of 2.5% in the spinal cord and 0.7% in the brain were observed at 1.5T, which is extrapolated to an echo time of zero. This study provided evidence for a non-BOLD contribution, termed SEEP, which is demonstrated to be three times larger in the spinal cord than in the brain.

Most spinal fMRI studies have obtained images in axial orientation. Greater volume coverage can be obtained with sagittal or coronal orientation slices, though. Coronally oriented images are not appropriate for the human spinal cord because of the anterior/posterior curvature of the spine. Sagittally oriented images display better because there is little left/right curvature. Sagittal images will suffer partial volume effects unless the slice thickness is as thin as possible. In most sagittal orientation images the range has been 4 to 8 mm (Backes et al., 2001; Madi et al., 2001). As the spinal cord is only 16 mm at its widest, partial volume effects would be expected. One proposed solution to this problem is to obtain contiguous sagittal slices with the thickness set to minimum, disregarding the SNR. The data is then reformatted into a three dimensional volume and smoothed across uniform tissue volumes in the rostral-caudal direction. This will increase the SNR without causing the partial volume effects. Neuronal activity

related signal changes are detected by computing the correlation between the pixel intensity time course and a model time course, on a pixel by pixel basis (See Figure 5). A detailed description of the data analysis can be found in Part Two, as the investigation of this technique is presented in this dissertation.

Figure 5: An example of how a pixel is determined to be active.

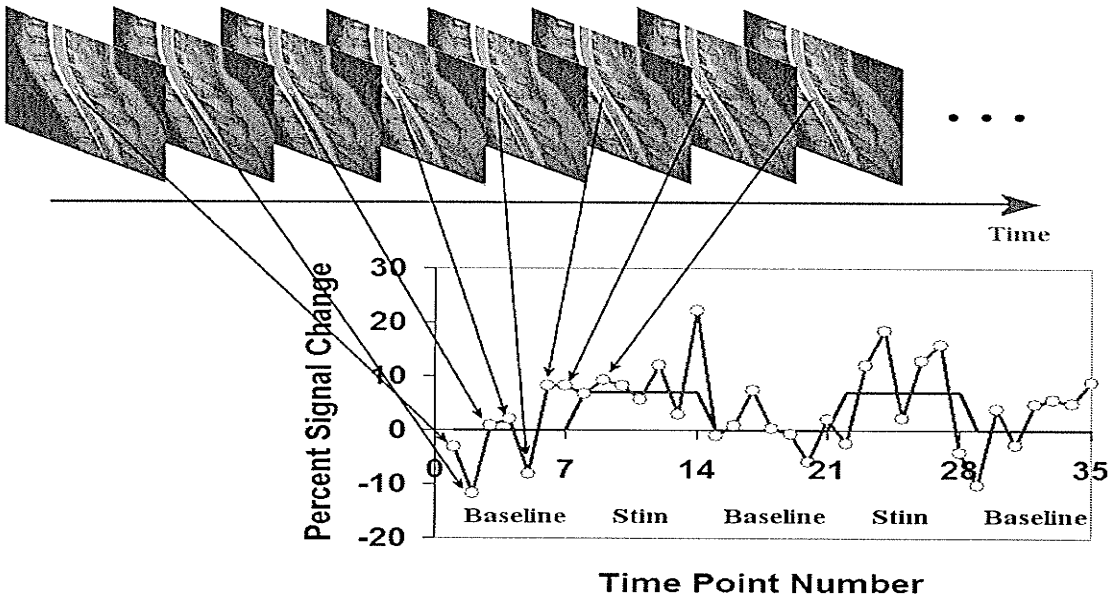

Correlation between the time course (red) and the pattern of rest/stimulation (blue): R = 0.515 or p = 0.00077

==> Significant correlation so the voxel is concluded to be active during the task

Spinal fMRI with healthy human volunteers

Development of the spinal fMRI method has been growing steadily since the first publication describing its feasibility by Yoshizawa et al. in 1996. It wasn't until 1999 that the next spinal fMRI paper was published by Stroman et al. In the past decade, more work has been published concerning spinal fMRI with human subjects (Yoshizawa et al., 1996; Stroman et al., 1999, 2001a,b, 2002a,b,c, 2004, 2005; Madi et al., 2001; Backes et

al., 2001; Kornelsen and Stroman, 2004; Ng et al., 2004; Kollias et al., 2004; Bergman et al., 2004a,b; Mackey et al., 2005; Stracke et al., 2005; Moffit et al., 2005) and concerning spinal fMRI with animal studies (Porszasz et al., 1997; Malisza et al., 2002, 2003; Lawrence et al., 2004; Majcher et al., 2005). The small number of publications in this area likely reflects the difficulty of acquiring functional images of the spinal cord. However, the available literature has shown spinal fMRI to be a reliable tool for assessing spinal cord neuronal function and this technique is currently in use for research purposes. In order for spinal fMRI to become a practical clinical tool, advances in some areas are necessary. Studies thus far have suggested that the use of spinal fMRI for clinical purposes is conceivable.

Spinal fMRI research has focused on imaging of the cervical and lumbar spinal cord during sensory and motor stimulation of the hands (Stroman et al., 2001a,b) and sensory stimulation of the lower leg (Stroman et al., 2002). Evidence that the signal changes observed are related to neuronal activity is provided by the correspondence between the patterns of activity and established neuroanatomy. In an early study involving a motor task and sensory stimulation of the hand, spinal fMRI proved reliable in displaying laterality and spread of activity in the spinal cord (Stroman et al., 2001a). A finger-tapping task elicited ipsilateral activity in the ventral regions spread over the C6 and C7 segments and contralateral ventral activity in the C7 segment. Subsequent spinal fMRI studies have shown that stimulation of specific dermatomes map to the corresponding spinal cord segments (Stroman et al., 2002a), and different types of sensory stimulation have mapped to the analogous gray matter regions (Stroman et al., 2002c). With thermal stimulation of different dermatomes of the hand and forearm, the

expected levels of the cervical cord were activated accordingly. Activity was detected in the dorsal horn in segments C7/C6 ipsilateral to a thermal stimulus applied to the palm of the hand. Shifting the stimulus to the forearm resulted in activity detected in the C6/C5 segments and reduced activity in the C7/C6 segments (Stroman et al., 2002a).

Signal intensity changes in the lumbar cord have been observed to depend on the temperature of cold stimulation, and have shown marked differences between innocuous and noxious cold stimulation (Stroman et al., 2002c). Presentation of an innocuous thermal stimulus to the lower leg (L4 dermatome) resulted in activity of the dorsal horn (lamina I-V) as well as activity in lamina VIII in the gray matter in the lumbar spinal cord. This activity was found primarily ipsilateral to the stimulus with a small contralateral contribution. A noxious thermal stimulus applied to the lower leg resulted in concentration of activity in the tip of the dorsal horn (lamina I/II) in the lumbar cord ipsilaterally, as well as an increase in lamina X activity and dorsal horn activity contralaterally. The signal intensity changes recorded at a temperature of 29°C averaged 2.6%, increased slightly to 3.2% at 15°C, but increased dramatically to 7.0% at 10°C, a temperature reported to be uncomfortable to painful by volunteers. A study by Madi et al. (2001) similarly showed that the magnitude of signal intensity changes in the spinal cord are dependent on the strength of the stimulus. The results indicated that spinal fMRI was capable of detecting reliable neuronal response to an isometric motor task of the hand and that the magnitude of the signal change is proportional to the force applied by the muscle.

Spinal fMRI is therefore able to detect neuronal activity in the appropriate spinal cord segments as well as specific gray matter areas in healthy spinal cords. Investigation

of neuronal response in the cervical and lumbar cord segments to sensory stimulation was performed initially as this generates fewer imaging difficulties due to volunteer movement. Neuronal activity in response to a motor stimulus was carried out after the spinal fMRI method was established as acquiring motion artefact free images proves more difficult during a movement task. Imaging the cervical cord during a motor task of the hand effects a lesser degree of movement to the trunk than does a lower limb movement task, and this was a sensible next step for building to the spinal fMRI literature.

Spinal fMRI with spinal cord injured volunteers

In the interest of advancing spinal fMRI towards clinical use, the spinal fMRI method has been applied to the study of injured spinal cords. The lumbar spinal cord was imaged during noxious thermal stimulation of the L4 dermatome of complete and incomplete spinal cord injured volunteers (Stroman et al., 2002c, 2004). The signal intensity changes for the injured groups were of similar magnitude and had a similar time course pattern as those of the healthy group. The areas of activity in gray matter were altered, however. Compared to the results of the healthy spinal cord group, the activity of the complete injury group was diminished ipsilateral to the stimulus but appeared enhanced on the contralateral side. Volunteers with complete injuries also showed absent or decreased dorsal gray matter activity but enhanced ventral activity particularly on the contralateral side to the stimulus, as compared to subjects with incomplete injuries, in response to the cold stimulus. Distribution of activity was not found to differ substantially between the healthy and incomplete injury groups. This could be accounted for by a complete interruption of the descending input to mediate the reflex response in

the complete spinal cord injured group, that could be partially or completely preserved in those with incomplete injuries. In the injured spinal cord, results demonstrated neuronal activity even when subjects could not feel the stimulus. Spinal fMRI is thus useful for revealing areas of impaired and preserved activity in spinal cord injured patients.

Introduction to physiology

Spinal cord anatomy

The central nervous system is composed of the brain, brainstem, and spinal cord (for a review, see Goshgarian, 2003). The spinal cord is composed of gray matter in a characteristic butterfly-shape cross-section surrounded by white matter, and two continuous rows of nerves enter or exit the cord on each side. These nerves are bundled together to form spinal nerve roots. Pairs of nerve roots enter on the dorsal side and exit on the ventral side of the cord. The segmental nerves divide outside of the column into anterior rami which provide information to the front of the body while the posterior rami supply the back side of the body. Although no obvious boundaries can be seen, the spinal cord is made up of segments that are defined by the vertebral level at which the corresponding spinal nerve exits the spinal canal. The spinal cord consists of 31 segments: 8 cervical (C), 12 thoracic (T), 5 lumbar (L), 5 sacral (S), and 1 coccygeal (Co), which lie within the vertebral canal. Between adjacent vertebrae there is an intervertebral foramina through which the roots enter and exit the column. The cord is shorter than the vertebral column and so the segments and the similarly numbered vertebrae do not align. The sensory and motor roots that enter and leave the cord at each segment do, however, enter and exit at each appropriately numbered vertebral level. In the cervical spine, the numbered nerve roots exit above the similarly numbered vertebrae.

The nerve root that exits between C7 and T1 is numbered C8, which explains why there are 8 cervical roots and only 7 cervical vertebrae. The remainder of the numbered nerve roots exit below the appropriately numbered vertebrae. Most of the lumbar spinal cord segments are typically aligned with the T12 vertebra although this varies from person to person. The conus medullaris, the tapered end of the cord, lies at approximately the L1 level in an adult human and is anchored to the sacrum by the filum terminale. At the caudal end of the cord is the cauda equina, which is a collection of the lumbar and sacral nerves extending down the column beyond the conus medullaris to the intervertebral foramina through which they exit.

Each spinal nerve innervates a region of body, which allows for a distribution map of myotomes and dermatomes to be made. The dermatome map represents the area of body from which a spinal segmental nerve receives sensory information. While each dermatome contains sensory receptors which transmit information predominantly to one segment of the spinal cord, there is some overlap in the distribution of sensory nerves of adjacent dermatomes, so that interruption of a single spinal nerve root may cause little sensory loss. A myotome map outlines the area of the body to which a spinal nerve provides motor information, which is generally a group of muscles. Again, there is some overlap in these maps from one segment to the next. This arrangement is clinically useful in that sensory or motor impairments confined to a specific area or muscle group implicates the spinal nerve and segment involved.

Gray matter

In cross section, it is possible to distinguish the gray and white matter of the spinal cord. The gray matter appears in the middle of the cord as a butterfly shape, while

the white matter surrounds the gray matter. This arrangement is converse to that of the brain, where the gray matter is outer most and the white matter is beneath. The gray matter may be subdivided into a ventral horn, dorsal horn, and intermediate zone. The different levels of the cord, in the rostral-caudal direction, are distinguishable by the size and shape of these matters, most noticeable in the cervical and lumbar enlargements. The enlargements of the cervical and lumbar cord reflect the greater number of nerve cell bodies and synapses in the gray matter, which give rise to the brachial and lumbosacral plexi, which innervate the upper and lower limbs, respectively.

The cross section of the gray matter is mapped into lamina, based on the concentration of certain cell types found in each area. The lamina have been labeled I through X, by Rexed (1952, 1954) and although this work was originally done on a cat spinal cord, the same general notation is still used today for human spinal cord. The laminae I-VI are found in the dorsal horns and are involved primarily in sensory information, with noxious stimuli concentrated at the tips of the horns in laminae I and II. Lamina VII is medial, or lateral, horn in the thoracic levels, and is primarily involved in interneuron activity. Lamina VIII and IX are located in the ventral horns, involved primarily in motor activity. Lamina X surrounds the central canal and is also involved with interneuron activity.

The dorsal horn of the spinal gray matter receives afferent input from axons in the dorsal nerve roots. The cell bodies for these axons lie in the dorsal root ganglia that are located in the intervertebral foramina along the dorsal roots. The dorsal root has two divisions. The lateral division contains small diameter fibers mediating sensation for pain and temperature, whereas the medial division contains large diameter fibers

mediating other sensory modalities such as touch and proprioception. The axons carrying different sensory modalities terminate and synapse in different lamina within the dorsal horn or pass through it to enter ascending tracts. The afferent fibers mediating the stretch reflex pass through the dorsal horn to synapse on motor neurons and interneurons in the ventral horn. In the thoracic and upper lumbar region, the intermediate zone also contains the nucleus dorsalis, which receives input from the muscle spindles and joint receptors. This information is relayed ipsilaterally in the spinal white matter in the posterior spinocerebellar tract.

Figure 6: Transverse section of spinal cord illustrating descending and ascending white matter tracts and gray matter lamina.

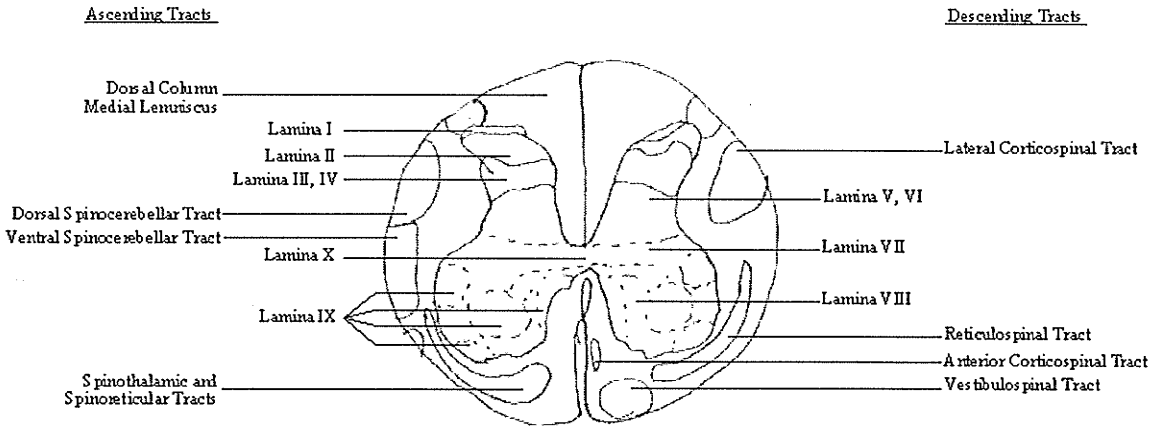

White matter

The white matter of the spinal cord is divided into three major regions; the posterior, lateral, and anterior funiculi. The white matter is comprised of the myelinated axons of the neurons in the cord. These axons tend to run together in what are called

tracts, each carrying a specific type of information or involved with a certain type of function. For example, in the dorsal aspect of the cord runs the ascending tract called the posterior column medial lemniscus tract (PCML), which is further divided into the fasciculus cuneatus and the fasciculus gracilis. These tracts convey information regarding position and movement, as well as touch and vibration sense. The lateral aspect of the cord, from dorsal to ventral, contains the posterior spinocerebellar tract which conveys information important for mediating smooth control of movement, and the spinothalamic tract which is involved primarily in pain and temperature sensation, for example. There are a number of other ascending tracts as well, such as the spinotectal and spinoolivary tracts within the lateral funiculi. The clinically important descending tracts of the white matter include the lateral corticospinal tract which is involved in voluntary movement, and the rubrospinal tract for facilitating flexor motor neuron activity, and the lateral vestibulospinal tract which is important in facilitating extensor muscle tone to maintain upright position and balance. There are other descending tracts as well, such as the tectospinal tract or reticulospinal tracts. Close to the gray matter there are propriospinal tracts in the white matter, in which intraspinal axons run in a rostral-caudal direction and integrate information between segments into reflex patterns. This results in both crossed and uncrossed pathways that connect neurons in one part of the spinal cord with those in others. These propriospinal tracts play a role in reflex activity, cyclic patterns of activity, and pattern generation within the spinal cord.

Relevant white matter pathways

The following ascending and descending tracts are expected to be recruited during participation in the tasks in my studies. Therefore, a detailed description of the pathways

is given here (for a complete review of the following ascending and descending tracts, see Goshgarian, 2003).

Ascending tracts

The posterior columns consist of the medially located fasciculus gracilis and the laterally located fasciculus cuneatus. Each contains myelinated sensory fiber axons from the dorsal roots. The axons within the posterior columns have a somatotopic organization where fibers originating caudally (lumbar and sacral cord segments) are located medially in the fasciculus gracilis and those originating more rostrally (thoracic and cervical segments) have axons in the fasciculus cuneatus. The axons ascend uncrossed in the posterior columns to synapse with second-order neurons in the gracile and cuneate nuclei in the medulla. Axons from these nuclei travel rostrally to decussate and ascend as the medial lemniscus. These synapse in the ventral posterolateral nucleus of the thalamus on neurons that send their axons to the cortex. The posterior columns transmit information concerned with the position and movement of the extremities.

Situated within the lateral funiculi, the spinothalamic tract is well known for its transmission of pain and temperature sensation, however, this tract also conveys information regarding less discriminative tactile sensation such as light touch and firm pressure. The fibers which give rise to the spinothalamic tract enter the dorsal horn through the medial division of the dorsal rootlets, and synapse on tract cells in the nucleus proprius in lamina IV and V-VI. The axons cross the midline in the ventral white commissure and continue through the ventral horn to ascend in the spinothalamic tract in the ventrolateral funiculi. The spinothalamic tracts are somatotopically organized such that the sacral fibers run laterally and the cervical fibers run medially. Within the brain,

the spinothalamic tract axons synapse in the ventral posterolateral nucleus and the posterior intralaminar nuclei of the thalamus.

Proprioceptive information of the lower limbs is obtained via receptors of the muscle spindles, joints and tendons and is relayed via the spinocerebellar tract. The neurons of the dorsal spinocerebellar tract originate in the nucleus thoracicus, or Clarke's column, which is located in lamina VII at the T1 through L3 levels. These ascend ipsilaterally and enter the cerebellum via the inferior cerebellar peduncles. These neurons also provide proprioceptive information from the lower limb to the ventral posterolateral nucleus of the thalamus through nucleus z in the medulla. The ventral spinocerebellar tract fibers arise from the ventral horn of the lumbosacral segments and the base of the dorsal horn. They cross initially and run close to the cord surface as far as the midbrain, where they turn into superior cerebellar peduncles to enter the cerebellum. They recross within the cerebellar white matter, and so both the dorsal and ventral spinocerebellar tracts provide ipsilateral proprioceptive information to the cerebellum from the lower limbs. The primary afferent fibers that enter the cord from the lumbar or sacral roots bifurcate into ascending and descending branches in the dorsal funiculus. It is the ascending branch that travels up the spinal cord and terminates in the nucleus dorsalis. The descending branch of the primary afferent terminates in gray matter to establish connections for spinal reflexes.

Descending tracts

A number of cortical structures give origin to the descending tracts, which form motor pathways between some of the motor centers in the brain and the motor neurons in the ventral horn of the spinal cord. Brain structures that are motor in function include

Brodmanns areas 4 and 6 in the primary motor cortex, the red nucleus, substantia nigra, corpus striatum, cerebellum, vestibular nuclei, inferior olivary nucleus, midbrain tectum, and reticular formation. About one third of the fibers arise from the motor cortex of the precentral gyrus (Brodmanns area 4), the remainder primarily from premotor and other precentral areas. The descending pathways are classified as either pyramidal or extrapyramidal pathways. The pathway involved in the control of voluntary movement is the corticospinal tract. The corticospinal neurons are located in the cerebral cortex and their axons descend to terminate within the spinal cord, either directly on lower motor neurons or on interneurons within the gray matter. After passing into the medullary pyramids, approximately 80% of the corticospinal fibers decussate to form the lateral corticospinal tract, which is in the dorsal portion of the lateral funiculus. Within the gray matter, corticospinal axons terminate in lamina IV-VII in the dorsal and ventral horns and in the intermediate gray matter. Some corticospinal neurons synapse directly with motor neurons in lamina IX, however, the majority synapse with interneurons. This distribution of termination of corticospinal neurons therefore contributes to activity in both the ventral and dorsal horns. The somatotopic organization of these tracts has the fibers controlling lumbar and sacral muscles running in the lateral aspect of the tracts, while fibers controlling cervical muscles run ventromedially. Approximately 10% of the corticospinal fibers do not decussate but rather descend in the spinal cord ipsilaterally in the anterior corticospinal tract within the anterior funiculus of the spinal cord white matter. These fibers cross the midline in the anterior white commissure to terminate in the ventromedial portion of the contralateral ventral horn.

A number of subcortical structures in the brain give rise to the descending tracts that connect to lower motor neurons that are concerned with automatic movements, such as walking, posture, and movement of muscle groups. The rubrospinal, tectospinal, vestibulospinal, reticulospinal and olivospinal tracts do not pass through the pyramid of the medulla as they descend through the brainstem into the spinal cord and so are called extrapyramidal pathways. The major nonpyramidal pathways located in the anterior funiculus of the spinal cord are the reticulospinal tracts and the vestibulospinal tract. These pathways innervate axial musculature and control muscle tone, reflex activity, posture, and balance. The vestibulospinal tract arises from the lateral vestibular nucleus (Dieter's nucleus) in the rostral part of the medulla and descends without decussating to control the muscles which maintain normal posture and balance. The reticulospinal tracts arise from the pontine and medullary reticular formation and are concerned with regulating automatic movements in locomotion.

Motor neurons

The fibers of the corticospinal tract synapse on motor neurons within the ventral horn. These neurons give rise to the nerve fibers that leave the cord by way of the anterior roots and innervate the skeletal muscle fibers. These neurons are composed of the larger (α) and smaller (γ) motor neurons (see Gordon and Ghez, 1991). The α motor neurons give rise to large type Aα nerve fibers that innervate extrafusal muscle fibers. The α motor neurons are important in mediating individual muscle movements. The γ motor neurons are much smaller neurons that transmit impulses through type Aα fibers to small skeletal muscle fibers called intrafusal fibers. The γ system is important in setting the gain of the spindles and also for maintaining muscle tone through supraspinal input.

Stimulation of a single nerve fiber can excite from as few as three to as many as several hundred skeletal muscle fibers, and these fibers are collectively called a motor unit. Corticospinal tract fibers terminate predominantly on interneurons. The signals from the corticospinal tract are integrated in an interneuron pool with signals from other spinal tracts or spinal nerves before they synapse with motor neurons to control the skeletal muscle.

The control of muscle function requires both the excitation of the muscle by the motor neurons as well as continuous sensory feedback of information from each muscle to the spinal cord, giving the status of the muscle at each instant. This is accomplished in two ways: the muscles and their tendons are supplied with two types of sensory receptors. The muscle spindles are distributed throughout the middle of the muscle and they send information to the nervous system about either the muscle length or rate of change of its length. The golgi tendon organs are located in the muscle tendons and transmit information about tendon tension or the rate of change of tension. These receptors transmit information to the spinal cord, which relays the information to the cerebellum and the cerebral cortex. The primary ending of a muscle spindle is supplied by a large myelinated fiber classified as group Ia fiber. This primary ending is responsive both to the rate of stretch of the spindle (dynamic response) and to the new length (static response). The secondary endings are supplied by afferent fibers of intermediate size, the group II fibers (Gordon and Ghez, 1991). Golgi tendon organs are located in the connective tissue of the muscle tendons and aponeuroses, and their terminals intertwine among bundles of collagen. Their afferent fibers are large myelinated axons classified as group Ib fibers. They respond at a high threshold to passive muscle stretch, but at a low

threshold to the contraction of muscle fibers ending on the tendon containing the receptor.

The spindle is built around the small intrafusal muscle fibers that are attached to the surrounding large extrafusal skeletal muscle fibers. The central region of each of these intrafusal fibers has either no or few actin and myosin filaments and therefore does not contract. The end portions that do contract are excited by small γ motor nerve fibers that originate from the small γ motor neurons (Gordon and Ghez, 1991). When the midportion of the spindle stretches, the receptor is stimulated. Thus, the muscle spindle receptor can be excited in two ways. By lengthening the whole muscle, the midportion of the spindle will stretch and therefore excite the receptor. Even if the length of the entire muscle does not change, contraction of the end portions of the spindle's intrafusal fibers will stretch the midportions of the fibers to excite the receptor. When there is even a slight amount of nerve excitation under normal conditions, the muscle spindles emit sensory nerve impulses continuously. Stretching the muscle spindles increase the rate of firing, whereas shortening the spindle decreases this rate of firing (Gordon and Ghez, 1991). Thus, the spindles can send to the spinal cord either positive signals, that is, an increased number of impulses indicates an increasing stretch of a muscle, or negative signals, a decreased number of impulses below the normal level indicates that the muscle is being unstretched.

The muscle spindle also plays a role in voluntary movement. Whenever signals are transmitted from the motor cortex or from any other area of the brain to the α motor neurons, in most instances, the γ motor neurons are stimulated simultaneously, an effect called co- activation of the α and γ motor neurons (Gordon and Ghez, 1991). This causes

both the extrafusal and the intrafusal muscle fibers to contract at the same time. The purpose of contracting the muscle spindle fibers at the same time that the large skeletal muscle fibers contract is twofold: first, it keeps the length of the receptor portion of the muscle spindle from changing and therefore keeps the muscle spindle from opposing the muscle contraction. Second, it maintains damping function of the muscle spindle regardless of change in muscle length.

Reflexes

An example of muscle spindle function at work is seen during the stretch reflex (see Gordon and Ghez, 1991). When a muscle is stretched, excitation of the spindles causes reflex contraction of the large extrafusal muscle fibers of the homonymous and synergistic muscles. The type Ia nerve fiber in the muscle spindle enters the dorsal root of the spinal cord and synapses directly with motor neurons in the ventral horn that send nerve fibers back to the homonymous muscle. This monosynaptic pathway allows a reflex to occur with the shortest possible delay back to the muscle after excitation of the spindle. Some type II fibers from the secondary spindle endings also terminate monosynaptically with the anterior motor neurons. However, most of the type II fibers (and many collaterals from the Ia fibers from the primary endings) terminate on interneurons in the cord gray matter, and these transmit signals to the motor neurons. Because these connections are polysynaptic they are of longer duration.

A negative stretch reflex also occurs when a muscle is suddenly shortened. If the muscle is taut, a sudden release of the load on the muscle that causes the muscle to shorten will elicit reflex muscle inhibition rather than reflex excitation. This negative stretch reflex acts to oppose the shortening of the muscle in the same way that the

positive stretch reflex opposes the lengthening of the muscle. The purpose of the stretch reflex then serves to maintain the length of a muscle and to provide the damping function that prevents jerkiness of movements.

The flexor reflex causes flexion of a limb in response to a sudden painful stimulus, which serves to withdraw the limb away from the stimulus to avoid tissue damage. A crossed extensor reflex can also occur which accompanies the flexor reflex by promoting extension of the contralateral limb in response to a stimulus that has caused flexion in a limb, which serves to keep the person from falling over. These reflexes are suppressed as a result of activity in descending tracts in healthy people, but can be troublesome for spinal cord injured patients due to lack of descending modulation.

Blood Supply to the Spinal Cord

The spinal cord is supplied by three branches of the verterbral arteries and from those by a number of radicular arteries that arise from segmental vessels (see Goshgarian, 2003). The three main arteries are the anterior spinal artery and a pair of posterior spinal arteries. The anterior spinal artery lies on the anterior surface of the cord and gives rise to the sulcal arteries that enter the cord through the anterior median fissure to supply the anterior two thirds of the cord. The posterior spinal arteries descend on the posterior surface of the cord medial to the posterior roots, and supply the posterior one third of the cord. The lateral funiculi are supplied by an anastomosis between the anterior and posterior spinal arteries called the arterial vasocorona.

The anterior spinal artery is most commonly formed in the region of the foramen magnum or upper cervical spine from branches of the vertebral arteries. The radicular arteries accompany each spinal nerve root, with some serving as tributaries to the anterior

spinal artery. The artery of Adamkiewicz is recognized as the largest and most constant radicular artery in the region. It is an unpaired artery located on the left side in two thirds of all cases. It is usually found at the spinal root of L1 or L2 and is a major source of blood flow to the anterior spinal artery region. The anterior spinal artery gives rise to a number of sulcal branches that enter the anterior median fissure and then divide into left and right branches to perfuse the gray matter and central white matter. The arterial vasocorona surrounds the spinal cord to provide another source of blood flow. Through these two arterial systems, the anterior spinal artery serve the anterior and lateral horn, the base of the dorsal horn and the central gray matter, and the anterior and lateral funiculi.

The paired posterior spinal arteries form a network of blood vessels. Rostrally, the posterior spinal arteries arise from the vertebral or the posterior inferior cerebellar arteries. Caudally, they arise from radicular arteries. In the cervical region, the blood flow is directed caudally, but in the thoracic and lumbar spine blood flows in the rostral direction. The posterior spinal arteries supply the posterior columns and lateral aspects of the dorsal horns.

The venous system follows a similar pattern to that of the arterial system. An anterior spinal vein is fed by sulcal veins and accompanies the anterior spinal artery. A single prominent median posterior draining vein is located near the posterior median septum. Radicular veins drain the anterior and posterior median veins. As is the case with radicular arteries, some of these veins are more prominent than others; in the lumbar region the most prominent vein is the vena radicularis magna. A network of veins called the internal vertebral venous plexus courses in the epidural space.

Spinal Cord Injury

Lesions of the spinal cord can result from trauma, degenerative or demyelinating disorders such as amyotrophic lateral sclerosis (ALS) or syringomyelia, tumor or infection, or vascular insult. Spinal cord transection can result from penetrating wounds, or by spinal fracture or dislocation as seen in traffic accidents or diving accidents (Byrne et al, 2000). A complete transection results in the total loss of sensation and voluntary movement below the lesion site, however, a complete transaction is a rarity. If a lesion is at the upper cervical level, tetraplegia results, with both upper and lower limbs affected. If a lesion is below the cervical segments, paraplegia results, with only the lower limbs affected. Lesions affecting the lower motor neurons result in a flaccid paralysis of the affected muscles, impaired tendon reflexes and progressive atrophy of the muscles. This is referred to as a lower motor neuron syndrome. Lesions in the cortex or cerebral hemisphere, the brainstem, or in the descending white matter tracts of the spinal cord result in an upper motor neuron syndrome. The symptoms of an upper motor neuron lesion include paralysis and spasticity with exaggerated tendon reflexes.

The basis for loss of function after injury is rooted in the absence of nerve impulse conduction through the lesion in the injured white matter (see Borgens, 2003 for a review). As the white matter tracts of the cord are the processes of the nerve cell bodies that carry the sensory and motor information to and from the brain and the rest of the body, disruption of these tracts results in a deficit or impairment of the function that tract was carrying. Should the spinothalamic tract be lesioned, for example, the sensation of pain and temperature would be impaired from areas innervating the cord below the injury site. Damage to gray matter causes a more local impairment. For example, the motor

unit that supplies a muscle, especially the large muscles of the limbs, is supplied by motor neurons contained in several contiguous spinal cord segments. A lesion to an individual segment of the cord, then, would normally cause muscle weakness or paresis, rather than paralysis. Damage to gray matter, therefore, results in an area of weakness whereas damage to a white matter tract results in a clearer separation of functioning and nonfunctioning sensory and/or motor abilities.

Spinal cord injury also causes damage to involuntary functions such as voiding reflexes, breathing, and control of blood pressure. The compartmentalization of involuntary function of the autonomic nervous system can be problematic. For example, the vagal nerve is part of the parasympathetic system that exits the vertebral column within the neck region. The sympathetic counterpart to this is located at thoracic cord levels. Therefore, an injury in the cervical cord would anatomically separate the two circuits that usually work together to balance heart activity. This disconnection results in autonomic dysreflexia, which is manifest as a dangerously uncontrolled spiking of blood pressure due to unopposed sympathetic stimulation. Similarly, bowel and bladder function are modulated by descending supraspinal inhibition to control voiding. The interruption of coordination of reflexes for voiding can cause incontinence and high pressure voiding. Breathing is controlled by the diaphragm with the aid of accessory musculature, the intercostal rib muscles and abdominal muscles. The diaphragm is innervated by C3-5, and thus people with injuries C4 and distal will retain independent breathing, however impaired due to the latter two muscles loss of innervation. Injury to C3 and above results in diaphragm paralysis and therefore the use of a ventilator is required to assist breathing.

Initially following injury, there is usually a period of spinal shock that can last from a few days to several weeks. In this time, all somatic and visceral reflex activity is absent. In suprasacral injuries these reflexes return, often accompanied by the spasticity of muscles and exaggerated tendon reflexes. The lower limbs can assume a position of flexion because of vestibulospinal tract damage, as this tract is involved in extensor stimulation. Damage to the cord is usually confined to a single segment and the condition of the cord immediately adjacent to the injury is usually unaffected for the period of spinal shock. However, injury to the affected cells is followed by cell death in the gray matter and secondary axotomy and wallerian degeneration in the white matter (Tator, 2002). Secondary injury results from the cell membrane being damaged. Ionic derangement is the result of the cell membrane damage, causing the mixing of ions across the membrane, specifically unregulated entry of Ca^{++} into the neurons or axons. This ion imbalance alone is known to destabilize the cytoskeleton, degrade microfilaments, destabilize the integrity of the membrane and turn off axoplasmic transport (Borgens, 2003). At the same time, Na^{+} is also moving in the wrong direction, as the Na^{+}/Ca^{++} exchanger begins to work in reverse due to the effects of the elevated Ca^{++} levels. In addition to this, glucose and oxygen deprivation occurs which contributes to the tissue damage during secondary injury (Borgens, 2003).

Spinal Cord Injury Assessment

The location of a lesion can be determined based on a patient's reflexes and neurological examination. Stretch reflexes of the biceps (C5/6), triceps (C6-8), quadriceps (L2-4), and gastrocnemius (S1/2) can be used to determine the general condition of the spinal nerves and segments. Absent reflexes suggest a lower motor

neuron disorder or damage at that level, whereas exaggerated reflexes suggest an upper motor neuron disorder or damage above that level. A commonly used measure is the American Spinal Injury Association (ASIA) Impairment scale (2000), which utilizes the distribution of dermatomes and myotomes to indicate the lesion location. The ASIA assessment involves systematically testing specific dermatomes and myotomes to determine the level and extent of the spinal cord injury. This is accomplished by calculating left and right side sensory and motor scores. These four scores combined give the neurological level which is an indication of the most caudal segment of the cord with normal preserved function on both sides of the cord. The levels are determined by testing a key sensory point within each of the 28 dermatomes on each side of the body, and a key muscle within each of 10 myotomes of each side of the body. Sensation is tested by sensitivity to pin prick and to light touch and is scored on a three-point scale corresponding to absent, impaired, or normal sensation. The strength of key muscles is scored on a six-point scale ranging from total paralysis through normal active full range of movement against resistance. The classification of 'incomplete' or 'complete' is made based on whether partial preservation of sensory and/or motor function is found below the neurological level and includes retained function of the lowest sacral segment. A 'complete' injury classification is used when there is an absence of sensory and motor function in the lowest sacral segment. Thus, retained sensation or voluntary contraction of the anal sphincter determines the complete versus incomplete classification.

The ASIA Impairment Scale, however, further distinguishes the injuries into the following categories. ASIA A represents a complete injury, with no sensory or motor function preserved in the sacral segments. This ASIA A classification is based on testing

of sensory (light touch and pin prick) and motor (strength) function only, and does not take into account possible retained function of other spinal tracts. ASIA B represents an incomplete injury with sensory but not motor function preserved below the neurological level and includes the lowest sacral segment. ASIA C represents an incomplete injury with motor function preserved below the neurological level and more than half of the key muscles involved have a score of less than three. ASIA D represents an incomplete injury with motor function preserved below neurological level and at least half of the key muscles have a muscle score greater than or equal to three. ASIA E represents normal sensory and motor function.

Although the ASIA Impairment Scale is useful in that it is an internationally recognized method of assessing the extent of damage in the spinal cord, there are a number of issues that require attention. One issue with ASIA is that it is a physical examination which requires a conscious, willing and able participant in the examination. This may not always be the situation. In addition, a patient may be inhibited by factors such as pain or impaired by unrelated physical issues. Regardless of patient participation, some myotomes are not clinically testable with this method, such as the C1 through C4, T2 through L1, and S2 through S5 segments. For these segments, the motor level can only be assumed the same as the sensory level. For the myotomes that can be tested with this method, the scoring of muscle strength is subjective. When a score of three is given, it is assumed that the muscle has intact innervation by the more rostral of the innervating segments, as long as the next rostral segment has a score of five. This scoring is based on the examiner's judgment, and although this is a subjective measure, the ASIA examination has good inter-rater reliability. Therefore, given that the patient is able to

participate in the examination and the best possible estimation is made regarding the sensory and motor levels, a neurological level can be assessed. However, no information is obtained regarding the condition of the cord below the most caudal functioning segments.

Recovery of function strategies

Injury in the CNS is catastrophic because of its inability to repair itself. This is because of a lack of sustained nerve regeneration and failure to form new functional synapses. Research concerning possible treatment for spinal cord injury is advancing in a number of different directions (Young, 2000; Tator, 2002; Brunelli, 2005). Restoring, repairing, and regenerating are a few of the strategies currently under investigation, as described in Borgens (2003). Restoration aims to use some of the anatomically spared tissue remaining after an injury. Even in a seemingly complete neurologic injury, there may still be a small amount of spared, although nonfunctioning, white matter. The white matter is nonfunctional because of its inability to conduct nerve impulses, likely due to loss of myelination, ionic derangement and autoimmune attack. The goal of restoration is to encourage nerve impulse conduction in the spared white matter. One such method involves the use of a fast potassium channel blocker, 4-aminopyridine (4-AP), which is theorized to improve conduction through white matter, has shown some promise in clinical trials (Shi et al., 1997), however large scale studies have failed to show significant improvements (DeForge et al., 2004). This failure to provide significant outcome differences is likely due to the lack of a sensitive measure to objectify change. Repair strategies aim to reverse or stop progressive destruction of the neural mechanisms at the lesion site. These strategies are geared to interfere with the processes of secondary

injury as they occur. The use of a Ca^{++} channel blocker in an attempt to ward off the destructive sequence of events that follow the unregulated movement of these ions is one such strategy (Pointillart et al., 2000). Regeneration strategies include peripheral nerve bridges, transplantation of fetal nervous tissue onto spinal cord lesions (Reier et al., 1988, 2002a,b) or insertion of stem cells (Vescovi and Snyder, 1999). These strategies will only be of use if they are able to not only survive the transplantation and form new cells, but also reconnect with existing structures to form new pathways for nerve impulse conduction. One other promising area of research in the hope of spinal cord injury recovery is the idea of inhibiting the innate inhibitors of nerve regeneration (Schwab and Bartholdi, 1996).

Specific Objectives

The purpose of this dissertation is to contribute to the development of spinal fMRI as a tool for investigating spinal cord physiology. To this end, I propose to test the efficacy of spinal fMRI during motor stimulation of the lower limbs with a healthy and spinal cord injured population. A number of issues need to be addressed: In addition to any information obtained regarding the neuronal activity of the healthy and injured spinal cords during the motor tasks, establishing spinal fMRI also involves the improvement of the imaging method with the use of sagittal orientation, determining if the motor study with the spinal cord injured people shows results comparable to the ASIA scale classification for each participant and in agreement with their recorded motor abilities, the comparison of the healthy and injured groups to determine whether spinal fMRI is capable of detecting differences between the two groups, and to determine the optimal analysis methodology for spinal fMRI. Details for these objectives follows.

Part 1: Spinal fMRI with healthy subjects

This work was submitted as MSc equivalent for transfer to PhD program.

Rationale: It is unknown if spinal fMRI is capable of detecting neuronal actvity in response to a lower limb movement task. Previous spinal fMRI studies have focused on either the upper limbs for motor activity studies or the upper and lower limbs for sensory activation studies, as these impart less movement to the trunk of the body and therefore less motion artefacts. A lower limb movement study has not yet been undertaken as the development of spinal fMRI is in its infancy and not all areas have been investigated to date. Movement of the lower limbs is understandably an undesirable first choice for developing spinal functional imaging, as the problems associated with motion during fMRI are expected to be substantial. An MR compatible pedaling device was specifically designed for investigating lower limb movement tasks in this study. This study, therefore, aims to test the pedaling device, to determine if the neuronal activity observed corresponds to the relevant known physiology, and to assess whether spinal fMRI is sensitive enough to detect neuronal differences between different movement tasks.

Hypothesis: Spinal fMRI will be able to detect appropriate sites of neuronal activity in the lumbar spinal cord of healthy volunteers with the use of the pedaling device and will be sufficiently sensitive to detect a difference in areas of neuronal activity elicited during participation in active and passive movement tasks.

Part 2: Development of improved spinal fMRI with sagittal slices

Rationale: Spinal fMRI has a serious weakness that needs to be amended in order for spinal fMRI to become a valuable clinical and research tool. The majority of spinal fMRI studies have been completed with images in the axial orientation, resulting in a very

small area of cord imaged. Increased areas of viewing and optimal efficiency of magnet time use are great improvements for spinal fMRI both clinically and for research purposes. Attempts at a larger view have been made in the past with sagittal orientation imaging but these attempts have met with poor results. The slice thickness used in the previous studies has been too large, and the resulting images therefore suffer from partial volume effects from a low sensitivity to neuronal activity related signal changes. In order for spinal fMRI to be practical for research and clinical use, a larger extent of cord must be observed, but adequate temporal resolution must be preserved. A method of obtaining such images is proposed. The information obtained in this study is two-fold. In addition to testing the sagittal imaging method, further validation of the spinal fMRI technique is obtained, with imaging of the cervical spinal cord during thermal stimulation.

Hypothesis: The proposed sagittal imaging method will be effective in increasing the extent of spinal cord that can be imaged at one time with continued high resolution. The neuronal activity observed will correspond to known physiology in response to thermal stimulation.

Part 3: Spinal fMRI of spinal cord injured subjects during a motor task

Rationale: Spinal fMRI has proved useful in detecting neuronal activity in healthy and injured subjects during sensory stimulation and in healthy subjects while performing a motor task. However, spinal fMRI of the injured spinal cord during a lower limb motor task is unexplored and requires investigation. This study will provide information regarding neuronal activity elicited during an active motor task and during a passive motor task, as well as provide information for determining differences in signal intensity changes and patterns of neuronal activity in subjects with incomplete and complete

injuries and for comparison with previously collected data with healthy volunteers. Individual data sets will be analyzed to see if spinal fMRI is sensitive enough with this method and imaging technique to be used as clinical diagnostic tool.

Hypothesis: Spinal fMRI will be able to detect neuronal activity below the site of injury in the lumbar spinal cord of spinal cord injured participants during motor activity, and these differences in neuronal activity will correspond with the task performed and with the extent of the volunteers injury.

Paper 4: Cluster Analysis of Spinal fMRI of a Leg Motor Task

Rationale: Paradigm dependent statistical methods such as correlation analysis or t-tests are commonly used in analyzing fMRI data. A statistical analysis method that is independent of the paradigm is desirable when you do not want to impose any bias on the data. Clustering is one such method used to supplement correlation or t-test analyses. Clustering groups pixels together based on their signal intensity time courses or magnitude of signal intensity change from baseline. These clusters can be displayed to demonstrate their locations and thereby identify spatial relationships that exist between the pixels. Spatial and temporal relationships between pixels provide confidence that the mechanisms contributing to the signal intensity changes are related and also help to identify these mechanisms. Therefore, cluster analysis can be used to discover structures in data without the requirement of fitting to a study paradigm and without providing any explanation as to their cause.

Hypothesis: Cluster analysis of spinal fMRI data will help to identify and separate true positive activations from false positive activations.

Contributions to multi-authored papers:

Paper 1) Involved in study design, data acquisition, data analysis, manuscript preparation.

Paper 2) Involved in study design, data acquisition, data analysis, manuscript preparation.

Paper 3) Involved in study design, data acquisition, data analysis, manuscript preparation.

Paper 4) Involved in study design, data acquisition, data analysis, manuscript preparation.

FMRI of the lumbar spinal cord during a lower limb motor task

J. Kornelsen[1], P. W. Stroman[1,2]

[1]Department of Physiology, University of Manitoba, Winnipeg, Manitoba, Canada.
[2]Institute for Biodiagnostics, National Research Council of Canada, Winnipeg, Manitoba, Canada.

Running Title: Spinal fMRI of lumbar motor activity

Word count: 2659 words and 3 figures

Correspondence:

Patrick W. Stroman, PhD
Institute for Biodiagnostics
National Research Council of Canada
435 Ellice Avenue
Winnipeg, Manitoba, Canada
R3B 1Y6
phone (204) 984-6564
fax (204) 984-7036
Patrick.Stroman@nrc.ca

In: Magnetic Resonance in Medicine 52:411-414 (2004)

Submitted as MSc equivalent for transfer to PhD program

Abstract:

This study applies spinal fMRI to the lumbar spinal cord during lower limb motor activity. During active ankle movement, activity was detected in the lumbar spinal cord motor areas and sensory areas bilaterally. During passive ankle movement, activity was detected in the motor and sensory areas in lower lumbar spinal cord segments, and motor activity in higher lumbar spinal cord segments. Spinal fMRI detects patterns of activity consistent with known physiology and can be used to reliably assess activity in the lumbar spinal cord during lower limb motor stimulation. This study affirms spinal fMRI as an effective tool for assessing spinal cord function and increases its potential as a clinical tool.

Key words: Spinal fMRI; spinal cord; motor; human; imaging

Introduction

Previous work with functional magnetic resonance imaging of the spinal cord (spinal fMRI) has shown that it is a reliable tool for assessing condition and localizing activity in both healthy and injured spinal cords (1-4). To date, spinal fMRI has proven to be useful in investigating sensory and motor activity in the cervical spinal cord and sensory activity in the lumbar spinal cord. The present study is the first to apply spinal fMRI to the lumbar spinal cord during lower limb motor activity.

Spinal fMRI reveals neuronal function indirectly by way of changes in blood flow and blood oxygen levels that occur near metabolically active gray matter, as with conventional fMRI of the brain (5-7). Blood oxygen-level dependant contrast is linked to the metabolic activity that occurs in active neuronal tissues. When neuronal firing rates increase, nerve cell bodies take up more oxygen. To compensate, an over-abundant increase in blood supply to neurons occurs resulting in a decrease in the concentration of deoxygenated hemoglobin. Deoxygenated hemoglobin in blood acts as a MR contrast agent that causes the MR signal to decay quickly. At the time of recording, the MRI signal is stronger from metabolically active areas because the signal has not decayed as quickly as in the adjacent less active tissues. The MR image intensity increases as the spiking rate increases (8). However, the more dominant contrast mechanism in spinal fMRI is due to signal enhancement from extravascular water protons (SEEP) which is more closely related to the blood flow increase to the active neural tissues (9-11). When blood flow increases, the intravascular pressure also increases, particularly on the arterial side of the capillary system. This pressure change alters the normal fluid balance and increases movement across blood vessel walls into extracellular space, resulting in a

slight increase of water protons near active neural tissues. This is a normal physiological process and serves to compensate for the absence of lymphatics in the central nervous system. Spinal fMRI is able to detect both primary neuron activity as well as interneuron activity in spinal cord gray matter. The sensitivity to primary neuron and interneuron activity allows for mapping of sensory and motor activity as well as reflex activity.

With spinal fMRI, stimulation of specific dermatomes has been shown to map to the corresponding spinal cord segments, and different types of sensory stimulation have mapped to the analogous gray matter regions (1,2,4). Previous work has focused on imaging of the cervical spinal cord during sensory and motor stimulation of the hands, as well as lumbar spinal cord imaging during sensory stimulation of the lower leg. Results have shown activity in the cervical cord dorsal horn and the lumbar cord dorsal horn, and these areas correlate to sensory stimulation of the hand and lower leg, respectively. In a study involving a motor task and sensory stimulation of the hand, spinal fMRI also proved reliable in displaying laterality and spread of activity in the spinal cord (4). Signal intensity changes in the lumbar cord have also been observed to depend on the temperature of cold stimulation, and have shown marked differences between innocuous and noxious cold stimulation (1,3). Recently, the spinal fMRI method has been applied to the study of injured spinal cords (1,3,12). These results are in agreement with known physiology and electrophysiology (13). Spinal fMRI is therefore able to detect neuronal activity in the appropriate spinal cord segments as well as specific gray matter areas in healthy spinal cords, and can demonstrate areas of impaired and preserved activity in spinal cord injured patients.

The implications that follow from the findings are not only important for understanding normal sensory/motor function and reflexes, but also for comprehending impaired function. The information attained by spinal fMRI regarding spinal cord condition is invaluable for designing and assessing rehabilitation programs and for evaluating potential recovery of function in those with either incomplete or complete injuries. In addition, spinal fMRI can provide information that self-report and physical examination techniques are unable to acquire, such as where the cord is preserved. Significantly, this information can be obtained despite a patients' inability to report a sensation or produce a movement. The purpose of the present study is to test the efficacy of spinal fMRI during motor stimulation of the lower limbs and further establish spinal fMRI as a valuable clinical and research tool by expanding the repertoire of stimuli and responses that can be assessed.

Methods

Six healthy subjects (5 male, 1 female) were studied in a 1.5 T GE Signa Horizon LX clinical MR system. Subjects were supine on a GE phased-array spine receiver coil, with their feet secured to a MR-compatible pedaling device specifically designed for the study. The device consisted of two pedals with adjustable straps over the toes, and over and below the ankle, which was secured on a base designed to fit the MR bed (Figure 1). The device allowed for alternating rhythmic flexion and extension movements of the ankles. The device was custom made to assist in keeping the movements alternate and equal. Placing a cushion under the knee stabilized the thighs and reduced movement of the upper body thereby minimizing motion effects. The study was reviewed and

approved by our Institute's Human Research Ethics Board, and informed consent was obtained from all participants before entering the magnet room.

Spinal fMRI was carried out in a block design with two stimulation periods. During active pedaling, the subject moved the pedals with their feet in the alternating pedaling motion. During passive pedaling, the experimenter moved the pedals manually while the subject was asked to relax and let their feet be moved by the pedals. Each subject completed two series of active pedaling and one series of passive pedaling in each study. Images were acquired repeatedly during alternating rest and stimulation periods, resulting in a total of 56 time points recorded.

Functional time course data were obtained using single-shot fast spin-echo imaging with sets of eight contiguous slices from approximately the 3rd sacral spinal cord segment (S3), and spanning the entire lumbar spinal cord, up to the 1st lumbar spinal cord segment (L1). This required a repetition time of 11 seconds. The single-shot fast spin-echo method employed for this study was a product sequence developed by GE, without any modification. The matrix was 128 x 128 with an echo time of 42.3 msec, and an echo train length of 72 with the 8th echo at k-space center. Slices were oriented transverse to the spinal cord and the thickness was adjusted so that every second slice was aligned with either the intervertebral discs or centers of the vertebrae, spanning the entire lumbar cord. Adjusting the slice thickness accordingly resulted in a slice thickness range of 7.0 to 7.5 mm. Spatial saturation pulses were applied to eliminate signal from surrounding areas to avoid aliasing, and to reduce motion artefacts arising from regions anterior to the spine. A reference image was obtained with the first subject to ensure that the same extent of the spinal cord was being imaged with all subsequent subjects.

Custom-made analysis programs written in MatLab software (The Mathworks Inc. Natick MA) were used to analyze the individuals' data using a correlation method with a p-threshold of 0.05. Images were registered to reduce the effects of motion by means of rigid-body translation and rotation. However, only a small sub-region of the images spanning the spine was used for the registration process to avoid influence from changes in the surrounding muscle tone. A region of interest (spinal cord white and gray matter) was outlined manually for each slice. The correlation between the time-course for each pixel and a box-car reference paradigm was then used to create individual activation maps, as in previous studies (1,3,4).

After all studies had been completed, the individual activation maps were superimposed to generate combined activation maps of the 12 active runs and 6 passive runs, from the 6 subjects. The resulting maps were thresholded to indicate activity only where it was duplicated in two or more series and these activations were colour coded to indicate level of overlap. The signal intensity changes were calculated and time courses were plotted.

Results

During active pedaling, activity was detected in the lumbar spinal cord ventral horn and dorsal horn bilaterally (Figure 2). Activity was observed in the left ventral and dorsal regions of spinal cord segments S3 and S2, in the bilateral ventral horns in L5, and in the bilateral ventral and dorsal horns in L4 through L1, with increased activity in L2 and L1. The amount of activity increased at higher levels of the cord. The amount of overlap ranged from a minimum of two (yellow) up to a maximum of five (red) active

pixels at one location. The average signal intensity change was 11.9% ± 1.0% (mean ± standard error of the mean) averaged over the duration of all active conditions (Figure 3).

During passive pedaling, activity was detected in the central region and dorsal horn in lower lumbar spinal cord segments and ventral activity was detected in higher lumbar spinal cord segments. Activity was observed in the bilateral dorsal horns in the S3 and S2 spinal cord segments, in the right ventral and central regions of the spinal cord segment L4, and in the bilateral ventral horns in the L3 through L1 spinal cord segments, with increased activity in L1. More activity was observed at higher spinal cord segments than in lower spinal cord segments for both active and passive maps. The average signal intensity change was 12.4% ± 1.1% averaged over the duration of all passive conditions.

Discussion

The observed activity corresponds well with known spinal cord physiology. Movement of the ankle flexor and extensor muscles corresponds to myotomes that innervate the spinal cord at levels S1, L5, and L4. With alternating movements of antagonistic muscle groups there is reflex activity, which is relayed to other areas of the spinal cord by interneurons. This activity is seen in the central region of the spinal cord gray matter. Active pedaling involved use of the motor area as indicated by the bilateral activation of the ventral horns. This activity was seen in the lumbar spinal cord segments L5 and L4 as would be expected during active movement of the ankles. Dorsal horn activity also occurred as proprioceptive information was relayed to the spinal cord during motion.

Passive pedaling incurred sensory activity in the dorsal horn due to proprioception and central region activity due to reflexes relayed by interneurons at lower lumbar segments. Higher segments revealed ventral horn activity, which could be accounted for by reflexes. The increased activity at higher ventral levels could also be due to the subjects' tensing their thigh muscles while attempting to remain motionless as their feet were moved for them. Passive movements generated less activity overall, but the locations of the activity remained true to the physiology. The findings are reliable in that there is overlap in up to five activated pixels in locations consistent with the physiological response expected during the performed motor task, from the 6 subjects.

The average signal intensity changes were notably higher than that observed in previous spinal fMRI studies with thermal sensory stimulation, in which values of approximately 8% have been reported (1,2,3,12). The values obtained in this study after initial analysis were observed to be 15.4% ±1.3% and 18.3% ± 1.4%, for active and passive motion, respectively. The signal intensity changes were lower when voxels identified as apparent activity that were at edge of the spinal cord, and therefore were presumed to be due to motion, were set apart from the analysis (2,3). Areas of apparent activity that were clearly the result of motion were readily identifiable based on their location and relatively high signal intensity changes. After eliminating these identifiable false activations, the signal changes observed with passive and active motion were much more similar, and these were still significantly higher than with sensory stimulation observed in previous studies. Average signal intensity changes were reduced to 11.9% ± 1.0% and 12.4% ± 1.1% when the presumed motion associated voxels were removed, for active and passive motion, respectively. This would suggest that the elevated signal

changes initially observed in the present study may have been due to motion effects. However, different average signal changes were observed when comparing the dorsal activity and the ventral activity after excluding the motion induced activations. During active motion, the average signal changes were 13.3% ± 1.8% for dorsal activity and 10.7% ± 1.0% for ventral activity, p=0.2 (two-tailed student's t-test). During passive motion, the average signal changes were 14.7% ± 2.1% for dorsal activity and 10.6% ± 1.1% for ventral activity, p=0.07. Although these values likely contain residual motion effects, comparing overall dorsal activity to overall ventral activity revealed significantly different signal changes. Given that the areas of activity are mere millimeters apart in the spinal cord and are induced by the same stimuli, they should be affected equally by noise and motion. The overall signal changes were 13.8% ± 1.4% for dorsal regions and 10.7% ± 0.7% for ventral regions, for active and passive tasks combined (p=0.04). The signal changes are therefore significantly different in the dorsal and ventral areas and are both significantly higher than the signal changes observed in studies with thermal stimulation. This suggests that the signal changes are indeed larger with a motor task than with sensory stimulation, and that the difference is not artefactual or due only to the task-related motion. This higher signal change seen with a motor task could originate from a greater change of neuronal activity with a motor task than with sensory stimulation. In consideration of spinal cord neuroanatomy, this could be accounted for by a larger number of neurons involved, a greater difference in spiking rate, or, based on the work of Logothetis et al. (8), greater afferent input to the gray matter with motor activity than with sensory.

Conclusions

This initial motor study demonstrates that the problems associated with motor-related tasks can be overcome, and spinal fMRI can be used to assess reliably the activity in the lumbar spinal cord during lower limb motor stimulation. In spite of the effects of motion, we were able to detect consistent areas of motor and sensory activity, which correspond well with spinal cord neuroanatomy. The effects of motion were identified primarily at the high-contrast boundaries at the edge of the spinal cord. Fortunately, spinal cord gray matter does not extend to the edge of the spinal cord, and with the imaging methods we employ there is very little contrast between white and gray matter. Motion effects arising at gray/white boundaries are therefore expected to be very small, with a very low probability of contributing to the identification of false-positive activations. The observed spatial characteristics of the individual and combined activity maps serve to demonstrate the reliability of our results. We propose that motion contributions to the data can be assessed at the cord boundaries, and may be used in future motor studies as a quality assurance marker, without significantly degrading the spinal fMRI results. Nonetheless, the signal changes observed with edge regions excluded were larger than observed with sensory stimulation in previous studies. This difference is presumed to have some contribution from task-related motion, but we conclude that the signal changes we have observed are accurate to within less than ±2% standard error. The signal changes observed with active and passive motor tasks (~12%) are therefore significantly higher than with thermal stimulation (~8%) employed in previous studies, and so are presumed to be due to a larger degree of neuronal activity with the motor task. This difference will be more readily investigated in future studies

with spinal cord injured subjects.

The data reported here conclude the basic spinal cord physiological testing that was required to affirm spinal fMRI as an effective tool for assessing spinal cord function. Spinal fMRI has now been proven successful at identifying sensory, motor, and reflex activity in both the cervical and lumbar spinal cord.

References

1. Stroman PW, Kornelsen J, Bergman A, Krause V, Ethans K, Malisza KL, Tomanek B. Non-invasive Assessment of the Injured Human Spinal Cord by means of Functional Magnetic Resonance Imaging. Spinal Cord. 2003;

2. Stroman PW, Krause V, Malisza KL, Frankenstein UN, Tomanek B. Functional magnetic resonance imaging of the human cervical spinal cord with stimulation of different sensory dermatomes. Magn Reson. Imaging 2002;20:1-6.

3. Stroman PW, Tomanek B, Krause V, Frankenstein UN, Malisza KL. Mapping of neuronal function in the healthy and injured human spinal cord with Spinal fMRI. NeuroImage 2002;17:1854-1860.

4. Stroman PW, Ryner LN. Functional MRI of motor and sensory activation in the human spinal cord. Magn Reson. Imaging 2001;19:27-32.

5. Ogawa S, Lee TM, Kay AR, Tank DW. Brain magnetic resonance imaging with contrast dependent on blood oxygenation. Proc. Natl. Acad. Sci. U. S. A 1990;87:9868-9872.

6. Menon RS, Ogawa S, Kim SG, Ellermann JM, Merkle H, Tank DW, Ugurbil K. Functional brain mapping using magnetic resonance imaging. Signal changes accompanying visual stimulation. Invest Radiol. 1992;27 Suppl 2:S47-S53.

7. Ogawa S, Tank DW, Menon R, Ellermann JM, Kim SG, Merkle H, Ugurbil K. Intrinsic signal changes accompanying sensory stimulation: functional brain mapping with magnetic resonance imaging. Proc. Natl. Acad. Sci. U. S. A 7-1-1992;89:5951-5955.

8. Logothetis NK, Pauls J, Augath M, Trinath T, Oeltermann A. Neurophysiological investigation of the basis of the fMRI signal. Nature 7-12-2001;412:150-157.

9. Stroman PW, Krause V, Malisza KL, Frankenstein UN, Tomanek B. Extravascular proton-density changes as a non-BOLD component of contrast in fMRI of the human spinal cord. Magn Reson. Med. 2002;48:122-127.

10. Stroman PW, Malisza KL, Onu M. Functional Magnetic Resonance Imaging at 0.2 Tesla. NeuroImage 2003;20:1210-1214.

11. Stroman PW, Krause V, Malisza KL, Frankenstein UN, Tomanek B. Characterization of contrast changes in functional MRI of the human spinal cord at 1.5 T. Magn Reson. Imaging 2001;19:833-838.

12. Stroman PW, Krause V, Malisza KL, Kornelsen J, Bergman A, Lawrence J, Tomanek B. Spinal fMRI of spinal cord injury in human subjects. ISMRM 2003, Toronto, ON, July 10-16 2003;13-

13. Craig AD, Dostrovsky JO. Differential projections of thermoreceptive and nociceptive lamina I trigeminothalamic and spinothalamic neurons in the cat. J. Neurophysiol. 2001;86:856-870.

Figures and figure captions:

Figure 1: MR compatible pedaling device; in place in the magnet with a healthy volunteer positioned for imaging.

Figure 2: Combined activity map of the lumbar spinal cord, during passive pedaling (top row) showing motor and reflex activity, and during active pedaling (bottom row) showing bilateral motor activity and sensory activity. Images are axial and in radiological orientation, with the right side of the body to the left of the image, and dorsal is toward the bottom. Eight image slices are shown, spanning from the 3rd sacral spinal cord segment (S3) on the left, moving rostrally along the spinal cord, reaching the 1st lumbar spinal cord segment (L1) on the right.

Figure 3: Average signal intensity time course averaged across all active regions in six healthy subjects. The subjects performed a rhythmic alternated ankle flexion task during time points 9-16, 25-32, and 41-48, and rested otherwise.

Figure 1

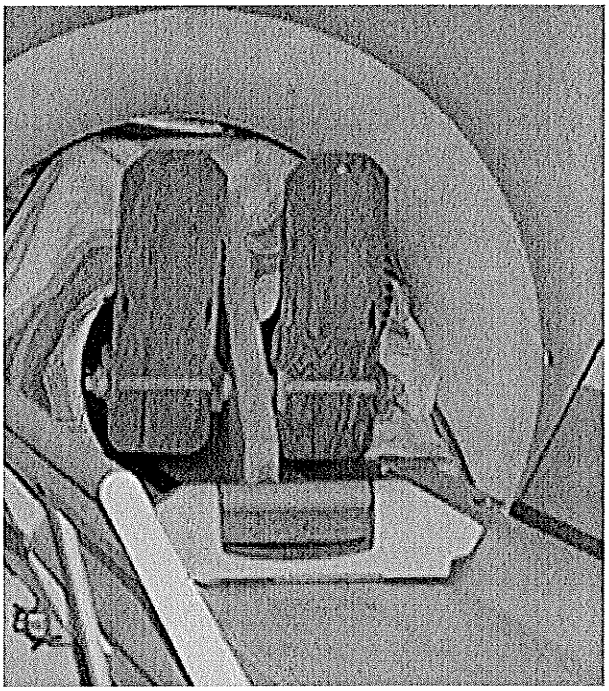

Figure 2

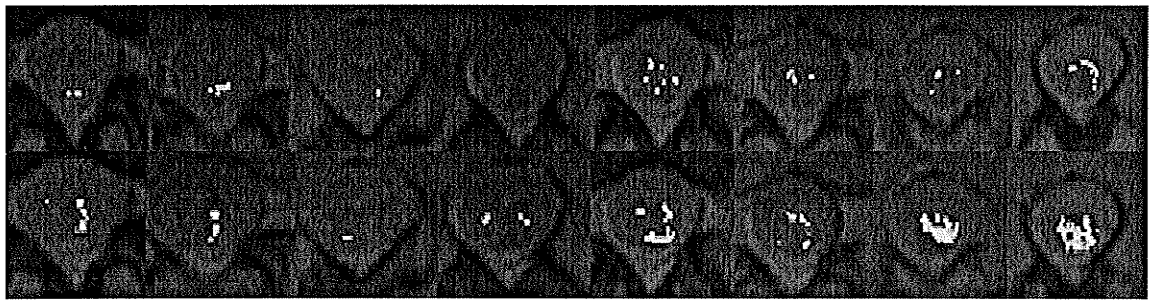

Figure 3

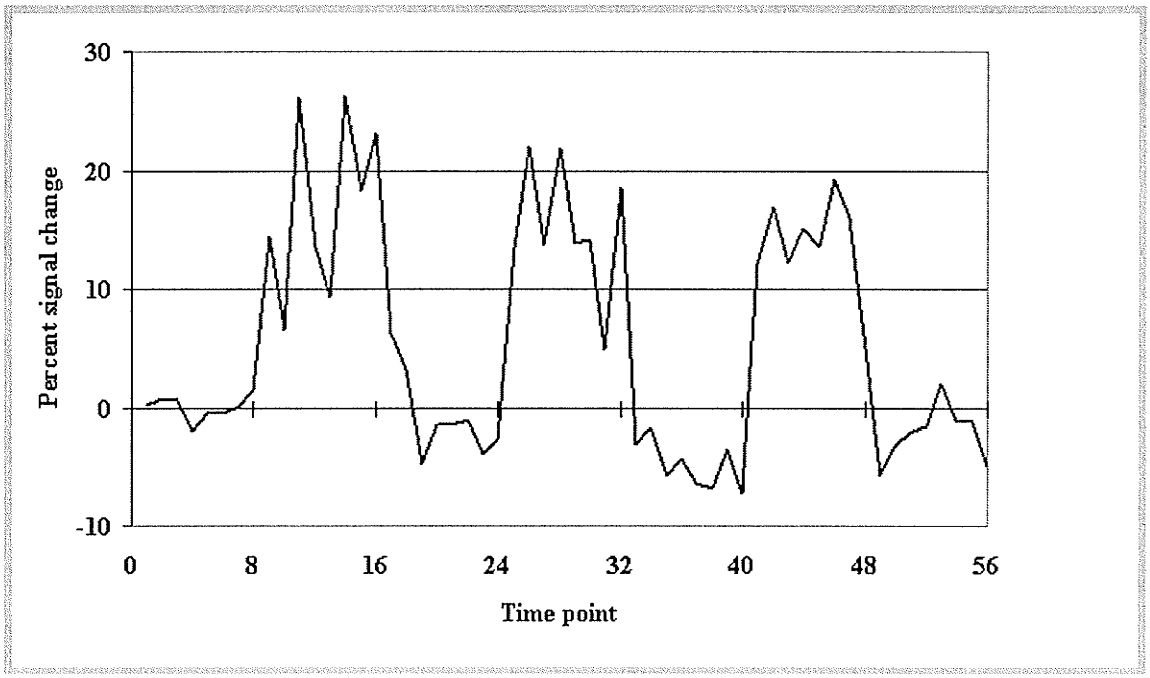
30
20
10
0
-10
Percent signal change
0
8
16
24
32
40
48
56
Time point

An improved method for spinal fMRI with large volume coverage of the spinal cord

Patrick W. Stroman, Ph.D.[1,2,3], Jennifer Kornelsen B.A.[2], Jane Lawrence B.Sc.[2]

[1] Dept. of Diagnostic Radiology, Queen's University, Kingston, Ontario, Canada
[2]Dept. of Physiology, University of Manitoba, Winnipeg, Manitoba, Canada
[3] Institute for Biodiagnostics, National Research Council of Canada, Winnipeg, Manitoba, Canada

Running Title: Spinal fMRI with large volume coverage

Word count: ~3600 words + 4 figures

Correspondence:

Dr. P. W. Stroman
Dept of Diagnostic Radiology
c/o Center for Neuroscience Studies
231 Botterell Hall
Queen's University
Kingston, Ontario
Canada K7L 2V7
Phone 613-533-3245
Fax 613-533-6840
stromanp@post.queensu.ca

In: Journal of Magnetic Resonance Imaging 21:520-526 (2005)

Abstract

Purpose: To develop a spinal fMRI method with three-dimensional coverage of a large extent of the spinal cord with minimal partial volume effects

Materials and Methods: Functional MRI data of the cervical spinal cord were obtained at 1.5 T with a single-shot fast spin-echo imaging method, from thin contiguous sagittal slices spanning the cord. Thermal stimulation was applied to the palm of the hand in a block pattern with 15 °C for stimulation, and 32 °C during baseline periods. Prior to analysis, the image data at each time point were reformatted into three-dimensional volumes and re-sliced perfectly transverse to the spinal cord. Smoothing was applied only in the S/I direction across uniform tissue types. Active voxels were then identified by means of a correlation to a model paradigm.

Results: The resulting activity maps demonstrate activity primarily in ipsilateral sensory areas and in some motor areas, consistent with the spinal cord neuroanatomy. These data also demonstrate detail of the sub-segmental organization of the spinal cord, as well as anatomical detail of the spinous processes and positions of nerve roots.

Conclusion: The spinal fMRI method described enables large volume coverage of the spinal cord in three-dimensions, with reliable and reproducible results.

Key Words:
spinal cord, human, magnetic resonance imaging, fMRI

Introduction

Functional magnetic resonance imaging of the human spinal cord has been demonstrated to be effective at demonstrating areas of neuronal activity in the spinal cord, in response to an external stimulus, in both healthy and injured people (1-7). However, there are several challenges that must be overcome before this method will be sufficiently practical and reliable for use as a tool for clinical assessment or for spinal cord research. These challenges are caused by the flow of cerebrospinal fluid (CSF) around the cord, the magnetic susceptibility differences between the cord and the surrounding bone, and the relatively small cross-sectional dimensions of the cord (~16 mm x 10 mm at the cervical enlargement) with a large superior-inferior (S/I) extent (~45 cm). Artefacts arising from CSF flow can be reduced with flow-compensating gradients, and the motion this imparts to the cord has been shown to be a likely source of error in spinal fMRI results (8), but is yet to be fully addressed. The effects of susceptibility gradients have been overcome by acquiring spinal fMRI data with proton-density weighted spin-echo imaging methods. Neuronal-activity related contrast changes arise from the BOLD (blood-oxygenation level dependent) contrast, as well as from SEEP (Signal Enhancement by Extravascular water Protons) (4,9). The underlying physiological mechanism which has been proposed for SEEP is a local change in extravascular water content driven by changes in perfusion pressure and production of extracellular fluid (ECF) (4,10,11). Local water content changes related to cell swelling, and changes in the extracellular volume, may also contribute because it has been shown that these processes may play an important role in neuronal signaling (12-16). The small cross-sectional dimensions of the cord result in problems of partial volume effects or a

trade-off with the extent of the cord that can be imaged. The method that has been demonstrated to be effective for spinal fMRI employs transverse slices because this orientation is superior for distinguishing gray and white matter (less partial-volume effect) and slices can be positioned to be aligned with the centers of the vertebral bodies or the intervertebral discs where the through-slice field homogeneity is optimal (2). However, this slice orientation provides only a limited view of the cord with low resolution in the rostral-caudal direction. The alternative of employing sagittal or coronal slices has been employed (17-20), but the slices acquired have been ½ to ¼ of the cord width or depth in order to achieve an adequate signal-to-noise ratio and the results have suffered from severe partial volume effects. In the present study we propose that spinal fMRI data can be acquired with thin contiguous sagittal slices, with smoothing applied only across consistent tissues to increase the signal-to-noise ratio without incurring partial-volume effects.

In the present work we therefore describe a new method, based on sagittal slices, but with several very significant differences from the methods used previously by others (18-20). This new method makes use of a single-shot fast spin-echo technique to image contiguous sagittal slices of the spinal cord that are as thin as the hardware will allow, regardless of the signal-to-noise ratio of the resulting images. The slices are then reformatted into a three-dimensional volume, and re-sliced perfectly transverse to the spinal cord. Smoothing is applied only in the rostral-caudal direction across consistent tissue types, and spinal fMRI analysis is applied to the resultant axial slices as per our usual method (5,6). The functional maps resulting from this method are in the form of isotropic voxels spanning a three-dimensional volume, and can be reformatted into any

desired slice orientation. This permits visualization of areas of activity in relation to anatomical markers such as vertebrae, spinous processes, and spinal nerve roots. Here we demonstrate the effectiveness and reliability of this new method, and propose that it provides the practical spinal fMRI tool needed for clinical assessment or research.

Previous spinal fMRI studies employing thermal sensory stimulation of various areas of the hand, forearm, or leg have demonstrated a consistent pattern of activity in the corresponding spinal cord segments (2,3,5,21). Activity is primarily in ipsilateral dorsal areas and projects to ipsilateral ventral regions, with some activity also in contralateral ventral areas and around the central canal (5,6). The magnitude of the signal intensity changes has also been observed to vary with the stimulation temperature, including a clear transition in the response between cold sensation, and noxious or painful cold, demonstrating the correspondence between the observed signal changes and neuronal activity (5). Recent studies in an animal model (rat) have demonstrated a close correspondence between areas of activity identified with spinal fMRI and with direct histological detection of neuronal activity (21). Signal intensity changes in the cervical spinal cord have been consistently observed to be 6.4% ± 1.3% (mean ± s.d.) with thermal stimulation of the palm of the hand at 15 ^{o}C, and 7.0% ± 0.9% with 10^{o}C stimulation, in healthy volunteers(3,4). In the lumbar spinal cord the signal intensity changes were 6.6% ± 0.9% and 7.2% ± 1.5% with 10^{o}C stimulation of the leg in healthy and injured subjects respectively (5). In order to validate the new method, we have employed the same stimulus in the present study in order to elicit the same consistent pattern of response.

Methods

Spinal fMRI studies of 7 healthy volunteers were carried out at 1.5 T in a GE Signa Horizon LX clinical MR system. In most of the subjects experiments were duplicated and a total of 22 sets of spinal fMRI data were obtained. Data were acquired with single-shot fast spin-echo imaging with a 12 cm x 12 cm field of view, 128 x 128 matrix, and an effective echo time of 36 msec. A commercial GE phased-array spine coil was used for signal reception and a body coil used for transmission of spatially uniform RF excitation pulses. K-space data were zero-filled to 256 x 256 prior to reconstruction. Eight contiguous sagittal slices, each 2.8 mm thick, were selected to span the cord, requiring a repetition time of approximately 10 seconds. This provided a resolution of 2.8 mm x 0.9 mm x 0.9 mm (R/L x A/P x S/I), in the original image data. Thermal stimulation of the palm of the right hand was applied with a 3 cm x 3 cm thermode with temperature controlled by a Medoc TSA-II thermal sensory analyzer with input from a PC. This was used to elicit reproducible activity in the 6^{th} to 8^{th} cervical spinal cord segments without incurring task-related motion. The thermode temperature was set to 15 °C for stimulation and 32 °C during baseline periods, with the transition occurring in one TR period (10 sec). A block design was used with two stimulation periods of 50-60 seconds duration interleaved with rest periods of 60-70 seconds. The total acquisition time for each experiment was 350 seconds, with the spinal cord imaged 35 times to describe the fMRI time course.

Data were analyzed using custom-made software written in MatLab (The MathWorks Inc., Natick MA). Prior to analysis a line was drawn manually along the anterior edge of the spinal cord in a mid-line sagittal image taken from the functional data set, and this

was used as a reference for the spinal cord position and curvature. The sagittal slice data at each time point of the functional series were combined into a three-dimensional volume and linearly interpolated to obtain cubic voxels 0.5 x 0.5 x 0.5 mm^3. The volume was then re-sliced perfectly transverse to the spinal cord and smoothing was applied only in the rostral-caudal direction to be across consistent anatomy. The correlation between a model paradigm and the signal intensity time course of each voxel was computed in order to construct a map of correlation T-values. A T-value threshold of 2.0 was chosen to identify voxels as being active, corresponding to a p-value threshold of 0.05, and were plotted in colour over a gray-scale average image of the volume. An intensity threshold was set manually on the background image to identify the higher intensity CSF, and a mask was created to exclude false activations arising from within the CSF. The volume map demonstrating the areas of activity was then also reformatted back into thin sagittal slices for viewing.

The results obtained were normalized to a consistent size to facilitate comparison between experiments and across subjects. This was achieved by defining reference lines on the three-dimensional interpolated data that resulted from the analysis as described above. Reference lines were drawn manually along the dorsal, ventral, left and right edges of the cord, overlying axial, sagittal, and coronal slices of the volume data. Approximate boundaries of the spinal cord segments were identified by means of the positions of dorsal nerve roots, and the shapes and sizes of the spinous processes, as references. Using these manually defined references, the spinal cord image data and the correlation T-value map were normalized by linear interpolation and translation to a cord cross-section of 18 pixels x 30 pixels (anterior-posterior x left-right) at each S/I location.

Each spinal cord segment was then normalized to be 30 pixels long. Activation maps were produced by thresholding the T-value maps at $T \geq 2$ to identify active voxels which were labeled in colour overlying the averaged and normalized reference image data. Image data spanning 210 pixels in the S/I direction therefore spans spinal cord segments C4 to T2 with a width of 30 pixels each.

In order to allow a comparison to be made with the previously employed axial-slice method, the data that had been re-sliced into 0.5 mm thick transverse slices was averaged across blocks of 15 slices to create a data set of 7.5 mm thick transverse slices. The correlation with the model paradigm was again calculated with this data and active voxels identified with a T-value threshold of 2.0. The signal intensity time courses of the active voxels in the spinal cord which would have been determined with the axial-slice method were thus determined.

Results

Spinal fMRI data obtained from seven volunteers with thermal stimulation of the right hand demonstrated consistent patterns of activity (Fig 1). The three-dimensional distribution of activity is demonstrated in normalized results in Figure 2. In the dorsal gray matter ipsilateral to the stimulus, active regions were observed at typically three to five locations at the levels of the 5^{th}, 6^{th} and 7^{th} cervical vertebrae, corresponding approximately with the 6^{th}, 7^{th}, and 8^{th} cervical spinal cord segments, respectively. In each experiment, the activity was observed at numerous locations within each spinal cord segment with small (~ 2 mm) spatial extent in the S/I direction. In ventral gray matter, active areas were also observed and were slightly offset from those in dorsal regions, and in dorsal and ventral gray matter the pattern appeared to alternate along the rostral-caudal

direction within a segment. Activity was observed in both ipsilateral and contralateral ventral gray matter, each slightly offset in the S/I direction from the other, as well as being consistently offset (~1-2 mm) from that in dorsal regions. Activity was more consistently observed in contralateral ventral regions, however, as compared to in the ipsilateral ventral regions. Some contralateral activity in dorsal gray matter was also observed at locations that were offset in the S/I direction from that in ipsilateral dorsal areas. The spatial relationship between the ipsilateral and contralateral ventral activity and the ipsilateral dorsal activity appeared to produce a repeated pattern at more than one location within each active spinal cord segment. There were also noticeable gaps of a few millimeters in width at the approximate segment boundaries where activity was not observed. Some active regions were also observed in ventral gray matter at higher (4^{th}-5^{th} cervical) and lower (1^{st} - 2^{nd} thoracic) spinal cord segments. Representative examples of results of one experiment from each of the seven volunteers are shown in Figure 1. Each figure shows the activity within an interpolated 0.5 mm thick sagittal slice through the right side of the spinal cord, and demonstrates both the right dorsal and right ventral activity. The images are oriented with dorsal toward the bottom, and the rostral direction is toward the left side of the frame, as demonstrated by the appearance of the spinous processes. The magnitude of the signal intensity changes in all active regions were observed to be consistent and averaged 10.0% ± 1.0% (mean ± s.d.) as shown in Figure 3. In comparison, the signal intensity time courses obtained with data reformatted into 7.5 mm thick transverse slices demonstrated an average signal intensity change of 6.3% ± 0.5% (mean ± s.d.).

Discussion

The results obtained demonstrate that the spinal fMRI method we have developed can provide full three-dimensional coverage of a 12 cm extent of the cervical spinal cord, with high sensitivity to neuronal-activity-related signal changes. Normalized results shown in Figure 2 provide examples of the 3D coverage of the cervical spinal cord as any desired transverse, sagittal, and coronal slices can be selected for displaying functional maps. The detail obtained in the data is also demonstrated by the surrounding anatomical features such as spinous processes, which can be clearly identified and used as landmarks for the position in the cord.

The pattern of activity observed in the present study was identical to that observed previously in its R/L and A/P distribution, but differences were notable in the S/I distribution as a result of the finer resolution obtained. The sensory dermatomes on the palm of the hand are known to be innervated from the 6^{th} to 8^{th} cervical spinal cord segments, corresponding with the observed location of activity. There are also projections to motor areas in the same segment and adjacent segments, and if a stimulus is of sufficient type and intensity, a motor reflex to withdraw from the stimulus can be triggered. However, descending input from the brain can inhibit the reflex. In the present study the volunteers did not move their arms or hands when the 15 °C cold stimulus was applied. Nonetheless, in this study and previous studies with the same stimulus, motor activity was observed in ventral gray matter regions and around the central canal. Both the dorsal and ventral activity was also observed in every experiment to occur at multiple localized regions within a segment, demonstrating a finer-scale organization at the sub-segmental level. Similar fine-scale structure has been

demonstrated in electrophysiological studies in rats (22). However, this is the first time this structure detail has been observed with spinal fMRI. The areas of ventral activity on the right and left sides were observed to be consistently offset in the S/I direction from the dorsal activity as well as being slightly offset from each other, and the locations of activity in these three areas (right ventral, left ventral, right dorsal) were repeatedly observed in the same pattern. Examples of this pattern are shown in Figure 2.

Partial volume effects do not appear to be significant with the 2.8 mm thick sagittal slices employed for this study because very little contamination from CSF flow is apparent in the results. Such a contribution would be expected to appear as false positive activations around the edges of the cord and should be easily recognized. The effective size of the resolution element ("resel") (23) we have obtained with the sagittal-slice method is approximately 2.8 mm x 0.9 mm x 1.8 mm (R/L x A/P x S/I) because the smoothing was applied only in the S/I direction across 3 voxels that were first interpolated to 0.5 mm across, from an original resolution of 0.9 mm. We therefore approximate that we are mixing signal across 2 original voxels (i.e. 1.8 mm). These resel dimensions are expected to be a closer match to the dimensions of gray matter functional volumes than with the axial-slice method (resel size of approximately 0.9 mm x 0.9 mm x 7.5 mm). At the same time, the effective resel volume and SNR are maintained at similar values. The interpolation and re-slicing applied prior to analysis does not alter the resolution obtained in the original image data. The resolution obtained in the A/P and R/L directions was clearly adequate to demonstrate regions of dorsal and ventral gray matter in the image data. Moreover, partial volume effects in the S/I direction were notably reduced compared to the method described previously with axial slices (5,6), as

evidenced by the fact that the fractional signal intensity changes were significantly greater in the present study. Signal changes averaged 10.0% ± 1.0% during stimulation periods with sagittal slices, as compared to 6.4% ± 1.3% under the same stimulation conditions in previous studies, but with axial slices. Reformatting the data obtained in the present study into 7.5 mm axial slices to simulate the data obtained with the axial-slice method, yielded signal intensity changes of 6.3% ± 0.5%. This is consistent with the observation that the active regions each span only a few millimeters in the S/I direction, and so the magnitude of signal change would have been reduced when averaged over the 7.5 mm thick axial slices used previously. This signal change magnitude is much too large to be attributed to the BOLD effect, and is consistent with the proposed SEEP contrast mechanism being dominant in spinal fMRI (4).

The observation of small, localized areas of activity within the gray matter in each spinal cord segment that is related to sensory dermatomes being stimulated, the correspondence of the observed areas of activity with known neuroanatomy, and the relatively high signal intensity changes, all demonstrate a high degree of sensitivity with the sagittal-slice method described in the present study. This method is therefore expected to provide better sensitivity to neuronal-activity induced signal changes than was obtained with the previous axial-slice method. The sensitivity and reliability of the sagittal slice method are demonstrated by the consistency of the results obtained, both in repeated experiments with each subject, and across different subjects, and is demonstrated in Figures 1 and 4. Figure 4 shows maps indicating the reproducibility of the results, which were created at each voxel in the spinal cord by computing the inverse of the average distance to the nearest active voxel, after normalizing the results to

consistent dimensions. For example, if at a given voxel the average distance to the nearest active voxel in each repeated study was 3 voxel-widths (the voxel width is 0.5 mm in the normalized data), then that voxel in the reproducibility map would be assigned a value of 1/3. If the average distance was zero, meaning that every set of results being compared showed activity at that location, then the voxel in the reproducibility map was arbitrarily assigned a value of 10. Higher values thus indicate the locations of highly clustered active voxels in repeated experiments. In comparison, Figure 1 contains images demonstrating the distribution of activity in single experiments for each of the seven volunteers studied, through one selected 0.5 mm thick sagittal slice through the right side of the spinal cord. The same segmental level of the spinal cord is indicated in each image with green corner marks. Figures 1 and 4 demonstrate highly reproducible areas of activity across repeated studies in each subject, and also show reproducibility in the pattern and locations of activity across different subjects. However, it is important to note that some differences between subjects are to be expected because the distribution of sensory dermatomes varies between individuals, and the thermode used for stimulation did not rest within the palm of each volunteer's hand precisely the same way. In repeated experiments for each subject it is expected that the thermode position was consistent.

The benefits of carrying out spinal fMRI with thin sagittal slices, and post-processing to improve the SNR (by means of averaging across consistent tissue types) are the increased spatial coverage of the spinal cord, greater flexibility in how results can be displayed, and the improved spatial resolution in the S/I direction. An added benefit of acquiring data in sagittal slices to span a continuous three-dimensional volume is that it is possible to normalize the data to constant dimensions to facilitate viewing of the results,

and comparison of results within, or across, subjects. The results shown in Figures 2 and 4 have been normalized using the method described above, and demonstrate the effectiveness of the method. This is the first attempt at defining a normalization technique for spinal cord image data, and more detailed studies are required to determine the optimum normalization for all situations.

Conclusion

In conclusion, a new method for spinal fMRI acquisition with thin sagittal slices, and post-processing to attain an adequate signal-to-noise ratio, has been demonstrated. Compared to data obtained with axial slices, this method has been shown to provide at least equal sensitivity and reliability, with significantly greater resolution in the S/I direction, to demonstrate a larger extent of the spinal cord, and to yield effectively three-dimensional data. We have also demonstrated the ability to normalize the spinal fMRI data, and produce consistent R/L and A/P dimensions along the cord length. Moreover, with the larger volume imaged with sagittal slices it is possible to identify approximate boundaries of spinal cord segments based on the shape/size of the spinous processes and positions of nerve roots. The sagittal-slice method we have developed for spinal fMRI therefore provides a tool that is practical, and better suited for routine use for clinical assessment and spinal cord research.

Acknowledgements

We gratefully acknowledge helpful input from Dr Spyros Kollias, Dr. Boguslaw Tomanek, and Dr. Krisztina Malisza. This work was supported by a grant from the

Canadian Institutes of Health Research (CIHR), and was undertaken, in part, thanks to funding from the Canada Research Chairs Program (P. W. Stroman).

References

1. Yoshizawa, T., Nose, T., Moore, G. J., and Sillerud, L. O. Functional magnetic resonance imaging of motor activation in the human cervical spinal cord. Neuroimage. 1996: 4: 174-182.

2. Stroman, P. W. and Ryner, L. N. Functional MRI of motor and sensory activation in the human spinal cord. Magn Reson.Imaging 2001: 19: 27-32.

3. Stroman, P. W., Krause, V., Malisza, K. L., Frankenstein, U. N., and Tomanek, B. Functional magnetic resonance imaging of the human cervical spinal cord with stimulation of different sensory dermatomes. Magn Reson.Imaging 2002: 20: 1-6.

4. Stroman, P. W., Krause, V., Malisza, K. L., Frankenstein, U. N., and Tomanek, B. Extravascular proton-density changes as a non-BOLD component of contrast in fMRI of the human spinal cord. Magn Reson.Med. 2002: 48: 122-127.

5. Stroman, P. W., Tomanek, B., Krause, V., Frankenstein, U. N., and Malisza, K. L. Mapping of neuronal function in the healthy and injured human spinal cord with spinal fMRI. Neuroimage 2002: 17: 1854-1860.

6. Stroman, P. W., Kornelsen, J., Bergman, A. et al. Non-invasive assessment of the injured human spinal cord by means of functional magnetic resonance imaging. Spinal Cord 2004: 42: 59-66.

7. Kollias, S. S., Kwiecinski, S., and Summers, P. Functional MR Imaging of the Human Cervical Spinal Cord. In: American Society of Neuroradiology. Proceedings of the 42nd Annual Meeting, Seattle, June 7-11, 2004. (abstract 227).

8. Brooks, J., Robson, M., Schweinhardt, P., Wise, R., and Tracey, I. Functional magnetic resonance imaging (fMRI) of the spinal cord : a methodological study. In: American Pain Society. 23rd Annual Meeting, Vancouver, May 6-9, 2004 (abstract 667).

9. Stroman, P. W., Krause, V., Malisza, K. L., Frankenstein, U. N., and Tomanek, B. Characterization of contrast changes in functional MRI of the human spinal cord at 1.5 T. Magn Reson.Imaging 2001: 19: 833-838.

10 Stroman, P. W., Tomanek, B., Krause, V., Frankenstein, U. N., and Malisza, K. L. Functional magnetic resonance imaging of the brain based on signal enhancement by extravascular protons (SEEP fMRI). Magn Reson.Med. 2003: 49: 433-439.

11. Stroman, P. W., Malisza, K. L., and Onu, M. Functional magnetic resonance imaging at 0.2 tesla. Neuroimage 2003: 20: 1210-1214.

12. Piet, R., Vargova, L., Sykova, E., Poulain, D. A., and Oliet, S. H. Physiological contribution of the astrocytic environment of neurons to intersynaptic crosstalk. Proc.Natl.Acad.Sci.U.S.A 2004: 101: 2151-2155.

13. Svoboda, J. and Sykova, E. Extracellular space volume changes in the rat spinal cord produced by nerve stimulation and peripheral injury. Brain Res. 1991: 560: 216-224.

14. Sykova, E., Vargova, L., Kubinova, S., Jendelova, P., and Chvatal, A. The relationship between changes in intrinsic optical signals and cell swelling in rat spinal cord slices. Neuroimage. 2003: 18: 214-230.

15. Sykova, E., Vargova, L., Prokopova, S., and Simonova, Z. Glial swelling and astrogliosis produce diffusion barriers in the rat spinal cord. Glia 1999: 25: 56-70.

16. Sykova, E. Modulation of spinal cord transmission by changes in extracellular K+ activity and extracellular volume. Can.J.Physiol Pharmacol. 1987: 65: 1058-1066.

17. Stroman, P. W., Nance, P. W., and Ryner, L. N. BOLD MRI of the human cervical spinal cord at 3 tesla. Magn Reson.Med. 1999: 42: 571-576.

18. Porszasz, R., Beckmann, N., Bruttel, K., Urban, L., and Rudin, M. Signal changes in the spinal cord of the rat after injection of formalin into the hindpaw: characterization using functional magnetic resonance imaging. Proc.Natl.Acad.Sci.U.S.A 1997: 94: 5034-5039.

19. Madi, S., Flanders, A. E., Vinitski, S., Herbison, G. J., and Nissanov, J. Functional MR imaging of the human cervical spinal cord. AJNR Am.J.Neuroradiol. 2001: 22: 1768-1774.

20. Backes, W. H., Mess, W. H., and Wilmink, J. T. Functional MR imaging of the cervical spinal cord by use of median nerve stimulation and fist clenching. AJNR Am.J.Neuroradiol. 2001: 22: 1854-1859.

21. Lawrence, J., Stroman, P. W., Bascaramurty, S., Jordan, L. M., and Malisza, K. L. Correlation of functional activation in the rat spinal cord with neuronal activation detected by immunohistochemistry. Neuroimage 2004: 22: 1802-1807.

22. Takahashi, Y., Chiba, T., Kurokawa, M., and Aoki, Y. Dermatomes and the central organization of dermatomes and body surface regions in the spinal cord dorsal horn in rats. J.Comp Neurol. 2003: 462: 29-41.

23. Worsley, K. J. and Friston, K. J. Analysis of fMRI time-series revisited--again. Neuroimage 1995: 2: 173-181.

Figures and Figure Captions:

Figure 1: Examples of results from 7 subjects, showing a single 0.5 mm thick (interpolated) sagittal slice through the dorsal and ventral gray matter on the right side of the body. Images are oriented with the rostral direction to the left, and the dorsal side is toward the bottom of the frames. Voxels with signal intensity time courses that are significantly correlated with the time course of thermal stimulation are shown in colour, overlying the gray-scale background. Sensory activity is therefore seen in the lower half of the spinal cord, whereas motor activity is seen in the upper regions. The same rectangular region of the spinal cord in each subject, containing the dominant activity, is indicated by the green corner marks. The spinous process of the 7^{th} cervical vertebra is marked with a green asterix in each image, and corresponds approximately to the level of the 8^{th} cervical spinal cord segment. The results shown in these images have not been normalized to consistent dimensions.

Figure 2: Examples of normalized results selected from three subjects, showing a number of axial slices (left side), and one sagittal and coronal slice for each subject (as indicated in the top frame). The positions of the axial slices are indicated in the sagittal and coronal views with green lines, and the positions of the sagittal and coronal slices are indicated in each axial slice. Axial slices are in radiological orientation with the right side of the body toward the left side of the frame, and dorsal is toward the bottom. Sagittal and coronal slices are oriented with rostral toward the left. Dorsal is toward the bottom in the sagittal slice, and the right side of the body is toward the top of the coronal

slices. The axial slices are in order from rostral to caudal, from left to right, and demonstrate the alternated pattern of dorsal (sensory) and ventral (motor) activity within a single spinal cord segment.

Figure 3: Signal intensity time courses of active regions observed in each experiment, plotted in gray. The average time course and errors bars showing the standard deviation are plotted in black. The stimulation paradigm is shown in black at the bottom of the plot.

Figure 4: Maps indicating reproducibility in repeated experiments with each of four selected subjects, with data normalized to a consistent size and position as described in the text. Colours indicate the inverse of the average distance to the nearest active voxel in each experiment, spanning from red (lowest distance) through orange to yellow (indicating an average distance of 3 pixels). Average distances above 3 pixels (inverse value of 1/3) are not displayed. Each figure shows one 0.5 mm thick sagittal slice through the right side of the spinal cord, one coronal slice through the dorsal region of the cord, and two selected axial slices. Axial slices are in radiological orientation with the left side of the body on the right side of the image frame. Sagittal slices are shown with the rostral direction to the left, and dorsal is down. Coronal slices are shown with the rostral direction to the left, and the right side of the body is toward the top of the frame. The green lines indicate the positions of the intersecting slices that are shown. Reproducibility was compared across: (top left) 2 experiments, (top right) 2 experiments, (bottom left) 5 experiments, and (bottom right) 4 experiments.

Figure 1

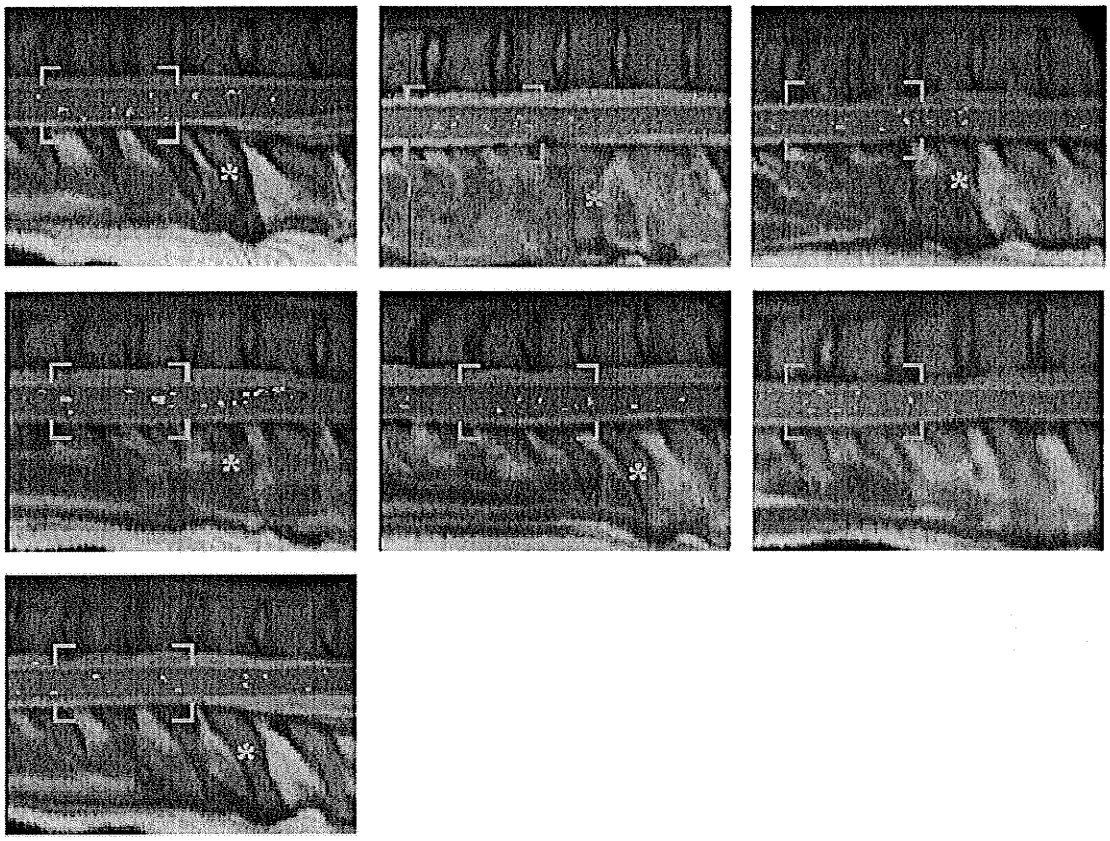

Figure 2

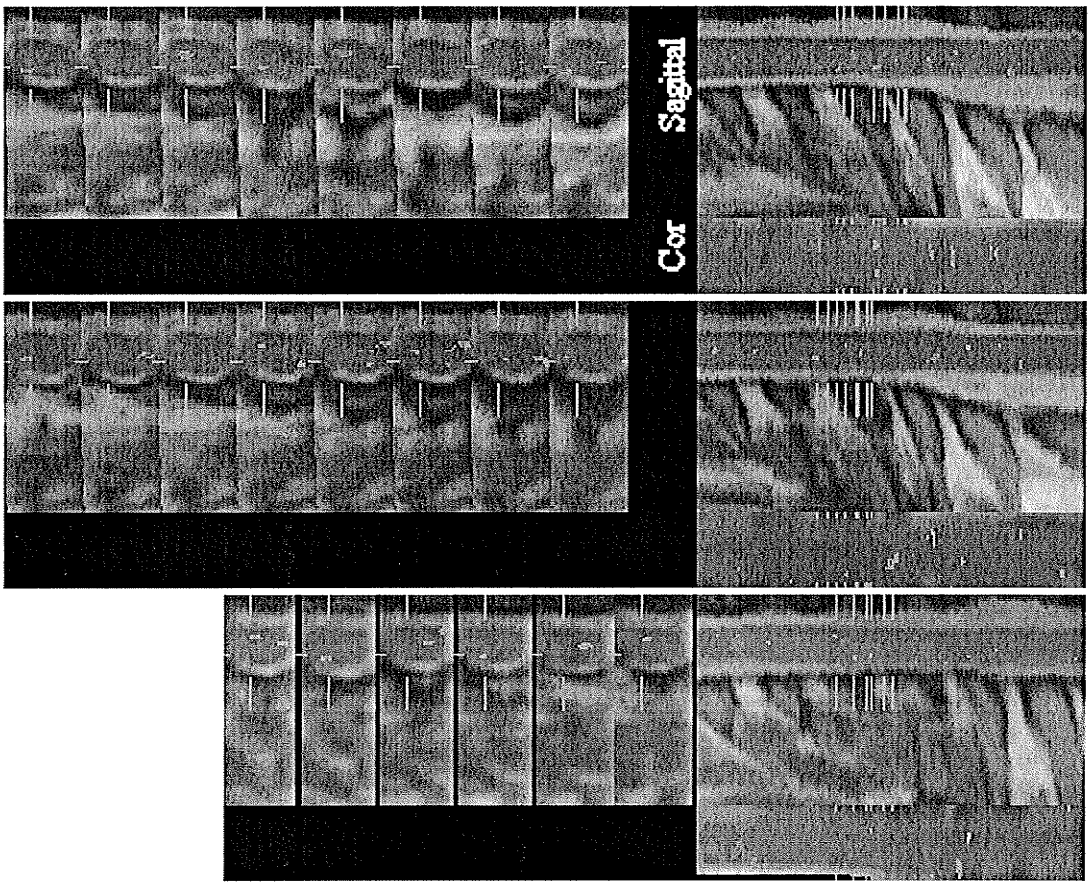

Figure 3

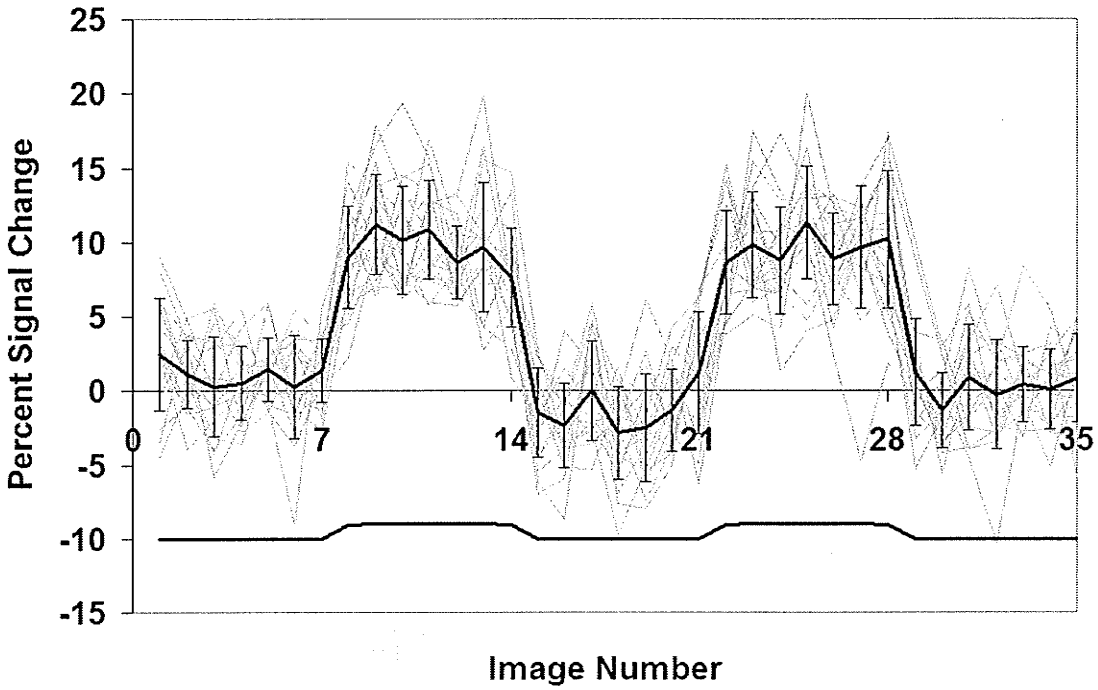
25
20
15
10
5
0
-5
-10
-15
Percent Signal Change
0
7
14
21
28
35
Image Number

Figure 4

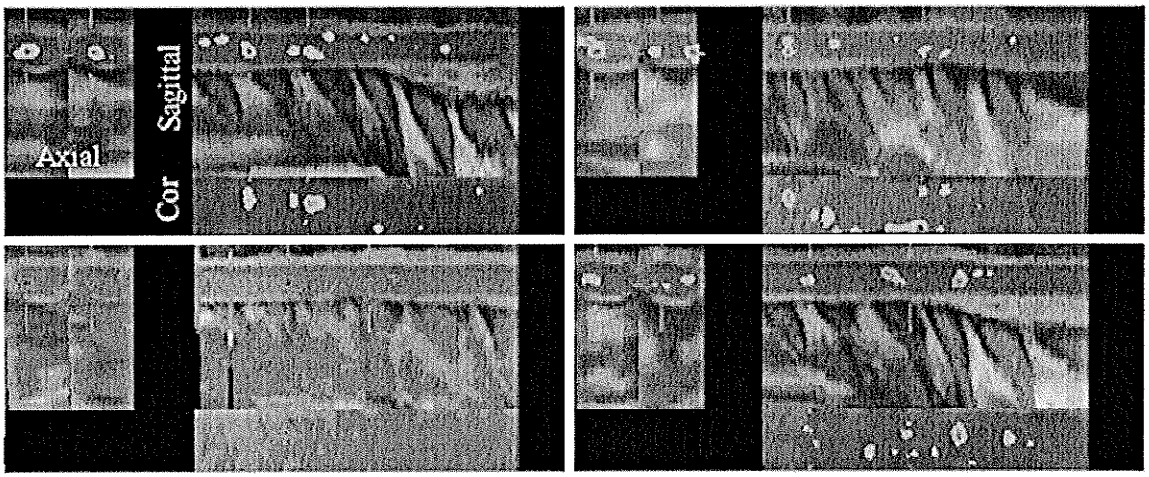

Detection of the neuronal activity occurring caudal to the site of spinal cord injury that is elicited during lower limb movement tasks

J Kornelsen, BA[1], PW Stroman, PhD [2]

[1] Dept of Physiology, U. of Manitoba, Winnipeg, Manitoba, Canada

Phone: (204) 984-6619

Fax: (204) 984-7036

Email: jennifer.kornelsen@nrc-cnrc.gc.ca

[2] Dept of Diagnostic Radiology, c/o Center for Neuroscience Studies, 231 Botterell Hall, Queen's University, Kingston, Ontario, Canada K7L 2V7

Running Title: Detection of neuronal function

Word Count: **3621** words + 2 figures

Correspondence:

Patrick W. Stroman, PhD
Associate Professor - Canada Research Chair in Imaging Physics
Depts of Diagnostic Radiology and Physics
c/o Center for Neuroscience Studies
231 Botterell Hall
Queen's University
Kingston, Ontario
Canada K7L 2V7
phone 613-533-3245
stromanp@post.queensu.ca

Abstract

Study design: Functional magnetic resonance imaging (fMRI) of the spinal cord (spinal fMRI) was used to detect neuronal activity elicited by passive and active lower limb movement tasks, in regions caudal to the injury site in volunteers with spinal cord injury.

Objectives: The objectives of this project are: 1) to assess the use of spinal fMRI as a tool for detecting neuronal function in the spinal cord below an injury, and 2) to characterize the neuronal response to active and passive movement tasks.

Setting: Institute for Biodiagnostics, National Research Council of Canada, Winnipeg, Manitoba, Canada.

Methods: fMRI of the spinal cord was carried out in 12 volunteers with cervical or thoracic spinal cord injuries. Spinal fMRI was carried out in a 1.5T clinical MR system using established methods. Active and passive lower limb movement tasks were performed, and sagittal images spanning the entire lumbar spinal cord were obtained.

Results: Neuronal activity was detected caudal to the injury site in all volunteers regardless of the extent of injury. During both active and passive participation, activity was seen caudal to the injury site, although the number of active voxels detected with passive movement was less than with the active movement task. Average percent signal change was 13.6% during active participation and 15.0% during passive participation.

Conclusions: Spinal fMRI is able to detect a neuronal response sufficient for characterization during both active and passive lower limb movement tasks in the spinal cord caudal to the injury site.

Sponsorship: This work was funded by a grant from the International Spinal Research Trust (U.K.) and the Canada Research Chairs Program.

Keywords: spinal cord; injury; MRI; fMRI; human; magnetic resonance

Statement on Ethics: We certify that all applicable institutional and governmental regulations concerning the ethical use of human volunteers were followed during the course of this research.

Introduction

Spinal cord repair strategies for recovery of function are becoming a possibility for those with spinal cord injury (1). As these repair strategies reach clinical trials, it is important to accurately assess the extent of the spinal cord so that the response to treatment can be monitored. Whereas self-report and physical examination techniques are useful in assessing spinal cord function rostral to the injury site, function caudal to the injury is not assessable in this manner. In this study, we investigate the value of functional magnetic resonance imaging (fMRI) of the spinal cord (spinal fMRI) in its ability to detect neuronal function caudal to the injury site during specific lower limb movement tasks.

Functional magnetic resonance imaging of the spinal cord is a non-invasive tool that can be used to investigate neuronal activity and reveal important information regarding spinal cord function (2,3). Spinal fMRI reveals neuronal function indirectly via changes in blood flow and blood oxygen levels that occur near metabolically active gray matter (4). The signal change arises in part from the blood oxygen-level dependant (BOLD) contrast, which is based on the metabolic activity that occurs in active neuronal tissues. When neuronal firing rates increase, nerve cell bodies take up more oxygen. To compensate, an excess increase in blood supply to neurons occurs resulting in a decrease in the concentration of deoxygenated hemoglobin. Deoxygenated hemoglobin in blood acts as a magnetic resonance (MR) contrast agent that causes the MR signal to decay more quickly. At the time of recording, the MRI signal is stronger from metabolically active areas because the signal has not decayed as quickly as in the surrounding non-active tissues. However, an equally important contrast mechanism in spinal fMRI is

caused by signal enhancement from extravascular water protons (SEEP) which results from an increase in water content in the active neural tissues (5,6). This mechanism is hypothesized to be related to swelling of neurons and/or glial cells that has been shown to arise at sites of neuronal activity (7-9). In addition, the increased blood flow to the active tissues has been shown to be accompanied by increased intravascular pressure, and increased production of extracellular fluid at sites of neuronal activity (10,11). The net effect is a local increase in water content near active neural tissues which causes a higher MR signal intensity. Thus, spinal fMRI detects neuronal activity in spinal cord gray matter, and this allows for mapping of spinal cord responses to sensory and motor stimulation. This method has proven useful for detecting neuronal activity in both healthy and injured spinal cords in response to innocuous and noxious thermal stimulation, in which the distribution of activity and the signal intensity change were found to differ between conditions (2). The neuronal response in the lumbar spinal cord to participation in active and passive lower limb movement tasks was characterized in a previous investigation involving healthy volunteers with spinal fMRI (12). The current study aims to detect and characterize the neuronal response to these same tasks with spinal cord injured volunteers.

Currently, the American Spinal Injury Association (13) assessment scale is the standard for classifying spinal cord injuries. This examination involves a battery of light touch and pin prick examinations to assess where a patient has preserved sensory perception. To determine preserved motor function the patient's ability to move specific key muscle groups is assessed. Patients are categorized as ASIA A, B, C, or D, indicating the preservation of sensory and/or motor functions below the injury level.

ASIA A indicates no sensory or motor function preserved, ASIA B indicates sensory but not motor function is preserved, ASIA C indicates motor function is preserved but in a substantially weakened condition, and ASIA D indicates motor function is preserved in a condition sufficient for near normal use. Further information regarding the condition of the spinal cord caudal to the level of injury must be obtained by invasive measures or deduced from reflex actions. Electrophysiological techniques such as somatosensory evoked potential, H-reflex or stretch reflexes are capable of assessing residual function following a spinal cord injury. The utility of these techniques is limited by the incomplete scope of information that is obtained with each measure, such that a combination of measures is required in order to determine residual function. For example, somatosensory evoked potentials examine conduction along large areas of the body and the results can be affected by peripheral damage, nerve root damage, or spinal cord damage without revealing where along the pathway the damage has occurred. Similarly, an increase in reflexes denotes an upper motor neuron disorder, but will not reveal the degree of damage, or whether the damage is complete or incomplete. Although these methods are useful for many research applications, they require specific equipment and are time-consuming, and are therefore not in routine clinical use. Thus, should spinal fMRI be successful at detecting neuronal activity below the injury site in spinal cord injured patients, this method would be of considerable value for those assessing an injury, planning a treatment strategy or monitoring recovery of function during and post-treatment. These methods are based on standard clinical MRI systems without special modifications. Analysis can be carried out at a later time on a separate computer using published methods (2-4). The resulting images reveal a large extent of

the spinal cord, which can be displayed in axial, coronal, or sagittal orientation resulting in an effectively 3D display. This non-invasive technique is able to show where functional activity occurs in response to a stimulus regardless of a patient's ability to feel the stimulus, a feature the ASIA assessment scale is lacking. The results can be assessed in relation to those from normal healthy control subjects such that the similarities and differences can be identified. Previous work involving healthy control subjects is available for this comparison (12).

We hypothesize that neuronal activity is detectable, using spinal fMRI, caudal to an injury site in response to lower limb movement, and that characterization of the neuronal activity in response to passive and active motor tasks in spinal cord injured (SCI) volunteers is possible.

Methods

Participation:

Twelve volunteers (11 male, 1 female) with spinal cord injury participated in this study. The participants' injuries, following the American Spinal Injury Association, were classified as four participants with ASIA A, three with ASIA B, three with ASIA C, and two with ASIA D. The volunteers participated in active and/or passive lower limb movement tasks according to their abilities. During the active task, participants with ASIA C and D moved their feet in an alternating flexion-extension manner. During the passive task, all participants passively allowed their feet to be moved by the experimenter. In both conditions, the movements were kept in time with the noise of the scanner in order for all volunteers' movements to be kept at the same pace. Subjects

were supine on a General Electric phased-array spine MRI coil, with their feet secured to a MRI-compatible pedaling device. The device consisted of two pedals with adjustable straps over the toes, and over and below the ankle, which was secured on a base designed to fit the MR bed. The device allowed for rhythmic flexion and extension movements of the ankles and was customized to assist in keeping the movements alternate and equal. Placing a cushion under the knee stabilized the thighs and reduced movement of the upper body thereby minimizing motion effects. The study was reviewed and approved by our Institute's Human Research Ethics Board, and informed consent was obtained from all participants before entering the magnet room.

Imaging :

Spinal fMRI was carried out in a block design with three stimulation periods. Images were acquired repeatedly during alternating rest and stimulation periods for a total of 56 time points recorded at 1.5 T in a General Electric Signa Horizon LX clinical MR system. Functional time course data were obtained using single-shot fast spin-echo imaging, as per our established methods (4,12) with sets of eight contiguous 2.8 mm thick sagittal slices. This required a repetition time of 1074 msec per slice, and provided a resolution of 2.8 x 0.9 x 0.9 mm [R/L, A/P, S/I], with a 12 cm x 12 cm field of view and a 128 x 128 matrix. The echo time was set at 37.2 msec. Spatial saturation pulses were applied to eliminate signal from surrounding areas to avoid aliasing and to reduce motion artefacts arising from regions anterior to the spine.

Analysis:

Data were analysed using custom-made analysis programs written in MatLab software (MathWorks, Natick MA). Prior to analysis, a line was drawn manually along

the anterior edge of the spinal cord in a midline sagittal image taken from the functional data set to indicate the spinal cord position and curvature. The data at each time point of the functional series were combined into a three dimensional volume and linearly interpolated to 0.5 x 0.5 x 0.5 mm cubic voxels. The volume was re-sliced transverse to the cord according to the manually drawn reference line, and smoothing was applied only in the rostral-caudal direction. The correlation between a model paradigm and the signal intensity time courses of each voxel was computed to produce a map of correlation t-values. A t-value threshold of 2.0 ($p=0.05$) was chosen to identify voxels as active, and these voxels were plotted in colour over a gray-scale reference image that was produced by averaging the images obtained at the 56 time points. The activity map was then converted to sagittal, axial and coronal slices for viewing. The percent signal change and the standard deviation for each task were calculated.

Results

Spinal fMRI was consistently able to detect neuronal activity caudal to the injury site in the lumbar spinal cord of injured volunteers in response to lower limb movement. Evidence of neuronal activity was seen regardless of the level or extent of injury. The number of active voxels that were detected was greater during active participation than during passive participation. Neuronal activity induced by active movement was seen in the dorsal, ventral and intermediate areas of the spinal cord. During passive movement, neuronal activity was also seen in these areas but there was an overall decrease in the number of active voxels.

The average percent signal change for data acquired during active participation

was 13.6% +/- 1.5% and for passive participation was 15.0% +/-2.8%, which is not significantly different (see Figure 1). The alternating periods of rest and movement (movement occurring during time points 9-16, 25-32, and 41-48) are indicated by a light gray line at the bottom of the graph. The time course of the signal changes fluctuate near baseline during periods of rest and increase dramatically during periods of activity, for both active and passive movement tasks, reflecting the neuronal response to the movement tasks.

As neuronal activity below the injury site was detected in all cases, general characterizations can be made of the distribution. The amount of activity, as indicated by number of active pixels, seen in the spinal cord in this investigation of the injured population is less than that seen in our earlier study involving healthy individuals as a control group (12).

Of the 4 volunteers with ASIA A injuries, spinal fMRI demonstrated bilateral dorsal and ventral neuronal response to the passive task. ASIA B volunteers had results similar in distribution to ASIA A volunteers. In the ASIA C volunteers during active participation, predominantly ventral activity was seen, bilaterally. During ASIA C volunteer passive participation, activity was detected mainly in the dorsal areas, with a small ventral contribution. With the ASIA D volunteers, one set of data was discarded due to motion artefacts caused by the volunteer's spasticity. The remaining ASIA D volunteer's active participation produced predominantly left dorsal activity, in a series in which the volunteer was better able to move the right leg. During passive participation, activity was seen bilaterally in the dorsal and ventral horn with less activity on the right.

In six of the thirty-four series of data collected, it occurred that movement was generated in one limb only (although the contralateral limb was passively moved out of phase by the pedaling device). This unilaterally generated movement corresponded to neuronal activity predominantly on the contralateral side of the spinal cord, in all six cases. For example, one ASIA C volunteer was able to move the right leg only, and neuronal activity was seen bilaterally but with a greater number of active voxels on the left, in the ventral and dorsal horns.

Specific examples from each of the ASIA classification categories are shown and are discussed below (see Figure 2). Apparent activity in the CSF is likely the result of CSF flow and/or blood vessels on the surface or on nerve roots. CSF flow and large blood vessels do not occur inside the cord, and so these same errors are not a concern.

Figures 2A and 2B illustrate the neuronal activity detected in the spinal cord caudal to the injury level in volunteers with no lower limb motor abilities during participation in a passive task. In Figure 2A, results show activity caudal to the injury site of an ASIA A volunteer, on both left and right sides of the cord, in the dorsal and ventral areas. In Figure 2B, an ASIA B motor complete injury volunteer experienced clonus in the right leg during the passive task condition. Results indicate ventral activity on the left side of the cord, contralateral to the recorded movements. Activity is seen in the spinal cord below injury level, although the overall number of active voxels is less than that of healthy volunteers and less than that of the ASIA C and D volunteers.

Figures 2C and 2D represent neuronal activity in response to an active and passive task, respectively, performed by an individual with an ASIA C injury. Activity was decreased in response to the passive task compared with the activity during the active

task, although similar to that seen in response to the passive task in Figure 2B. This volunteer was able to move the right foot only, but the left foot continued moving out of phase by the pedaling device. The activity seen in the lumbar cord consists of left and right ventral and dorsal activity, although activity on the left is predominant. During the passive task, activity was seen in the right dorsal and ventral area, and the left dorsal area.

Figures 2E and 2F show activity in response to active and passive movement in an individual with ASIA D motor incomplete injury. This individual was better able to move the right than left foot during the active task, and results show increased activity on the left side of the cord in both the dorsal and ventral areas. During the passive task, the experimenter was able to move both feet equally, and activity is shown evenly distributed on both sides of the cord, and is found in the dorsal and ventral horns.

Discussion

Neuronal activity was detected caudal to the injury site in all volunteers during passive and active movement tasks. The results demonstrate that neuronal activity occurs in the lumbar spinal cord caudal to an injury site, both in complete and incomplete injured volunteers, and that spinal fMRI is capable of detecting this neuronal response. During active participation, neuronal activity is seen bilaterally in the dorsal and ventral horns, indicating a neuronal response to motor and sensory stimulation as would be expected with purposeful movement. During passive participation, some ventral horn activity is seen, possibly indicating reflex activity, however the bulk of the activity is seen in the dorsal horn, indicating both the dorsal component of the motor terminations as well as the response to sensory stimulation that would be expected with the mechanical

and proprioceptive information produced by this type of movement.

The main pathway involved in the control of voluntary movement, and therefore recruited during the active movement task, is the corticospinal tract. Within the gray matter, corticospinal axons terminate in lamina IV-VII in the dorsal and ventral horns and in the intermediate gray matter (14). This broad distribution of termination of corticospinal neurons contributes to the activity seen in both the ventral and dorsal horns and intermediate areas of the spinal cord in response to the voluntary movement during the active task. Further contribution to the activity in the dorsal horns can be accounted for as the tactile sensory pathways also synapse here (15). The ventral spinothalamic tract conveys light touch and modified forms of tactile sensation such as firm pressure, as would occur during the passive as well as active movement tasks. Proprioceptive feedback, also expected to occur in both passive and active movement tasks, is detected by receptors of the muscle spindles, joints and tendons. The descending branch of these primary afferents terminate in gray matter to establish connections for spinal reflexes, which contributes to the neuronal activity seen in the dorsal horn accounted for by proprioception.

The activity is similar to that seen in healthy volunteers, in that the distribution of activity is similar during active and passive movement tasks and that the amount of activity (i.e. number of active voxels detected) is decreased with passive movement (see Figure 3). Active pedaling with healthy volunteers revealed neuronal activity in the ventral horn and dorsal horn bilaterally with an average percent signal change of 11.9 +/- 1.0%. During passive pedaling, the healthy volunteers elicited neuronal activity in the dorsal and intermediate areas bilaterally at lower lumbar segments and in the ventral horn

and dorsal horns bilaterally at upper lumbar segments with an average percent signal change of 12.4+/- 1.1%. The magnitude of signal change with the spinal cord injured group was 13.6+/- 1.5% and 15.0 +/- 2.8% during active and passive participation, respectively.

Our results show that in cases where the movement is bilaterally generated, the neuronal activity appears to be distributed across both sides of the cord. However, in the cases where the movement was generated unilaterally, the neuronal activity appears to be prominent on the contralateral side of the cord in the ventral horn. Indeed, this contralateral neuronal activity was observed in all six of the incidences where unilateral movement was observed. The activity detected is in agreement with known physiology and together with previous findings of increased contralateral activation in response to sensory stimulation of the injured spinal cord suggest that spinal fMRI is providing reliable results (2). The contralateral activity in the spinal cord seen in response to movement by incomplete spinal cord injured volunteers can be accounted for by circuits that have been implicated in other spinal cord injury studies (16-18) by the ipsilaterally descending corticospinal fibers, or the bilaterally operating neuronal networks that are proposed to form detour circuits in response to spinal cord injury (19). It is possible that the distributions of activity seen in our study are due to a strengthening of ipsilateral corticospinal pathways, or an overactive reflex circuit responding to the afferent input in the absence of descending inhibition. These pathways and their implications for recovery of function in injured persons have recently come under closer investigation (19).

Although it is clear from our results that spinal fMRI is capable of detecting differences in neuronal function in response to a stimulus, it is not possible to determine

the causes of the neuronal activity observed with the data presented in this study. Conversely, the current ASIA assessment scale lacks sensitivity to neural changes. Supplementing the ASIA assessment with detailed activity maps obtained by means of spinal fMRI may prove to be invaluable for the comprehension of spinal cord physiology and for the design of rehabilitation programs. Investigating neuronal function pre-, during-, and post-rehabilitation programs will provide a quantitative measure of rehabilitation progress. Similarly, there is great potential for spinal fMRI to objectively measure neuronal change in response to pharmaceutical intervention, such as for spasticity or neuropathic pain. The use of spinal fMRI for such investigation is shown here to be appropriate. In addition to the benefits of non-invasively detecting neuronal activity caudal to an injury, spinal fMRI can be carried out on any standard clinical MR scanner without requiring special modification.

Further investigation of neuronal circuitry caudal to a spinal cord injury site is required. There are specific difficulties with this clinical population that hinder spinal fMRI progress. The flexor reflex and the crossed extensor reflex are suppressed as a result of activity in descending tracts in healthy people, but can be bothersome for spinal cord injured patients due to lowered threshold (15). The deficiency in descending inhibitory modulation can result in an excessive amount of neuronal activity in the spinal cord caudal to the injury site, manifest as spasticity. In our study, for example, a volunteer who displayed clonus in response to the stimulation of the lower limb task produced motion artefacts too severe for the data to be analyzed with confidence. Similarly, other limitations of our data in this preliminary study, such as the small number of participants and the heterogeneous spinal cord injury sample, prohibit even

general conclusions regarding the physiology of specific spinal cord injuries. Nevertheless, we were able to successfully achieve the goals of this study by demonstrating that spinal fMRI is capable of detecting neuronal activity caudal to a spinal cord injury and that it is possible to characterize this neuronal response.

Conclusions

The results of this study indicate that the quantity and distribution of active voxels demonstrating neuronal activity in the spinal cord in response to both active and passive lower limb movements can be assessed using spinal fMRI in individual patients, with adequate sensitivity to reveal areas of neuronal activity in the cord caudal to an injury, with motor and sensory stimulation. This information is expected to aid with the assessment of spinal cord injury and subsequent rehabilitation. This technique reveals information regarding neuronal function in the spinal cord beyond that which the current ASIA assessment scale is able to provide and is simultaneously less invasive and more informative than electrophysiological methods. This information can be obtained in a non-invasive manner in standard clinical MRI systems, a clear advantage over the existing caudal-to-injury investigation methods.

References

1. Borgens R. Restoring Function to the Injured Human Spinal Cord. Springer-Verlag 2003, pp 138-139.

2. Stroman PW, Kornelsen J, Bergman A, Krause V, Ethans K, Malisza KL, Tomanek B. Noninvasive assessment of the injured human spinal cord by means of functional magnetic resonance imaging. Spinal Cord 2004; 42: 59-66.

3. Stroman PW, Tomanek B, Krause V, Frankenstein UN, Malisza KL. Mapping of neuronal function in the healthy and injured human spinal cord with spinal fMRI. NeuroImage 2002; 17: 1854-60.

4. Stroman PW. Magnetic resonance imaging of neuronal function in the spinal cord: spinal FMRI. Clin Med Res 2005 Aug; 3(3): 146-56.

5. Stroman PW, Krause V, Malisza K, Frankenstein U, Tomanek B. Extravascular proton-density changes as a non-BOLD component of contrast in fMRI of the human spinal cord. Magnetic Resonance in Medicine 2002; 48:122-127.

6. Stroman PW, Kornelsen J, Lawrence J, Malisza KL. Functional magnetic resonance imaging based on SEEP contrast: Response function and anatomical specificity. Accepted with revision Magnetic Resonance Imaging (revised ms accepted June 16 2005).

7. Sykova E, Vargova L, Prokopova S, Simonova Z. Glial swelling and astrogliosis produce diffusion barriers in the rat spinal cord. Glia 1999; 25(1): 56-70.

8. Svoboda J, Sykova E. Extracellular space volume changes in the rat spinal cord produced by nerve stimulation and peripheral injury. Brain Res 1991; 560(1-2): 216-24.

9. Sykova E. Modulation of spinal cord transmission by changes in extracellular K+ activity and extracellular volume. Can J Physiol Pharmacol 1987; 65(5): 1058-66.

10. Fujita H, Meyer E, Reutens DC, Kuwabara H, Evans AC, Gjedde A. Cerebral [15O] water clearance in humans determined by positron emission tomography: II. Vascular responses to vibrotactile stimulation. J Cereb Blood Flow Metab 1997; 17(1): 73-9.

11. Ohta S, Meyer E, Fujita H, Reutens DC, Evans A, Gjedde A. Cerebral [15O]water clearance in humans determined by PET: I. Theory and normal values. J Cereb Blood Flow Metab 1996; 16(5): 765-80.

12. Kornelsen J, Stroman PW. FMRI of the lumbar spinal cord during a lower limb motor task. Magnetic Resonance in Medicine 2004; 52: 411-414.

13. American Spinal Injury Association: International Standards for Neurological Classification of Spinal Cord Injury, Revised 2002; Chicago, IL, American Spinal Injury Association; 2002.

14. Lin VW. Spinal Cord Medicine: Principles and Practice.Demos Medical Publishing, Inc. New York 2003.

15. Kiernan JA. Barr's The Human Nervous System An Anatomical Viewpoint. 7th Edition Lippincott-Raven Publishers 1998.

16. Kawashima N, Nozaki D, Abe M O, Akai M, Nakazawa K. Alternate leg movement amplifies locomotor-like muscle activity in spinal cord injured persons. Jneurophysiol 2005; 93: 777-785.

17. Kautz SA, Patten C, Neptune RR. Does unilateral pedaling activate a rhythmic locomotor pattern in the non-pedaling leg in post-stroke hemiparesis? JNeurophysiol Feb 2006, in press.

18. Ferris DP, Gordon KE, Beres-Jones JA, Harkema SJ. Muscle activation during unilateral stepping occurs in the nonstepping limb of humans with clinically complete spinal cord injury. Spinal Cord 2004; 42: 14-23.

19. Jankowska E, Edgley SA. How can corticospinal tract neurons contribute to ipsilateral movements? A question with implications for recovery of motor functions. The Neuroscientist 2006; 12(1): 67-79.

Figures and Figure captions:

Figure 1: Signal intensity time courses of active regions averaged across participants during active and passive movement follow closely with periods of rest and lower limb movement task, as indicated.

Figure 2: Image orientation: Figures 2A-2F each show six sagittal slices spanning the spinal cord with lumbar segments approximately mid-image. The top row of each figure shows slices taken from the right side (R) of the spinal cord, the bottom row shows slices taken from the left side (L) of the spinal cord. Images are oriented with rostral to the left of each slice, caudal to the right. Dorsal (D, sensory information) is toward the bottom of the cord, ventral (V, motor information) toward the top. Figures 2A and 2B are taken from an ASIA A and ASIA B volunteer, respectively, during passive participation. Figures 2C and 2D are taken from an ASIA C volunteer and 2E and 2F are taken from an ASIA D volunteer, during active and passive participation, respectively.

Figure 3: Two selected sagittal images from Figure 2 are displayed with the rostral toward the top of the image. Selected axial slices are displayed which correspond to the marked level on the sagittal image.

Figure 1

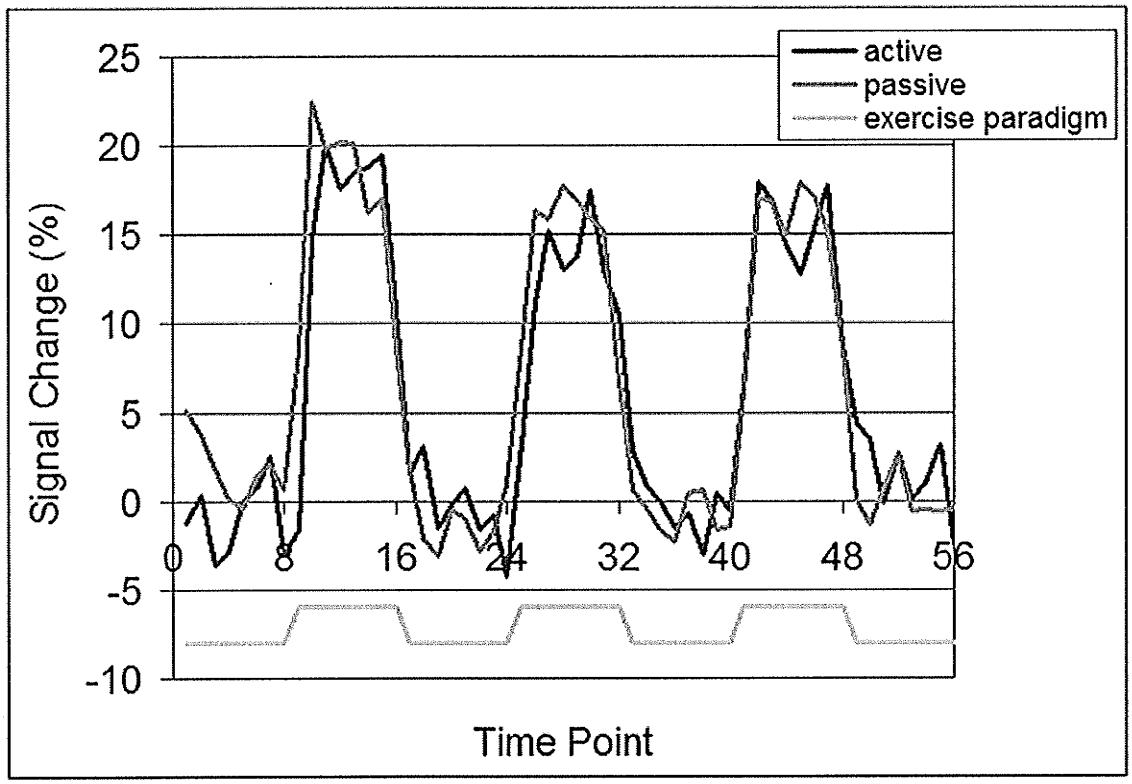
active
passive
exercise paradigm
25
20
15
10
5
0
-5
-10
Signal Change (%)
0
8
16
24
32
40
48
56
Time Point

Figure 2

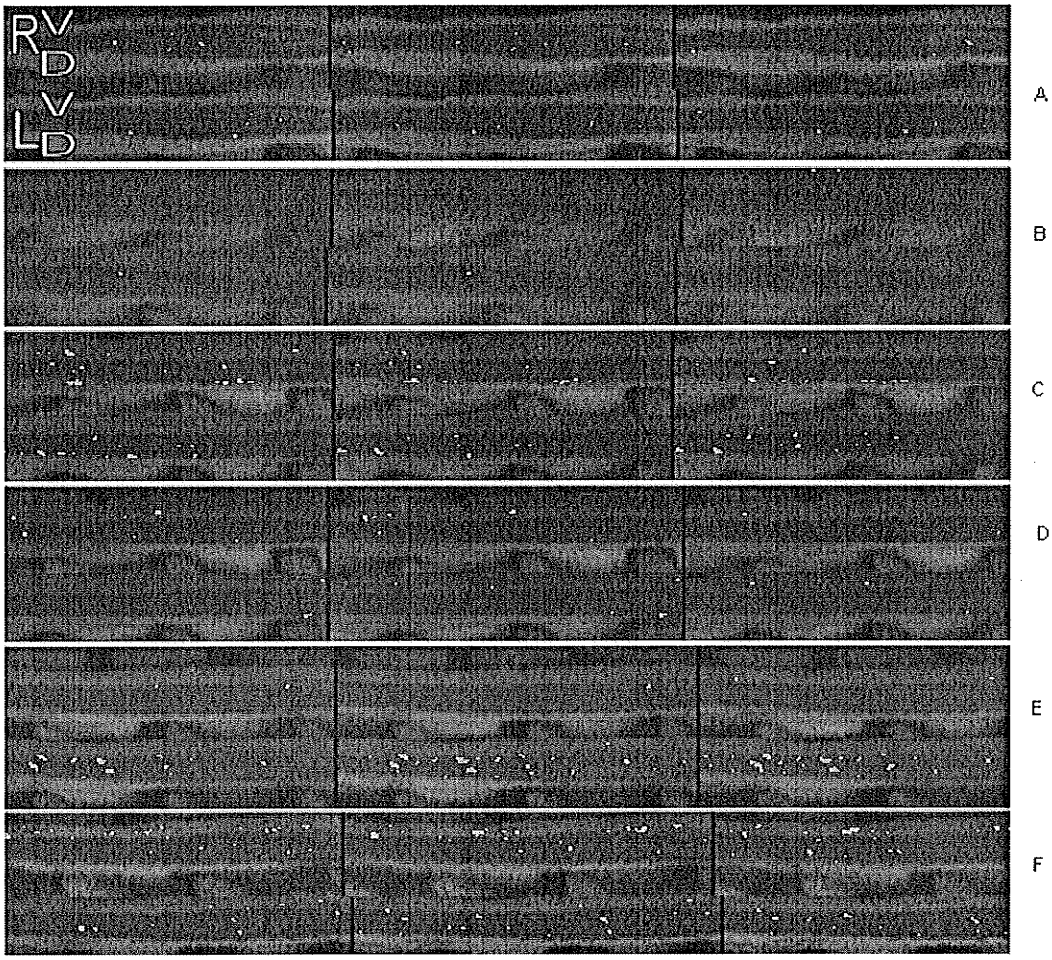

Figure 3

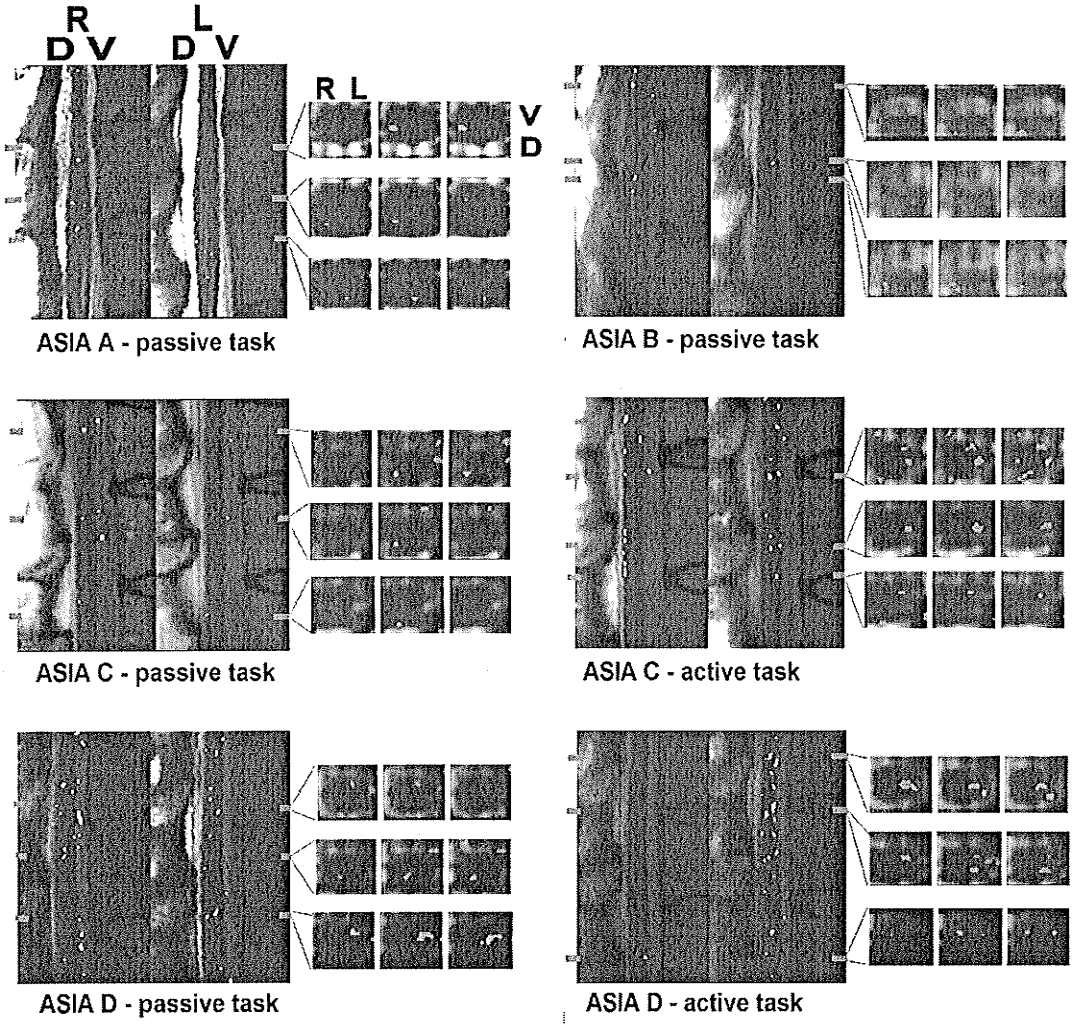
R
L
D V D V
R L
V
D
ASIA A - passive task
ASIA B - passive task
ASIA C - passive task
ASIA C - active task
ASIA D - passive task
ASIA D - active task

Cluster Analysis of Spinal fMRI of a Leg Motor Task

J Kornelsen, BA[1], PW Stroman, PhD [2]

[1] Dept of Physiology, U. of Manitoba, Winnipeg, Manitoba, Canada

Phone: (204) 984-6619

Fax: (204) 984-7036

Email: jennifer.kornelsen@nrc-cnrc.gc.ca

[2] Dept of Diagnostic Radiology, c/o Center for Neuroscience Studies, 231 Botterell Hall,

Queen's University, Kingston, Ontario, Canada K7L 2V7

Running Title: Cluster analysis of spinal fMRI data

Word Count: 2425 words + 7 figures

Correspondence:

Patrick W. Stroman, PhD
Associate Professor - Canada Research Chair in Imaging Physics
Depts of Diagnostic Radiology and Physics
c/o Center for Neuroscience Studies
231 Botterell Hall
Queen's University
Kingston, Ontario
Canada K7L 2V7
phone 613-533-3245
stromanp@post.queensu.ca

Abstract

Purpose: To identify false positive activations in spinal fMRI data obtained during a lower limb movement task.

Materials and Methods: Functional MRI data of the lumbar spinal cord were previously obtained at 1.5 T with a single-shot fast spin-echo imaging method, from thin contiguous sagittal slices spanning the cord. Volunteers participated in active and/or passive lower limb movement tasks during stimulation periods and remained still during baseline periods. Active voxels were identified by means of a correlation to a model paradigm. Cluster analysis is carried out to separate active pixels based on the signal intensity change to produce activation maps and time course graphs for each cluster.

Results: The resulting clustered activity maps demonstrate active pixels in the spinal cord gray matter occurring in the range of 5 through 15% signal intensity change, randomly located active pixels in signal intensity change below 5%, and active pixels located primarily in the area surrounding the spinal cord in the signal intensity change above 15%. Accompanying time course graphs support the findings.

Conclusion: Cluster analysis of the spinal fMRI data acquired during the movement tasks reveals important information regarding the identification of true and false positive activations.

Key Words:
Cluster analysis, false positive, spinal cord, human, fMRI

Introduction

Functional magnetic resonance imaging (fMRI) reveals functional activity of the spinal cord and brain by means of signal intensity changes between different activity states (1). The signal change that is important in revealing neuronal activity is that which occurs consistently in response to a presented stimulus and not in the absence of the stimulus. There are, however, additional mechanisms which can contribute to signal changes which do not represent a neuronal response to the stimulus obtained, including thermal noise, physiological noise, and motion (2), which confound the detection of neuronal-activity-related signal changes. Thermal noise arises from receiver electronics and the tissue being imaged, whereas physiological noise arises from metabolic changes, blood flow, CSF flow, spinal cord and brain pulsation or motion with the heart beat, cardiac and respiratory motion, etc. Noise arising from motion in this context is meant to be any other motion of the person being imaged. As a result of the motion of the spinal cord and proximity to the lungs and heart, fMRI of the spinal cord is particularly sensitive to these sources of physiological noise. Finally, motion associated with the functional task itself can give rise to additional noise (3). In the present study, functional MRI of the spinal cord is carried out in order to investigate motor activity involved with active and passive leg movement. This is therefore expected to represent effectively the worst-case-scenario for fMRI in terms of the potential sources of noise.

Paradigm dependent statistical methods such as correlation analysis or t-tests are commonly used in analyzing fMRI. A statistical analysis method which is independent of the paradigm is desirable when attempting to avoid imposed structure on the data. Clustering is one such method used to supplement correlation or t-test analyses and can

be as simple as grouping pixels based on their signal intensity time courses or magnitude of signal intensity change from baseline. These clusters can be displayed to demonstrate their locations and thereby identify spatial relationships that exists between the pixels. Spatial and temporal relationships between pixels provide support for identifying that the mechanisms contributing to the signal intensity changes are related (4). Therefore, cluster analysis can be used to discover patterns in data without the requirements of fitting to a study paradigm or being subjected to experimenter expectation or bias.

Clustering is particularly useful for detecting Type I errors which, in the context of this study is defined as a voxel being identified as being active, in error. Characterization of signal intensity changes from baseline is typically achieved by averaging over all active voxels in the image data regardless of whether they fall within anatomically relevant areas such as the gray matter. By clustering, it is possible to detect if the active pixels that occur within the gray matter, and are thus considered to be true positives, tend to occur within a particular range of signal intensity magnitude, that is acceptable according to conventional fMRI theory. The pixels occurring outside of the gray matter, with corresponding signal intensities that are either too low or too high based on conventional fMRI theory (5,6), can be considered false positives. These activations are likely due to physiological motion or artefacts rather than neuronal function.

In this study, clustering was based solely on the percent signal change from baseline during the stimulation periods. This approach is based on the hypothesis that Type I errors are believed to arise due to physiological noise and task-related motion, which can cause relatively large signal changes. Therefore, clustering based on the magnitude of signal intensity change may be able to discriminate errors from true

neuronal-activity-related signal changes. This identification can be made based on the anatomical location of the areas of activity given that true neuronal activity can occur only in the spinal cord gray matter, and this is a clearly localized anatomical region. As clustering is independent of the paradigm, it is also helpful to view the time course of the pixels in a given cluster to see if the activity follows the pattern of the stimulus.

Methods

Data acquired in a previous study was subjected to investigations by means of cluster analysis for the present study (7). In the previous study, spinal fMRI was carried out in a block design with three stimulation periods. Images centred on the T12 vertebra were acquired repeatedly during alternating rest and stimulation periods for a total of 56 time points recorded at 1.5 T in a General Electric Signa Horizon LX clinical MR system. Functional time course data were obtained using single-shot fast spin-echo imaging, as per our established methods with sets of eight contiguous 2.8 mm thick sagittal slices. Data were analysed using custom-made analysis programs written in MatLab software (MathWorks, Natick MA). Prior to analysis, a line was drawn manually along the anterior edge of the spinal cord in a midline sagittal image taken from the functional data set to indicate the spinal cord position and curvature. The data at each time point of the functional series were combined into a three dimensional volume and linearly interpolated to 0.5 x 0.5 x 0.5 mm cubic pixels. The volume was re-sliced transverse to the cord according to the manually drawn reference line, and smoothing was applied only in the rostral-caudal direction. The correlation between a model paradigm and the signal intensity time courses of each pixel was computed to produce a map of correlation t-

values. A t-value threshold of 2.0 (p=0.05) was chosen to identify pixels as active, and these pixels were plotted in colour over a gray-scale reference image that was produced by averaging the images obtained at the 56 time points.

Cluster analysis was performed for each series of data and the resulting activation maps were displayed in the axial orientation. Clusters were formed into groups based on multiples of 5% signal intensity change from baseline. Cluster 1 contained all active pixels with signal intensities ranging from 0.1% up to less than 5%, Cluster 2 contained all active pixels with signal intensities ranging from 5% to less than 10%, and so on. Cluster 6 contained all active pixels with signal intensities above 25%. Negative clusters were also formed in these same ranges, with Cluster -1 containing all active pixels with signal intensities ranging from -0.1% to greater than -5%, through Cluster -6 containing all active pixels with signal intensities below -25%. A map displaying the active pixels for each cluster for each series of data collected was created along with a graph of the average time course for that cluster's activity. With 33 series of data and 13 maps per series, this produced a total of 429 maps and accompanying time course graphs.

All negative and positive activations were also displayed on a combined activity map for each series. To represent magnitudes of signal changes, the active pixels were colour coded through shades of red for all positive activations and through shades of blue for all negative activations. This enabled display of the overall distribution of positive and negative activity for each series of data.

Results

The distribution of the apparently active voxels in the positive clusters follows the expected pattern both in terms of location as well as time course (See Figures 1-6). In general, cluster 1 revealed little activity, with a few isolated voxels following no apparent spatial pattern. Cluster 2 revealed activity distributed partly in gray matter as well as the surrounding areas. Cluster 3 contained the majority of the activity that fell in the gray matter. More active pixels were detected in cluster 3 than in cluster 2. Cluster 4 revealed apparent activity falling mainly toward the edges of the cord with a moderate amount of activity remaining in the gray matter. Cluster 5 revealed activity falling mostly in the area surrounding the cord. Little to no cluster 6 activity fell within gray matter regions. The average time course data for cluster 1 shows an apparently random pattern. Clusters 2 through 6 are all in good agreement with the boxcar model paradigm, but clusters 2 and 3 have the least variation across the clusters at each time point during the exercise periods.

The negative clusters loosely followed the same general pattern, however the clusters -1 through -3 seemed to have a more wide spread distribution of activity over the entire image, while active pixels in clusters -4 through -6 had a tendency to fall towards the edges of the images as did the positive clusters.

In the combined activity maps it is also clear to see that the negative signal intensity changes tend to fall within the CSF regions. (See Figure 7) The positive activations are less prominent and tend to occur in the gray matter and at the top centre of the image. The pattern of positive distribution appears to follow a segmental pattern

whereas the distribution of the negative clusters does not appear to follow any segmental pattern, in other words, it appears to occur evenly distributed over all slices.

Discussion

Clustering of spinal fMRI data is able to reveal and separate true neuronal activity from false positive activity. As predicted, the active pixels that occur in the appropriate range of magnitude according to conventional fMRI (5-15%) occurred in the gray matter and the time courses followed the study paradigm. The high signal intensity (>25%) active pixels occur in the CSF or the area surrounding the cord, where both physiological and/or stimulus correlated motion artefacts can occur. The low signal intensity (<5%) active pixels thought to be due to random noise were expected to occur in any area of the image and the time courses were not expected to follow the paradigm, and was as observed in cluster 1 in all series of data.

The results show that the largest signal changes were quite well localized to the spinal cord/CSF boundary and surrounding cord areas. These signal changes are too large to be attributed to any known or theorized fMRI contrast mechanism, and are therefore not believed to arise as a consequence of neuronal activity. Similarly, negative signal changes were also localized to this region of CSF and the boundary in the larger signal change range. The meaning of negative signal changes has not yet been determined, but in this case they appear to arise as a result of CSF movement or other physiological noise. In contrast, activity within the gray matter mainly occurred in clusters in the 5-15% signal change range. This intensity range is consistent with the combination of BOLD and SEEP contrast that is employed in the established spinal fMRI

method. This finding further supports the validity of spinal fMRI as an important tool in the study of spinal cord function.

It is not an assumption of this study that all areas of activity within the gray matter and within the acceptable signal intensity range, can be concluded to be true positives. There is still the possibility that these remaining activations are also false positives. As shown in Figure 1a and 1b, the time course of the signal changes occurring in the 0.1%-5% range appeared random and the location of the active pixels occur randomly across the image. These active pixels could potentially lie within gray matter, representing a possible false positive activation within the gray matter. It would be beneficial to eliminate these active pixels from the activation map, as they are may misrepresent true positive activity brought about by neuronal activation. Although it is unlikely that we can eliminate the source of random noise as it cannot be anticipated during image acquisition, it is shown here to be possible to eliminate a contribution from random noise during the data analysis and therefore produce an activation map that reveals true positive activity with greater confidence.

Similarly, the active pixels occurring in Cluster 5 and Cluster 6 are unlikely to be true positive activations based on signal changes that are too large based on fMRI theory and the tendency for the active pixels to lie outside of the cord. The time courses for these signal changes reveal that the activations do roughly follow the study paradigm and so are surmised to originate from trunk motion as the volunteer participates in the task in addition to the bulk motion of the spinal cord due to CSF flow, which is influenced by cardiac pulsation. It would be beneficial to eliminate these active pixels from the activation map as well in order to produce a map that reveals the most likely candidates

of true neuronal activity.

In an earlier study (3), the signal intensity change for active pixels during the identical lower limb motor task were reduced substantially by identifying pixels at the edge of the spinal cord and setting these apart from the analysis, under the assumption that they were caused by motion. After eliminating the active pixels surrounding the cord, the signal changes observed with active and passive tasks were reduced to 11.9+/-1.0% and 12.4+/-1.1% from 15.4+/-1.3% and 18.3+/-1.4%, respectively. In the present study, the activations which occur in the 10 to less than 15% range, cluster 3, are the best fit to the paradigm both in terms of the time course map as well as the location of pixels. This further supports the theory that true neuronal activity related activations occur within this range of signal intensity change.

Conclusions

In order for spinal fMRI to be improved as a reliable method for both research and clinical purposes, it is important that the signal intensity changes we are detecting are those that arise as a consequence of a change in neuronal activity. In order to determine this, it was necessary to first identify areas of signal change that are correlated with the stimulation paradigm but are not arising from neuronal activity. Cluster analysis has been shown to be useful in identifying and separating the true from false positive activations. This will allow future fMRI studies to be carried out in such a way that false positive activation will be reduced, or that these false positive activations will be identifiable and possible to eliminate during analysis. This study has enabled us to gain an understanding of the source or origin of the false positive activations which allows

these areas of signal change to be identified, and we are therefore able to identify with greater confidence the true positives, that is, those signal changes that are occurring in response to neuronal activity induced by the stimulus.

References

1. Ogawa,S. *et al.* Functional brain mapping by blood oxygenation level-dependent contrast magnetic resonance imaging. A comparison of signal characteristics with a biophysical model. *Biophys. J.* **64**, 803-812 (1993).

2. Hyde,J.S., Biswal,B.B., & Jesmanowicz,A. High-resolution fMRI using multislice partial k-space GR-EPI with cubic voxels. *Magn Reson. Med.* **46**, 114-125 (2001).

3. Kornelsen,J. & Stroman,P.W. fMRI of the lumbar spinal cord during a lower limb motor task. *Magn Reson. Med.* **52**, 411-414 (2004).

4. Baumgartner,R., Windischberger,C., & Moser,E. Quantification in functional magnetic resonance imaging: fuzzy clustering vs. correlation analysis. *Magn Reson. Imaging* **16**, 115-125 (1998).

5. Logothetis,N.K., Pauls,J., Augath,M., Trinath,T., & Oeltermann,A. Neurophysiological investigation of the basis of the fMRI signal. *Nature* **412**, 150-157 (2001).

6. Logothetis,N.K. & Wandell,B.A. Interpreting the BOLD signal. *Annu. Rev. Physiol* **66**, 735-769 (2004).

7. Kornelsen,J. & Stroman,P.W. Detection of the neuronal activity occurring caudal to the site of spinal cord injury that is elicited during lower limb movement tasks. Submitted to Spinal Cord, May, 2006.

Figures and Figure Captions:

Figures 1-6:

Figures 1 through 6 show a representative (a) cluster map and (b) accompanying time course graph obtained for clusters 1 through 6, respectively, for one series of data from one subject. Positive activations are shown in colour over a gray-scale image. The spinal cord is shown in axial orientation, with the right side of the cord to the left of the image, and the dorsal aspect of the cord towards the bottom of each image, displayed in 0.5 mm thick slices. The images begin rostrally at the top left square and continue caudally to the bottom right square.

Figure 7:

Spinal cord slices are shown in axial orientation, with the right side of the cord to the left of the image, and the dorsal aspect of the cord towards the bottom of each image, displayed in 0.5 mm thick slices. The images begin rostrally at the top left square and continue caudally to the bottom right square. Positively activated pixels are shown colour coded through shades of red, and negatively activated pixels are shown colour coded through shades of blue. The overall distribution of positive and negative activations reveals that negative activations appear to surround the spinal cord and this distribution is constant in the rostral/caudal direction, whereas the positive activations appear to occur mainly in the spinal cord gray matter following a segmental distribution and in the edges of the images again constant in the rostral/caudal direction.

Figures 1-6

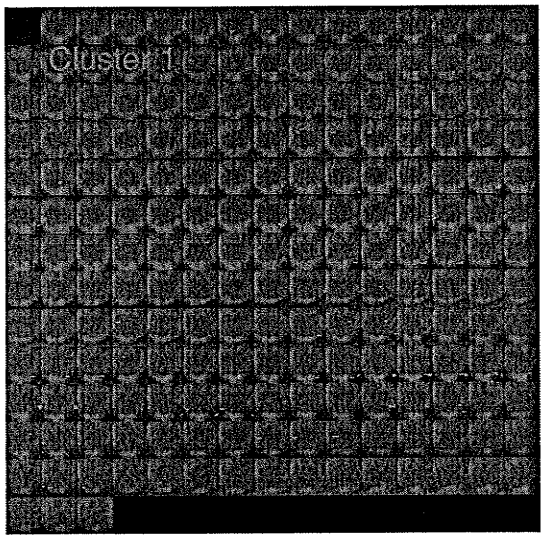
Cluster 1

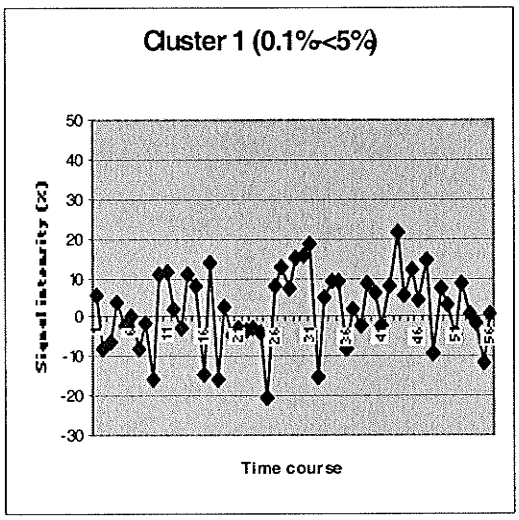
Cluster 1 (0.1%<5%)
Signal intensity (%)
Time course

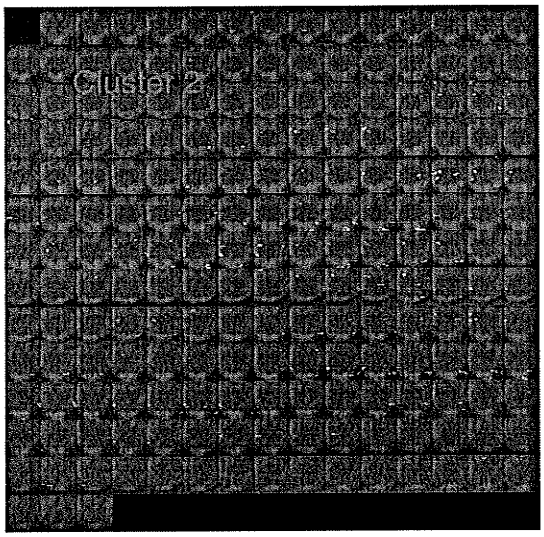
Cluster 2

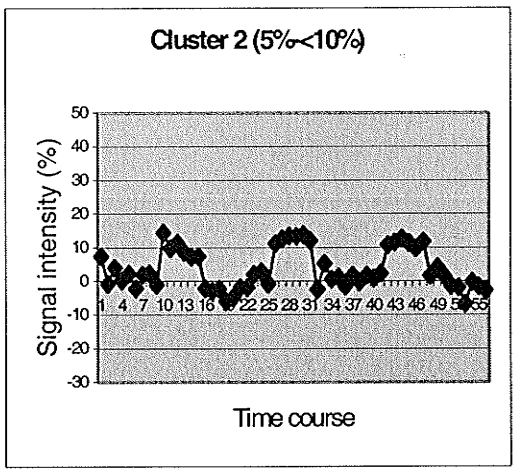
Cluster 2 (5%<10%)
Signal intensity (%)
Time course

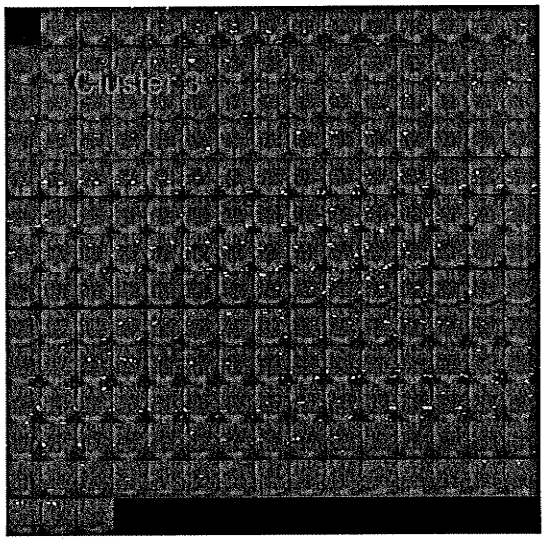
Cluster 3

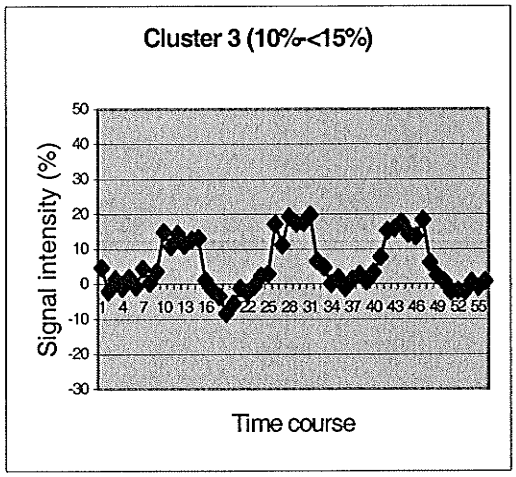
Cluster 3 (10%<15%)
Signal intensity (%)
Time course

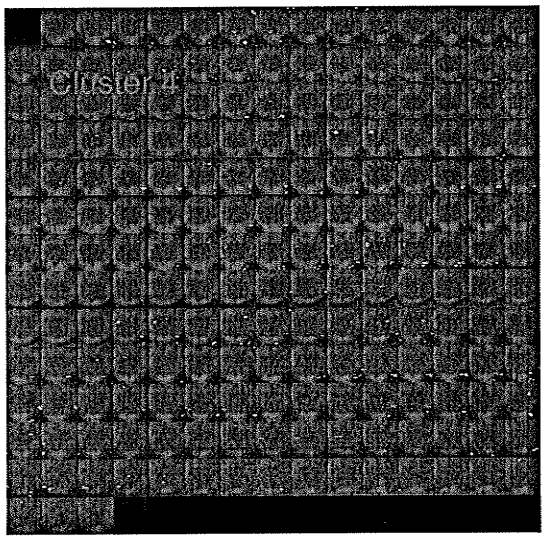
Cluster 4

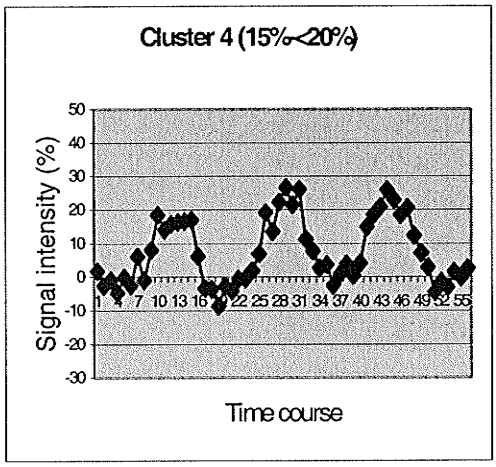
Cluster 4 (15%-<20%)
Signal intensity (%)
50
40
30
20
10
0
-10
-20
-30
1 4 7 10 13 16 22 25 28 31 34 37 40 43 46 49 52 55
Time course

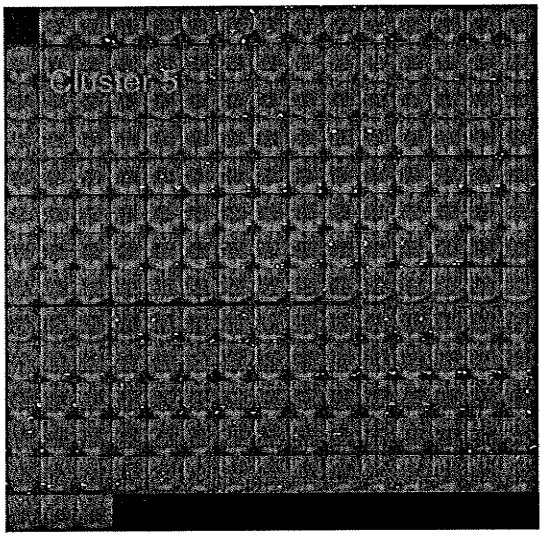
Cluster 5

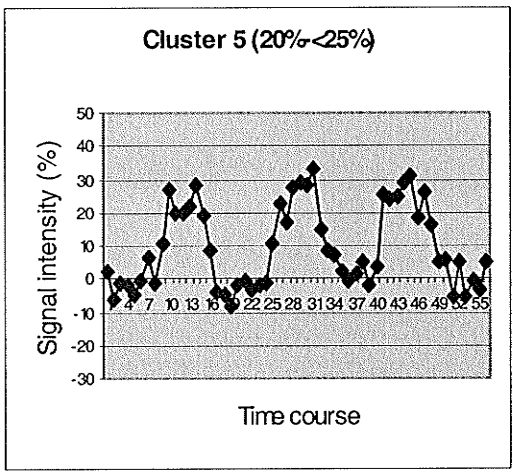
Cluster 5 (20%-<25%)
Signal intensity (%)
50
40
30
20
10
0
-10
-20
-30
Time course

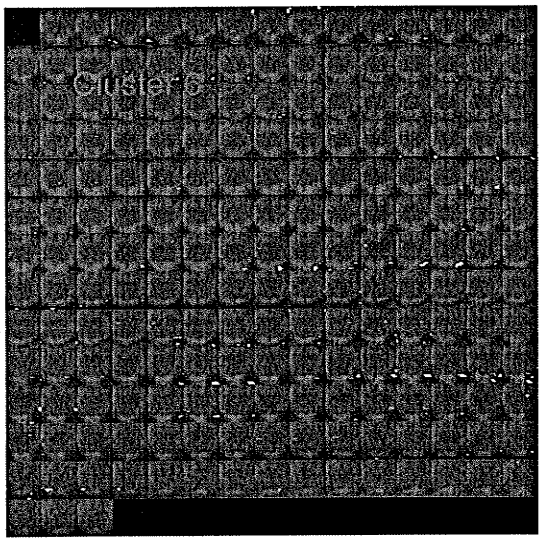
Cluster 6

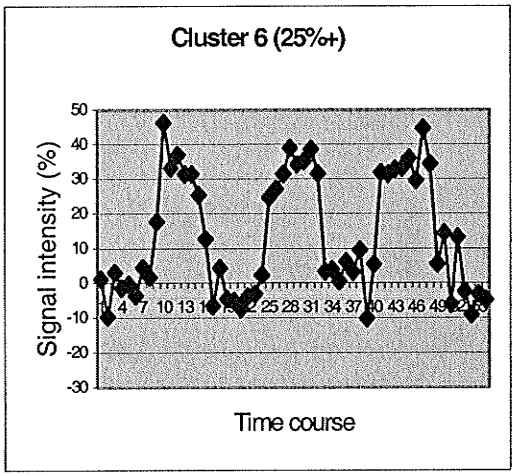
Cluster 6 (25%+)
Signal intensity (%)
50
40
30
20
10
0
-10
-20
-30
Time course

Figure 7

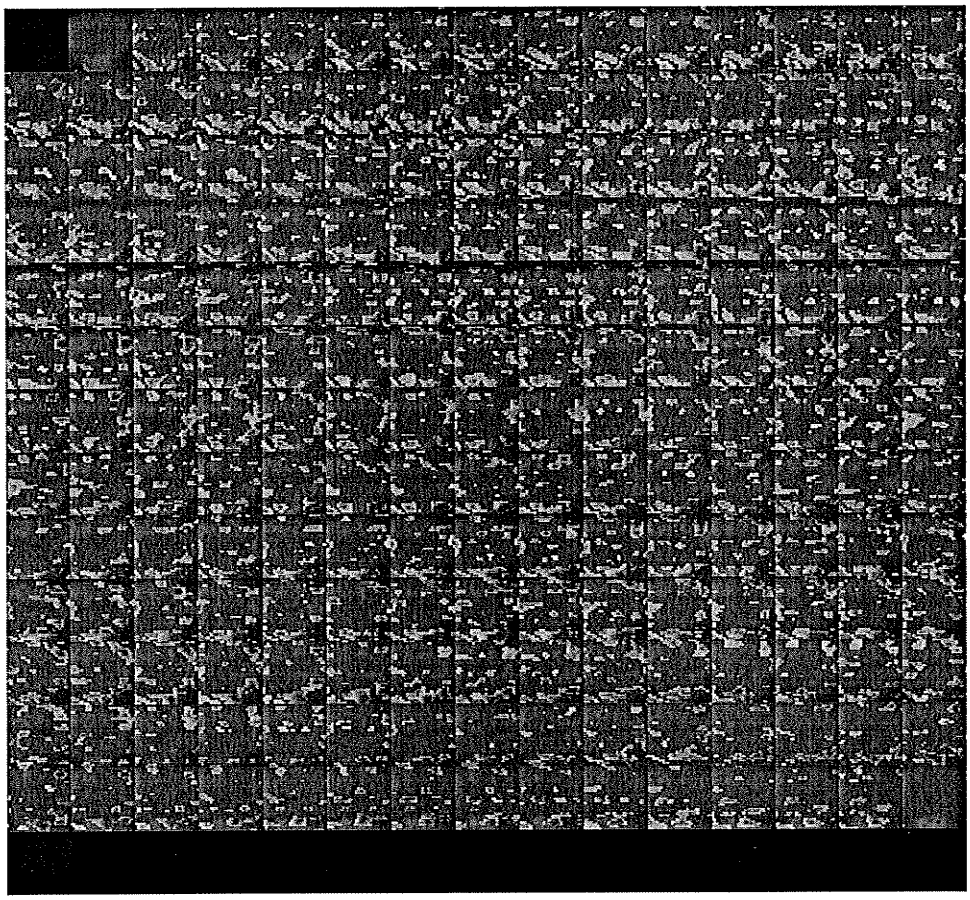

General Discussion

The goal of this dissertation was to contribute to the development of spinal fMRI as a tool for investigating spinal cord physiology. To achieve this, four investigations were performed. The first was aimed at establishing a method for studying lower limb movements with spinal fMRI. The second aimed to establish a sagittal imaging technique that increases the area of spinal cord we can image while reducing the artefacts that commonly afflict this type of imaging. The third aimed to detect and characterize the activity in lumbar cord caudal to an injury that arises from lower limb movement, using spinal fMRI. The fourth aimed to distinguish true from false positive activations in spinal fMRI data so that images can be acquired optimally and we can be confident in our results. Each investigation was successful in reaching its goal and important progress was made toward the advancement of spinal fMRI for reliable research and practical clinical use.

Part 1 was inspired by the need for a method with which to investigate lower limb movement tasks with spinal fMRI. The literature at the time included investigations of the use of spinal fMRI of the cervical cord during movement tasks of the hands; although this requires movement of the volunteer, movement of the hands does not cause any substantial movement of the trunk (Yoshizawa et al. 1996; Stroman et al., 1999; Madi et al., 2001). Spinal fMRI with sensory stimulation of the upper and lower limbs was also investigated, as this causes no movement of the volunteer and was therefore a good choice for beginning development of spinal cord functional imaging (Stroman et al., 2001a,b). A method was required for investigating motor activity of the lumbar spinal cord, but in such a way that did not bring about movement of the trunk. A device was

needed that would allow for a standardized motor activity to be performed that could be regulated to allow for comparison across subjects, constructed of a material that was compatible with an MR environment and that would fit the scanner. Initially, a pedal similar to a bicycle wheel was designed and built, but during hardware testing it became apparent that the movement of the entire leg required to pedal the device caused taller people's knees to hit the top of the inside of the magnet bore. In addition, this full limb movement caused too much movement of the trunk and therefore would cause motion artefacts in the images. The pedal was then redesigned in such a way that the volunteer could perform a movement task of the ankle. The pedal was built such that the feet could be secured to the pedals and perform an alternating flexion and extension movement while the thighs were stabilized. This incurred less motion of the trunk, while still allowing a rhythmic alternating lower limb movement which could be performed actively or passively by the experimenter moving the pedals manually.

This pedal was then used to investigate the neuronal response detectable in the spinal cord during an active and passive lower limb movement task, using fMRI. Results showed that spinal fMRI is able to detect reliable neuronal responses in the cord to both tasks, that the time course of the signal intensity changes were in agreement with the study paradigm, and that the location of active pixels was in agreement with known spinal cord physiology. Active and passive pedaling was shown to elicit average signal intensity changes of similar magnitude, at approximately 12%. The main shortcoming in this study was that the images were acquired in axial orientation and so only a small extent of cord was imaged. This study was, however, instrumental in the development of

the use of spinal fMRI for investigating motor activity as it validated the technique and provided a control population with which to compare further clinical populations.

The purpose of Part 2 of this dissertation was to improve the spinal fMRI method so that a larger extent of cord could be imaged. In order to accomplish this, a method was developed that resulted in a greater length of cord to be imaged, approximately 12 cm, as well as results that could be displayed in three dimensions. This method provides voxel dimensions that match more closely to the shape and size of the anatomical volumes of the Rexed's laminae, so that each voxel spans homogeneous tissue volumes as much as possible. This method is distinct from the sagittal slice methods attempted by others (Backes et al., 2001; Madi et al., 2001) because the slices are set as thin as the MR hardware allows, disregards the signal-to-noise ratio and leaves no space between slices. The difficulty with obtaining this volume of coverage is due to partial volume effects, an issue which was overcome by obtaining the images as thin as possible and reformatting the data into a three dimensional volume which was interpolated and resliced for analysis with our established methods (Kornelsen and Stroman, 2004). Again, the resulting activity maps demonstrated activity consistent with spinal cord neuroanatomy. In fact, it revealed subsegmental distribution of activity, which has been shown previously in electrophysiology studies of the rat (Takahashi et al, 2003) but not before with spinal fMRI. This subsegmental distribution was again shown in Part 3 which also used the improved method.

The development of the sagittal imaging method is of great value for both research and clinical purposes. Obtaining functional images with this improved methodology allows for activity maps to be displayed in axial, coronal and sagittal

orientation with improved spatial resolution in the superior/inferior direction. In addition to demonstrating details of subsegmental organization in the spinal cord, neuroanatomical detail such as spinous processes and position of nerve roots, as well as the cervical and lumbar enlargements were identifiable, structures beneficial for landmarking. In addition, results were normalized and consistent right/left and anterior/posterior dimensions were constructed, which facilitates comparison within and across subjects. With further investigations using this method, optimal normalization dimensions can be produced, from which a spinal cord atlas could be assembled. This would be an important advancement in spinal cord physiology research, as it would greatly facilitate comparison between subjects and between studies.

Part 3 combined the investigation of lower limb active and passive movement from Part 1 with the improved imaging method developed in Part 2, and was successful in showing that spinal fMRI is capable of detecting neuronal activity caudal to an injury site. This is a crucial step in bringing spinal fMRI closer to practical clinical use. In this study, active and passive movement tasks were performed by spinal cord injured volunteers. Activity was detected in all volunteers regardless of the extent of injury. During both active and passive participation, activity was seen caudal to the injury site, although the number of active voxels detected with passive movement was less than with the active movement task. The average percent signal changes were 13.6% during active participation and 15.0% during passive participation, which are slightly larger than those of healthy volunteers during the identical tasks. This could be accounted for, however, by the increased resolution and the reduced partial volume effects with the improved sagittal imaging method over the original axial orientation method. The activity is

similar to that seen in healthy volunteers, in that the distribution of activity is similar during active and passive movement tasks and that the amount of activity (i.e. number of active voxels detected) is decreased with passive movement.

An interesting pattern was identified in the data that is worth discussion, although further investigation of this phenomenon is required before conclusions can be made regarding the underlying physiology. Our results show that in cases where the movement was bilaterally generated, the neuronal activity appeared to be distributed across both sides of the cord. However, in the cases where the movement was generated unilaterally, the neuronal activity appeared prominent on the contralateral side of the cord in the ventral horn. Indeed, this contralateral neuronal activity was observed in all six of the incidences where unilateral movement was observed. However, the literature shows that with complete spinal cord injured volunteers locomotor-like activity in one limb can activate rhythmic locomotor activity in the contralateral limb. Kawashima et al. (2005) carried out an investigation focused on alternating leg movements of human bipedal locomotion to determine if the spinal central pattern generator (CPG) is involved in the neural mechanisms of locomotor-like muscle activity in the contralateral limb by employing the leg movement pattern which should contribute to the generation and coordination of this muscle activity. Results suggested that the afferent input from the contralateral leg plays a role in amplifying the induced locomotor-like muscle activity in the lower limbs and that the contralateral leg movement should be out of phase for the muscle activity of the ipsilateral leg to be well amplified. In addition to the reflex response induced by the rhythmic muscle and tendon stretches, contribution from the interaction of the CPG in the spinal cord was implicated. This suggests the existence of

neuronal circuits enabling interlimb coordination within the spinal cord, which they reveal to be intact in spinal cord injured persons. Similarly, this phenomenon has been studied in persons with injury due to stroke, where it was suggested that unilateral pedaling movement activated a pattern of rhythmic alternating muscle activity in the contralateral non-pedaling leg. Furthermore, this effect appeared to be more clearly demonstrated in the more severely impaired individuals (Kautz et al., 2006).

It has also been shown that the complete injured human spinal cord can use sensory information about ipsilateral limb loading to increase muscle activation even when there is no limb movement. It was shown that movement and loading in one limb can produce rhythmic muscle activity in the contralateral limb even when it is stationary and unloaded (Ferris et al, 2004). The results of these investigations into the ability of one limb to produce muscle activity in the other limb in complete spinal cord injured persons indicate intact spinal cord circuits, either in the form of reflexes or CPG activation. This could account for the neuronal activity induced by the movement tasks in the study described in Part 3. Alternately, the neuronal activity reported in Part 3 could be accounted for by the ipsilaterally descending corticospinal fibers and the bilaterally operating neuronal networks that are proposed to form detour circuits in response to spinal cord injury. Given that the lateral corticospinal tract is damaged unilaterally, and there is therefore no voluntary movement on that side of the body, it is possible that the ipsilateral corticospinal tract from the same hemisphere becomes strengthened. This strengthened tract descends on the contralateral side to the impaired limb, and synapses with interneurons in lamina VII on the contralateral side. These interneurons cross at the segmental level and branch extensively to lamina VII, VIII and

IX, which could account for the increase in neuronal activity seen in the ventral horn associated with the non-moving limb. As presynaptic potentials are known to correlate to the MR signal intensity more so than the neuronal spiking rate (Logothetis, 2001), it is possible that the accumulation of these sub-threshold potentials is represented in the MR images whereas the spiking of neurons on the functioning side of the cord produces comparatively lower signal intensity. These ipsilateral pathways and the implications for recovery of function in injured persons have recently come under closer investigation (Jankowska and Edgely, 2006). It is therefore possible that the altered distribution patterns seen in our study were due to a strengthening of ipsilateral corticospinal pathways, or more likely, an overactive reflex circuit responding to the afferent input in the absence of descending inhibition. It is also possible that these circuit pathways at the level of the spinal cord are more active in spinal cord injured persons than in non-injured persons in response to lower limb movements due to the CPG mechanisms that are thought to exist in the lumbar spinal cord levels. A detailed mapping of these reflex circuits could prove invaluable for the comprehension of spinal cord physiology and for the design of rehabilitation programs. Specifically, the role of the central pattern generator in bilateral as well as unilateral lower limb movement in healthy and spinal cord injured persons requires further investigation. The use of spinal fMRI for such an investigation has here been shown to be appropriate and could provide considerable insight into spinal cord physiology.

Although spinal fMRI is not yet ready for routine clinical use in examining spinal cord injuries, it is certainly fit for use in assessing recovery of function strategies. As discussed in Part 3, the ability of other measures such as somatosensory evoked

potentials or H-reflex that are able to assess residual function caudal to injury is limited, as they reveal the effect, but not the location, of damage along a conduction pathway. These methods are invasive and are not in routine clinical use. The ASIA assessment scale is routinely used to assess and classify injuries and residual function, but is lacking in sensitivity for neuronal change. Spinal fMRI will be useful in the future as intervention strategies develop, in that it can be used to detect differences in neuronal activity pre- and post- treatment. Spinal fMRI could become an important tool for assessing the efficacy of interventions, as currently the ASIA assessment scale is in use to follow progress in research interventions, and this is, as mentioned, unable to detect neuronal changes. Similarly, assessing improvement of conductivity across incompletely damaged tracts in response to 4-aminopyridine or other drug treatments would be possible with spinal fMRI. The suspected false negative findings of the 4-AP trials could be resolved with the use of spinal fMRI, as it is a measure with increased sensitivity to neuronal change. Likewise, spasticity drug trials could also greatly benefit, again because presently there are few non-invasive measures available to objectively see changes in neuronal activity.

In Part 3, the small number of volunteers, further confounded by the heterogeneous population, does not afford conclusions regarding physiology to be made. Future studies using the pedaling device with a spinal cord injured population would be required in order to draw conclusions regarding residual function in the spinal cord following injury. A number of other variables are also factors with this population; time since injury, later developments within the cord such as syrinx development, susceptibility to spasticity or clonus, medication history, etc. It would be difficult to find

a large number of patients with identical injuries at the same stage past initial injury with similar symptoms and on the same medications in order to test a homogeneous sample. This is an obvious difficulty with conducting studies with this patient population. Another factor to consider is that the physiology of autonomic control is altered after spinal cord injury. This can result in autonomic dysreflexia, a symptom of which is uncontrollable spiking of blood pressure. As the MR signal is dependent on the blood flow, for both BOLD and SEEP contrast, this could alter the results obtained for this population. The other difficulty specific to this population is the potential for spasticity or clonus to occur during imaging, especially upon participating in the movement tasks. Should spasticity or clonus occur as a result of sudden initiation of movement, this would occur during the stimulus time points of the paradigm, and the analysis would reveal neuronal activity during spasticity or clonus rather than neuronal activity during voluntary movement. If this could be induced reliably, this would be an interesting study in itself. This proposed study would be difficult, however, in that the data would need to be free of motion artefacts, which are likely to occur during clonus. In our study, we only lost one subjects' data due to motion artefacts caused by clonus, while the other eleven sets of data were sufficiently unaffected by motion for analysis and interpretation.

Part 4 dealt with the questions that remain about the source and identification of false positive activations. These are voxels that appear to change signal intensity each time a stimulus is applied and so are identified as active regions but are not related to neuronal activity. The cluster analysis revealed that the magnitude of the signal intensity changes can be used to separate the true from false positive activities and that those that occur within the acceptable signal change range also occur in the gray matter of the

spinal cord. Those active pixels with signal changes outside of the acceptable range were found to occur in the areas surrounding the spinal cord. This study showed that by using a paradigm independent analysis method, important features of the activity maps can be revealed. This information can be useful for determining the hemodynamic response function as well as the optimum time course model for future studies. With an optimal time course model for the true or false positive activations identified, distinguishing and separating true and false positives within the data and resulting activity maps is possible. Thus, cluster analysis based on magnitude of signal intensity change has proven to be an important step toward the goal of improving spinal fMRI data acquisition and analysis to eliminate the false positives from the acquisition, or at least, the results.

Future directions

The development of the pedal now affords the researcher a tool for investigating rhythmic alternating lower limb movement with spinal fMRI. Imaging of the lumbar spinal cord during pedaling could reveal important information regarding the function of the central pattern generator. Spinal cord physiology research can be greatly advanced with this technique.

Future spinal fMRI studies will likely benefit from the reduction of noise of cardiac origin. As this issue is currently being investigated, it is likely that in the near future modeling of the time course of the non-neuronal related activity will reduce or eliminate noise due to cardiac driven motion. This should increase the signal to noise ratio, and therefore be an important step towards establishing optimal spinal fMRI techniques. In addition, the technical advances made in the development of MR equipment, such as the 3T magnet versus the 1.5T magnet, will also allow for greater

quality images in the future. The greater overall signal obtained with a 3T magnet will aid in enhancing the ability to detect neuronal activity related signal changes. However, the enhanced sensitivity to magnetic susceptibility may be problematic for spinal fMRI, as the different tissue types are in close proximity in the spinal canal. For further discussion of these developments, see Tanenbaum (2006).

Ultimately, the goal is for spinal fMRI to be a useful and practical clinical tool. The neuronal response in the spinal cord both above and below the injury site can be monitored following injury and throughout rehabilitation. A protocol can be developed such that a standard battery of tests may be conducted to assess both ascending and descending information. Imaging can be carried out shortly after injury and repeated at set intervals following initial injury or commencement of a rehabilitation program or drug trial. Ideally, a software program would be available for technicians and clinicians to use for simple and quick analysis of the data. The results should be displayed in three dimensions in both the original and normalized format. Normalizing the results would allow for ease of comparison between patients and facilitate a standard method of documenting the results. Packaging a standardized spinal fMRI assessment protocol with an efficient and comprehensible analysis program would expedite spinal fMRI into clinical use.

Conclusion

Spinal fMRI has now been successful in assessing neuronal activity in the cervical and lumbar cord for both sensory and motor stimuli. It has been determined that spinal fMRI is capable of detecting neuronal activity caudal to complete and incomplete spinal cord injury, during participation in active and/or passive lower limb movement tasks.

The spinal fMRI method has been optimized with increased volume coverage of the cord, three dimensional display of resulting activity maps, and improved spatial resolution in the superior/inferior direction. Further insight into the characteristics of true and false positive activations was gained. The overall goal of contributing to the development and advancement of spinal fMRI towards reliable research and practical clinical use was achieved.

References

American Spinal Injury Association Neurological Standards Committee *International Standards for Neurological Classification of Spinal Cord Injury*2000).

Andrew,R.D. & MacVicar,B.A. Imaging cell volume changes and neuronal excitation in the hippocampal slice. *Neuroscience* **62**, 371-383 (1994).

Backes,W.H., Mess,W.H., & Wilmink,J.T. Functional MR imaging of the cervical spinal cord by use of median nerve stimulation and fist clenching. *AJNR Am. J. Neuroradiol.* **22**, 1854-1859 (2001).

Bergman,A., Leblanc,C., & Stroman,P.W. Spinal fMRI of Multiple Sclerosis: Comparison of Signal Intensity Changes with Healthy Controls. Proceedings of the International Society for Magnetic Resonance in Medicine 12th Annual Meeting, Kyoto, Japan, May 15-21, 2004, 1035. 2004.

Bergman,A., Leblanc,C., & Stroman,P.W. Spinal fMRI of Multiple Sclerosis in Human Subjects. Proceedings of the International Society for Magnetic Resonance in Medicine 12th Annual Meeting, Kyoto, Japan, May 15-21, 2004, 1126. 2004.

Bitar,R., Leung,G., Perng,R., Tadros,S., Moody,A.R., Sarrazin,J., McGregor,C., Christakis,M., Symons,S., Nelson,A., Roberts,T.P. MR pulse sequences: what every radiologist wants to know but is afraid to ask. *Radiographics.* **26**(2), 513-37 (2006).

Borgens,R.B. *Restoring function to the injured human spinal cord*(Springer-Verlag, Berlin, 2003).

Bouzier-Sore,A.K., Merle,M., Magistretti,P.J., & Pellerin,L. Feeding active neurons: (re)emergence of a nursing role for astrocytes. *J. Physiol Paris* **96**, 273-282 (2002).

Brooks,J., Robson,M., Schweinhardt,P., Wise,R., & Tracey,I. Functional magnetic resonance imaging (fMRI) of the spinal cord : a methodological study. American Pain Society 23rd Annual Meeting, Vancouver, May 6-9, 2004, 667. 2004.

Brunelli,G. Research on the possibility of overcoming traumatic paraplegia and its first clinical results. *Current Pharmaceutical Design* **11**, 1421-1428 (2005).

Byrne T.N., Benzel,E.C., & Waxman,S.G. *Diseases of the spine and spinal cord*(Oxford University Press, Inc., New York, 2000).

Chakeres,D.W. & Schmalbrock,P. *Fundamentals of magnetic resonance imaging*(Williams & Wilkins, Maryland, 1992).

Damadian,R., Goldsmith,M., & Minkoff,L. NMR in cancer: XVI. FONAR image of the live human body. Physiological Chemistry and Physics and Medical NMR 9, 97-100 (1977).

DeForge,D., Nymark,J., Lemaire,E., Gardner,S., Hunt,M., Martel,L., Curran,D., Barbeau,H. Effect of 4-aminopyridine on gait in ambulatory spinal cord injuries: a double-blind, placebo-controlled, crossover trial. *Spinal Cord.* **42**(12), 674-85 (2004).

Ferris,D.P., Gordon,K.E., Beres-Jones,J.A., & Harkema,S.J. Muscle activation during unilateral stepping occurs in the nonstepping limb of humans with clinically complete spinal cord injury. *Spinal Cord.* **42**, 14-23 (2004).

Fujita,H. *et al.* Cerebral [15O] water clearance in humans determined by positron emission tomography: II. Vascular responses to vibrotactile stimulation. *J. Cereb. Blood Flow Metab* **17**, 73-79 (1997).

Gordon,J. & Ghez,C. Muscle receptors and spinal reflexes: The stretch reflex. in *Principles of Neural Science* (eds. Kandel E.R, Schwartz,J.H. & Jessell,T.M.) 564-580 (Elsevier, New York, 1991).

Goshgarian,H.G. Anatomy and function of the spinal cord in *Spinal Cord Medicine: Principles and Practice* (ed. Lin,V.W.) 15-34 (Demos Medical Publishing, Inc., New York, 2003).

Haxby,J.V., Courtney S.C., & Clark,V.P. Functional magnetic resonance imaging and the study of attention. in *The Attentive Brain* (ed. R.Parasuraman) 123-142 (MIT Press, Cambridge, 1998).

Jankowska,E. & Edgley,S.A. How can corticospinal tract neurons contribute to ipsilateral movements? A question with implications for recovery of motor functions. *Neuroscientist.* **12**, 67-79 (2006).

Jezzard,P., Matthews,P.M., & Smith,S.M. *Functional MRI: An Introduction to Methods*(Oxford Univerisity Press, New York, 2001).

Kautz,S.A., Patten,C., & Neptune,R.R. Does unilateral pedaling activate a rhythmic locomotor pattern in the nonpedaling leg in post-stroke hemiparesis? *J. Neurophysiol.* **95**, 3154-3163 (2006).

Kawashima,N., Nozaki,D., Abe,M.O., Akai,M., & Nakazawa,K. Alternate leg movement amplifies locomotor-like muscle activity in spinal cord injured persons. *J. Neurophysiol.* **93**, 777-785 (2005).

Kollias,S.S., Kwiecinski,S., & Summers,P. Functional MR Imaging of the Human Cervical Spinal Cord. American Society of Neuroradiology Proceedings of the 42nd Annual Meeting, Seattle, June 7-11, 2004., 227. 2004.

Kornelsen,J. & Stroman,P.W. fMRI of the lumbar spinal cord during a lower limb motor task. *Magn Reson. Med.* **52**, 411-414 (2004).

Lauritzen,M. & Gold,L. Brain function and neurophysiological correlates of signals used in functional neuroimaging. *J. Neurosci.* **23**(10), 3971-80 (2003).

Lauterbur,P.C. Image formation by induced local interactions: examples employing nuclear magnetic resonance. *Nature* **242**, 190-191 (1973).

Lawrence,J., Stroman,P.W., Bascaramurty,S., Jordan,L.M., & Malisza,K.L. Correlation of functional activation in the rat spinal cord with neuronal activation detected by immunohistochemistry. *NeuroImage* **22**, 1802-1807 (2004).

Li,G., Ng,M.C., Wong,K.K., Luk,K.D., & Yang,E.S. Spinal effects of acupuncture stimulation assessed by proton density-weighted functional magnetic resonance imaging at 0.2 T. *Magn Reson. Imaging* **23**, 995-999 (2005).

Logothetis,N.K., Pauls,J., Augath,M., Trinath,T., & Oeltermann,A. Neurophysiological investigation of the basis of the fMRI signal. *Nature* **412**, 150-157 (2001).

Logothetis,N.K. & Wandell,B.A. Interpreting the BOLD signal. *Annu. Rev. Physiol* **66**, 735-769 (2004).

Mackey,S., Ludlow,D., Knierim,J., Hanelin,J., & Glover,G. FMRI activation in the human cervical spinal cord to noxious thermal stimulation. American Pain Society 22nd Annual Meeting, Chicago, March 20-23, 2003, Poster 750. 2003.

Madi,S., Flanders,A.E., Vinitski,S., Herbison,G.J., & Nissanov,J. Functional MR imaging of the human cervical spinal cord. *AJNR Am. J. Neuroradiol.* **22**, 1768-1774 (2001).

Magistretti,P.J. & Pellerin,L. Astrocytes Couple Synaptic Activity to Glucose Utilization in the Brain. *News Physiol Sci.* **14**, 177-182 (1999).

Magistretti,P.J. Cellular bases of functional brain imaging: insights from neuron-glia metabolic coupling. *Brain Res.* **886**, 108-112 (2000).

Majcher,K. *et al.* Simultaneous functional magnetic resonance imaging in the rat spinal cord and brain. *Exp. Neurol.*(2005).

Malisza,K.L. & Stroman,P.W. Functional imaging of the rat cervical spinal cord. *J. Magn Reson. Imaging* **16**, 553-558 (2002).

Malisza,K.L. *et al.* Functional MRI of the Rat Lumbar Spinal Cord Involving Painful Stimulation and the Effect of Peripheral Joint Mobilization. *J. Magn Reson. Imaging* **18**, 152-159 (2003).

Mansfield,P. & Grannell,P.K. NMR 'diffraction' in solids? *Journal of Physics C Solid State* **6**, L422-L426 (1973).

Menon,R.S. *et al.* Functional brain mapping using magnetic resonance imaging. Signal changes accompanying visual stimulation. *Invest Radiol.* **27 Suppl 2**, S47-S53 (1992).

Moffitt,M.A., Dale,B.M., Duerk,J.L., & Grill,W.M. Functional magnetic resonance imaging of the human lumbar spinal cord. *J. Magn Reson. Imaging* **21**, 527-535 (2005).

Moonen,C. & Bandettini,P. *Functional MRI*(Springer-Verlag, Berlin, 1999).

Nedergaard,M., Takano,T., & Hansen,A.J. Beyond the role of glutamate as a neurotransmitter. *Nat. Rev. Neurosci.* **3**, 748-755 (2002).

Ng,M.C. *et al.* Proton-density-weighted spinal fMRI with sensorimotor stimulation at 0.2 T. *NeuroImage*(2005).

Ogawa,S., Lee,T.M., Kay,A.R., & Tank,D.W. Brain magnetic resonance imaging with contrast dependent on blood oxygenation. *Proc. Natl. Acad. Sci. U. S. A* **87**, 9868-9872 (1990).

Ogawa,S. *et al.* Intrinsic signal changes accompanying sensory stimulation: functional brain mapping with magnetic resonance imaging. *Proc. Natl. Acad. Sci. U. S. A* **89**, 5951-5955 (1992).

Ogawa,S. *et al.* Functional brain mapping by blood oxygenation level-dependent contrast magnetic resonance imaging. A comparison of signal characteristics with a biophysical model. *Biophys. J.* **64**, 803-812 (1993).

Ogawa,S., Menon,R.S., Kim,S.G., & Ugurbil,K. On the characteristics of functional magnetic resonance imaging of the brain. *Annu. Rev. Biophys. Biomol. Struct.* **27**, 447-474 (1998).

Ohta,S. *et al.* Cerebral [15O]water clearance in humans determined by PET: I. Theory and normal values. *J. Cereb. Blood Flow Metab* **16**, 765-780 (1996).

Pauling,L. & Coryell,C.D. The magnetic properties and structure of hemoglobin, oxyhemoglobin, and carbon-monoxyhemoglobin. *Proceedings of the National Academy of Sciences (USA)* **22**, 210-216 (1936).

Paulson,O.B. & Newman,E.A. Does the release of potassium from astrocyte endfeet regulate cerebral blood flow? *Science* **237**, 896-898 (1987).

Pellerin,L. & Magistretti,P.J. Food for thought: challenging the dogmas. *J. Cereb. Blood Flow Metab* **23**, 1282-1286 (2003).

Pointillart,V. *et al.* Pharmacological therapy of spinal cord injury during the acute phase. *Spinal Cord.* **38**, 71-76 (2000).

Porszasz,R., Beckmann,N., Bruttel,K., Urban,L., & Rudin,M. Signal changes in the spinal cord of the rat after injection of formalin into the hindpaw: characterization using functional magnetic resonance imaging. *Proc. Natl. Acad. Sci. U. S. A* **94**, 5034-5039 (1997).

Raichle,M.E. & Minton,M.A. Brain work and brain imaging. *Annu. Rev. Neurosci.* **29**, 449-76 (2006).

Reier,P.J., Houle,J.D., Jakeman,L., Winialski,D., & Tessler,A. Transplantation of fetal spinal cord tissue into acute and chronic hemisection and contusion lesions of the adult rat spinal cord. *Prog. Brain Res.* **78**, 173-179 (1988).

Reier,P.J., Stokes,B.T., Thompson,F.J., & Anderson,D.K. Fetal cell grafts into resection and contusion/compression injuries of the rat and cat spinal cord. *Exp. Neurol.* **115**, 177-188 (1992).

Reier,P.J., Anderson,D.K., Thompson,F.J., & Stokes,B.T. Neural tissue transplantation and CNS trauma: anatomical and functional repair of the injured spinal cord. *J. Neurotrauma* **9 Suppl 1**, S223-S248 (1992).

Rexed,B. The cytoarchitectonic organization of the spinal cord in the cat. *J. Comp Neurol.* **96**, 414-495 (1952).

Rexed,B. A cytoarchitectonic atlas of the spinal cord in the cat. *J. Comp Neurol.* **100**, 297-379 (1954).

Schwab,M.E. & Bartholdi,D. Degeneration and regeneration of axons in the lesioned spinal cord. *Physiol Rev.* **76**, 319-370 (1996).

Shi,R., Kelly,T.M., & Blight,A.R. Conduction block in acute and chronic spinal cord injury: different dose-response characteristics for reversal by 4-aminopyridine. *Exp. Neurol.* **148**, 495-501 (1997).

Stracke,C.P., Pettersson,L.G., Schoth,F., Moller-Hartmann,W., & Krings,T. Interneuronal systems of the cervical spinal cord assessed with BOLD imaging at 1.5T. *Neuroradiology* **47**, 127-133 (2005).

Stroman,P.W., Nance,P.W., & Ryner,L.N. BOLD MRI of the human cervical spinal cord at 3 tesla. *Magn Reson. Med.* **42**, 571-576 (1999).

Stroman,P.W., Krause,V., Malisza,K.L., Frankenstein,U.N., & Tomanek,B. Characterization of contrast changes in functional MRI of the human spinal cord at 1.5 T. *Magn Reson. Imaging* **19**, 833-838 (2001).

Stroman,P.W. & Ryner,L.N. Functional MRI of motor and sensory activation in the human spinal cord. *Magn Reson. Imaging* **19**, 27-32 (2001).

Stroman,P.W., Krause,V., Malisza,K.L., Frankenstein,U.N., & Tomanek,B. Functional magnetic resonance imaging of the human cervical spinal cord with stimulation of different sensory dermatomes. *Magn Reson. Imaging* **20**, 1-6 (2002).

Stroman,P.W., Krause,V., Malisza,K.L., Frankenstein,U.N., & Tomanek,B. Extravascular proton-density changes as a non-BOLD component of contrast in fMRI of the human spinal cord. *Magn Reson. Med.* **48**, 122-127 (2002).

Stroman,P.W., Tomanek,B., Krause,V., Frankenstein,U.N., & Malisza,K.L. Mapping of neuronal function in the healthy and injured human spinal cord with spinal fMRI. *NeuroImage* **17**, 1854-1860 (2002).

Stroman,P.W., Tomanek,B., Krause,V., Frankenstein,U.N., & Malisza,K.L. Functional magnetic resonance imaging of the brain based on signal enhancement by extravascular protons (SEEP fMRI). *Magn Reson. Med.* **49**, 433-439 (2003).

Stroman,P.W., Tomanek,B., Malisza,K.L. Functional magnetic resonance imaging of the human brain and spinal cord by means of signal enhancement by extravascular protons. *Concepts in Magnetic Resonance*, **16A(1)**, 28-34 (2003).

Stroman,P.W., Malisza,K.L., & Onu,M. Functional magnetic resonance imaging at 0.2 tesla. *NeuroImage* **20**, 1210-1214 (2003).

Stroman,P.W. *et al.* Non-invasive assessment of the injured human spinal cord by means of functional magnetic resonance imaging. *Spinal Cord* **42**, 59-66 (2004).

Stroman,P.W., Kornelsen,J., Lawrence,J., & Malisza,K.L. Functional magnetic resonance imaging based on SEEP contrast: response function and anatomical specificity. *Magn Reson. Imaging* **23**, 843-*850 (2005).*

Taber,K.H., Herrick,R.C., Weathers,S.W., Kumar,A.J., Schomer,D.F., Hayman,L.A. Pitfalls and artifacts encountered in clinical MR imaging of the spine. *Radiographics.* **18**(6), 1499-521 (1998).

Takahashi,Y., Chiba,T., Kurokawa,M., & Aoki,Y. Dermatomes and the central organization of dermatomes and body surface regions in the spinal cord dorsal horn in rats. *J. Comp Neurol.* **462**, 29-41 (2003).

Talairach,J. & Tournoux,P. *Co-planar stereotaxic atlas of the human brain*(Thieme Medical Publishers, Inc., New York, 1988).

Talos,I.F., Mian,A.Z., Zou,K.H., Hsu,L., Goldberg-Zimring,D., Haker,S., Bhagwat,J.G., Mulkern,R.V. Magnetic resonance and the human brain: anatomy, function and metabolism. *Cell Mol Life Sci.* **63**(10),1106-24 (2006).

Tanenbaum,L.N. Clinical 3T MR imaging: mastering the challenges. *Magn Reson Imaging Clin N Am.* **14**(1),1-15 (2006).

Tator,C.H. Strategies for recovery and regeneration after brain and spinal cord injury. Inj. Prev. 8 Suppl 4, IV33-IV36 (2002).

Vescovi,A.L. & Snyder,E.Y. Establishment and properties of neural stem cell clones: plasticity in vitro and in vivo. *Brain Pathol.* **9**, 569-598 (1999).

Wong,K.K. *et al.* Functional MRI of the spinal cord at low field. Proceedings of the International Society for Magnetic Resonance in Medicine 12th Annual Meeting , 1534. 2004.

Yoshizawa,T., Nose,T., Moore,G.J., & Sillerud,L.O. Functional magnetic resonance imaging of motor activation in the human cervical spinal cord. *Neuroimage.* **4**, 174-182 (1996).

Young,W. Molecular and cellular mechanisms of spinal cord injury therapies in *Neurobiology of Spinal Cord Injury* (eds. Kalb,R.G. & Strittmatter,S.M.) 241-276 (Humana Press Inc., Totowa, 2000).